Copyright Warning & Restrictions

The copyright law of the United States (Title 17, United States Code) governs the making of photocopies or other reproductions of copyrighted material.

Under certain conditions specified in the law, libraries and archives are authorized to furnish a photocopy or other reproduction. One of these specified conditions is that the photocopy or reproduction is not to be "used for any purpose other than private study, scholarship, or research." If a, user makes a request for, or later uses, a photocopy or reproduction for purposes in excess of "fair use" that user may be liable for copyright infringement,

This institution reserves the right to refuse to accept a copying order if, in its judgment, fulfillment of the order would involve violation of copyright law.

Please Note: The author retains the copyright while the New Jersey Institute of Technology reserves the right to distribute this thesis or dissertation

Printing note: If you do not wish to print this page, then select "Pages from: first page # to: last page #" on the print dialog screen

NOISE SPECTRAL DENSITY AS A DIAGNOSTIC TOOL FOR RELIABILITY OF p-n JUNCTIONS

BY

YOUNG DUCK KIM

A DISSERTATION

PRESENTED IN PARTIAL FULFILLMENT OF

THE REQUIREMENTS FOR THE DEGREE

OF

DOCTOR OF ENGINEERING SCIENCE IN ELECTRICAL ENGINEERING

AT

NEWARK COLLEGE OF ENGINEERING

Newark, New Jersey

1968

APPROVAL OF DISSERTATION

BY

YOUNG DUCK KIM

FOR

DEPARTMENT OF ELECTRICAL ENGINEERING

NEWARK COLLEGE OF ENGINEERING

BY

FACULTY COMMITTEE

APPROVED _____
ADVISOR

_____

_____

_____

NEWARK, NEW JERSEY

JUNE, 1968

ABSTRACT

The feasibility of choosing noise-voltage spectral density as a prediction parameter for the degradation of p-n junctions has been examined both theoretically and through a series of life-tests.

Experimental facts show that the noise-voltage spectral density, $S_v(w)$, observed in a p-n junction under the breakdown condition tends to be "white" (which contradicts the 1/f-noise theory), and $S_v(w)$ is inversely proportional to the breakdown current (which contradicts the shot-noise theory). Furthermore, some p-n junctions display one or more multiple peaks of $S_v(w)$ at different current levels which can not be explained by any of the existing noise theories.

In the derivation of a new theory, four factors are proposed to explain the behavior of $S_v(w)$. They are: (1) the number of primary carriers entering the multiplication zone during the given time interval is a random variable, (2) the entry times of primary carriers into the multiplication zone is a random variable, (3) the number of impact ionization events caused by a primary carrier is a random variable, and (4) the carrier transit times are statistically distributed.

The noise current due to the above mentioned multi-fold random processes is approximated by an ensemble of a triangular current pulses, and the Wiener-Khintchine theorem is applied to the autocorrelation function of the noise current to obtain $S_v(w) \propto V_b^2 I_r^{-1}$ where V_b is the breakdown voltage, and I_r is the breakdown current. This new theory can explain both inverse proportionality between $S_v(w)$ and I_r as well as white noise spectrum of $S_v(w)$.

It has been shown that the multiple-peak phenomenon found in some units is due to the microplasmic breakdown channels in a p-n junction. To demonstrate this fact, a microplasma-free, and a microplasmic breakdown channel were simulated by two diodes in parallel, and the difference in the breakdown voltages of two channels was externally inserted in series with a diode. Experimental evidence was obtained that one can generate artificially multiple-peak phenomenon from the above two-channel model.

Life-test experiments indicate that units whose $S_v(w)$ have multiple peaks are highly correlated with degradation of leakage characteristic over a life-test period.

It is recommended that some unreliable units be eliminated by inspecting the multiple-peak phenomenon which indicates the existence of microplasmic breakdown channels in a p-n junction.

TO MY MOTHER

ACKNOWLEDGEMENTS

The author wishes to express his sincere appreciation and gratitude to the following:

Dr. Raj P. Misra who provided the enthusiastic encouragement and valuable critism as the author's advisor throughout this endeavor.

Drs. Frederick A. Russell, Joseph J. Padalino, and Leonard M. Salzarulo for the continuous guidance in the course of his graduate studies.

Mr. James L. Ramsey for the benefit of technical discussions and data supplied by him.

His wife, Chungsook, for her encouragement and patience.

Newark College of Engineering for providing financial assistant in the form of a fellowship during the years 1963-1967.

U.S. Naval Ammunition Depot, Crane, Indiana, for the financial support during the last year of this research.

TABLE OF CONTENTS

LIST OF FIGURES AND TABLES

LIST OF SYMBOLS

A	Area of a p-n junction
a	Grade-constant in atoms/cm^4
C_j	Junction capacitance
D.U.T.	Diode under the test
D_p	Hole diffusion coefficient
d	Length of the depletion layer
E	Electric field
$E(A)=\overline{A}$	Statistical expectation of A
e	Charge of electron, -1.602×10^{-19} coul
f	Frequency in Hz
G	Junction conductance
$G(t_{ds}, t_{ds}+t_{as})$	Gate-function, $u(t_{ds})-2u(t_{ds}+t_{as})$
G313	Diode type used in the life-test No. 1
G321	Diode type used in the life-test No. 2
$H(jw)$	Transfer characteristic
$H^*(jw)$	Complex-conjugate of $H(jw)$
h	Plank's constant, 6.625×10^{-34} J·sec
$\overline{I}$	d-c reverse current
$\overline{I}_o$	$E(I(t))$
I_j	Branch current of j-th channel
$\overline{I}_s$	d-c saturation current
$I(t)$	Multiplication noise current

$i_o(t)$	A current pulse due to a primary carrier
$i(t)$	Same as $i_o(t)$ except t_a is replaced by $\bar{t}_{as}$
$i_{M_k}(t)$	Current pulse train due to a primary carrier
j	$(-1)^{1/2}$
K	Number of carriers entering the multiplication zone during the time interval of 2T
k	Boltzman's constant, 1.380×10^{-23} J/°K
k	Spectral proportionality constant
$\bar{k}$	Average number of carriers entering the multiplication zone during the time interval of 2T, E(K)/2T
l_a	Width of avalanche zone
l_d	Width of drift zone
M_k	Number of carriers emerging from the multiplication zone due to a primary carrier
m	Effective mass of the carrier
ma	10^{-3} amperes
mv	10^{-3} volts
$p(A)$	Probability distribution of A
p_n	Equilibrium hole concentration
q	Charge of electron, 1.602×10^{-19} coul
$R(s)$	Autocorrelation function
R_{eq}	Equivalent noise resistance
R_L	External current limiting resistor
R_s	Parasitic series resistance at j-th channel
S2A	Diode type used in the life-test No. 3
$S_i(w)$	Noise-current spectral density

$S_v(w)$	Noise-voltage spectral density
$S_v(1\text{-kHz})$	Noise-voltage spectral density measured at f=1-kHz and Δf=1-Hz
$S_p(w)$	Noise-power spectral density
S_{vj}	Equivalent noise source in j-th channel
s	Time displacement
T	Temerature in ^oK
2T	Time interval from -T to +T
t	time
t_a	Carrier transit time
$\bar{t}_{as}$	Average of carrier transit time
t_{ds}	Ionization time delays
t_{eff}	Effective life-time, $(t_s^{-1}+t_v^{-1})^{-1}$
t_k	Entry times of primary carriers into the multiplication zone
$\bar{t}_n$	Average transit time at p-side depletion layer
$\bar{t}_p$	Average transit time at n-side depletion layer
t_p	Hole life-time
t_s	Surface life-time
t_v	Bulk life-time
$u_i(E)$	Ionization coefficient as a function of electric field
ua	10^{-6} amperes
uv	10^{-6} volts

V_b	d-c breakdown voltage at given current
V_{bj}	d-c breakdown voltage of j-th channel
V_j	d-c voltage across the junction
v_d	Saturation drift velocity, approximately 8×10^6 cm/sec if electric field is greater than 1.5×10^4 volts/cm for n-type silicon at 300 ^{o}K
W	Width of depletion layer, $W=W_n+W_p$
W_n	Width of n-side depletion layer
W_p	Width of p-side depletion layer
w	Angular frequency in radian/sec, $w=2\pi f$
w_a	Avalanche frequency, $w_a=2\bar{u}_i l_a \bar{I}_o / \mathcal{E} A \bar{t}_a$
x	Distance
$Z(jw)$	Junction impedance under the avalanche
ΔV_b	Difference in breakdown voltages
$\delta(w)$	Impulse function
$\mathcal{E}$	Dielectric constant
ρ	Space-charge density
θ	Avalanche transit angle, $\theta=wt_a$

CHAPTER I

INTRODUCTION

The prediction of failure in components is one of the major problems of contemporary electronics. This is particularly true for semiconductor devices. At present, the reliability of semiconductor devices is mainly estimated on the basis of statistical characteristics, such as Failure Rate, Probability of Survival, and Mean Time Between Failure. These methods, however, have a number of serious deficiencies, the most important of which are the following:

(1) The statistical characteristics are an averaged criterion, which does not permit us to estimate the reliability of each device individually,

(2) The data on Failure Rate, from which Probability of Survival, and Mean Time Between Failure are calculated, involves very lengthy measurements which require very elaborate and expensive equipment. Therefore the measurements are performed only on sample lots. The vast majority of the devices are not checked with respect to these parameters.

It follows that no parameter is available at present that could be used as a criterion for the potential unreliability of a device. It would be ideal if one

would be able to establish a single reliability prediction parameter which enables one to estimate the reliability of each device individually rather than a given sample lot.

Misra[25] postulated that internal defects and potential instability mechanisms in the semiconductor devices may be readily, or at least partially* detected and analyzed from the noise spectral densities under foward and reverse biased conditions. Based on this postulate, the author's endeavor in this research has been aimed at determining whether noise spectral density alone can be used as the parameter to predict the reliability of individual p-n junctions.

---

* Misra also proposed a theory that the reliability of semiconductor devices is, in general, influenced by the following factors:

E lectric field
S urface protection
P ackage
A mbient (Gases)
T emperature and Temperature gradient

(ESPAT Theory). He foresightedly warned against the danger of selecting the noise spectral density alone as the reliability prediction parameter, since it may fail to predict some potential defects due to one or more factors such as Package, and Ambient.

For practical purposes, two electrical characteristics are considered to be of importance in the reliability of a p-n junction. They are:

(1) Degradation in reverse leakage characteristic for a given period,

(2) Degradation in foward voltage drop characteristic for a given period.

Although these two characteristics are equally important, and may be related to each other, the author has restricted himself in this research to investigating the noise spectral density with respect to the first characteristic alone. The second problem will be left for futrue study.

Fig. 1-1 shows a typical leakage degradation found in a commercially purchased diffused silicon rectifier. This undesirable degradation in leakage characteristic is attributed to "built-in" instability mechanisms which create high local current density as time goes on, and may also lead to the ultimate destruction of the device under certain conditions. It is sensed that some of these built-in instability mechanisms should be related to the noise spectral density, and if it is so, that they may be detected without performing lengthy life-test.

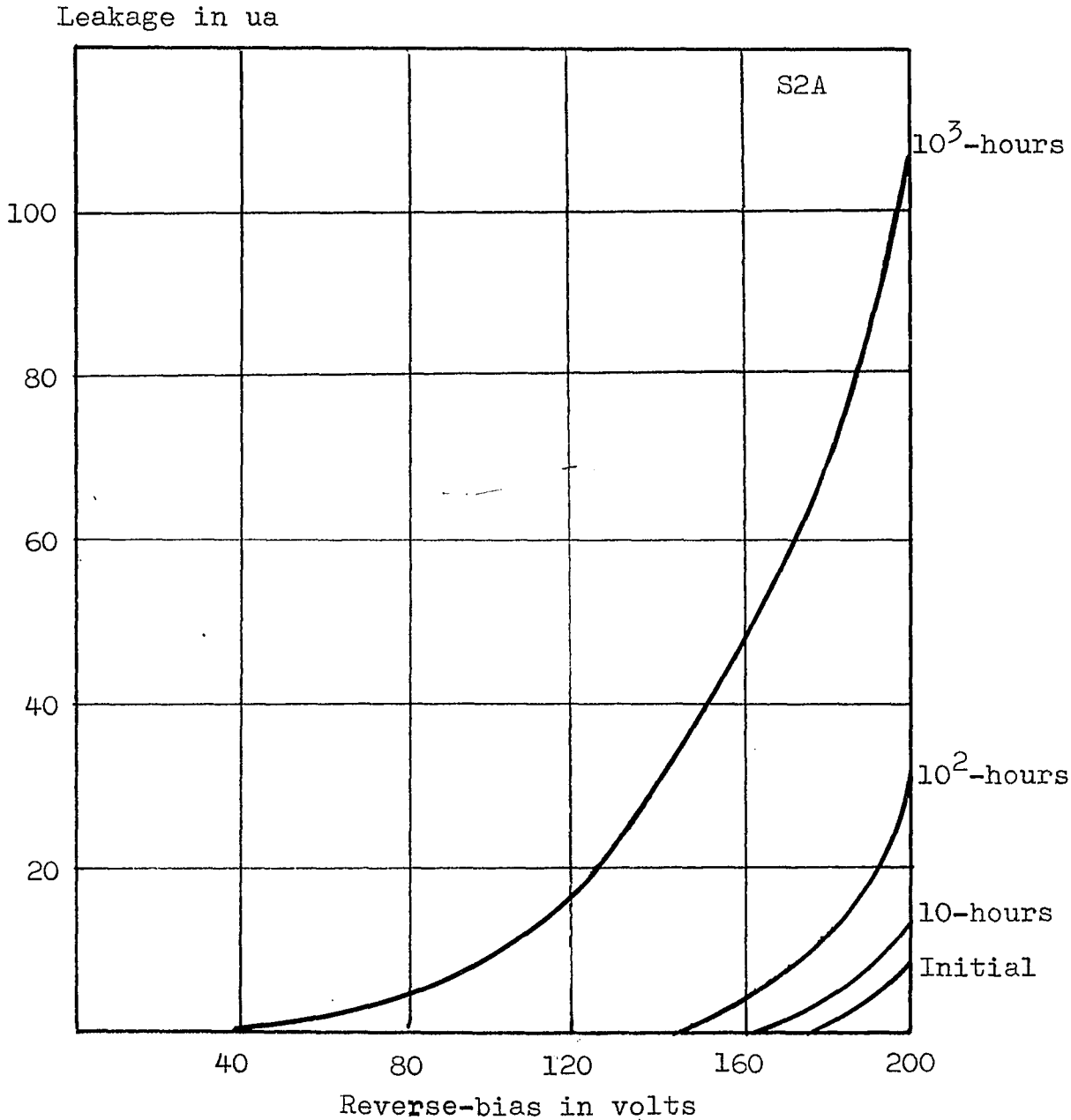

Fig. 1-1 Typical junction degradation in leakage characteristic found in a commercially purchased diffused silicon rectifier. 200 volts of d-c reverse-bias alone has been applied for 1000 hours at room temperature.

To investigate possible correlation, if any, between the degradation in leakage characteristic and the noise spectral density, the following steps were undertaken:

(1) The evaluation of the noise spectral density of a p-n junction at different bias conditions, especially near the breakdown knee,

(2) The identification of the noise sources, and their physical mechanisms,

(3) The construction of an equivalent noise model which consists of a given junction configuration and applied bias condition,

(4) The development of the hypothesis which can lead to the establishment of a screening technique to improve the reliability and performance of the device,

(5) The establishment of a test routine for the reliability prediction, hopefully at low-frequencies, and with standard equipment for high volume samples.

To carry out the research steps outlined above, it was considered to be most essential to investigate the noise spectral density around the breakdown knee because the author found, during his experimental research, that there is a somewhat peculiar "multi-peak" behavior* of

---

* Chapter 5 will be devoted to explain multi-peak phenomenon in the noise-voltage spectral density.

spectral density when the breakdown current is controlled. This phenomenon can not be explained by any existing noise theory, and the author was motivated to investigate sudden transitions of the noise spectral density in a p-n junction under breakdown condition as it was suspected that the multi-peak phenomenon was related to built-in instability mechanism.

In general, the theoretical study of the noise-voltage spectral density observed in a p-n junction under given bias condition requires investigation of two major factors:

(1) The determination of the physical noise generating mechanism as a form of the noise current-spectral density, $S_i(w)$, under given bias condition, and given p-n junction configuration,

(2) The transfer characteristic, H(jw), of the system which consists of the junction impedance (or admittance) under given bias condition, and noise measuring system as shown in Fig. 1-2.

Once $S_i(w)$ and H(jw) are determined, the observed noise-voltage spectral density, $S_v(w)$, may be determined from the following linear operation

$$S_v(w) = H(jw)H^*(jw)S_i(w) \qquad (1\text{-}1)$$

where $H^*(jw)$ denotes complex conjugate of H(jw).

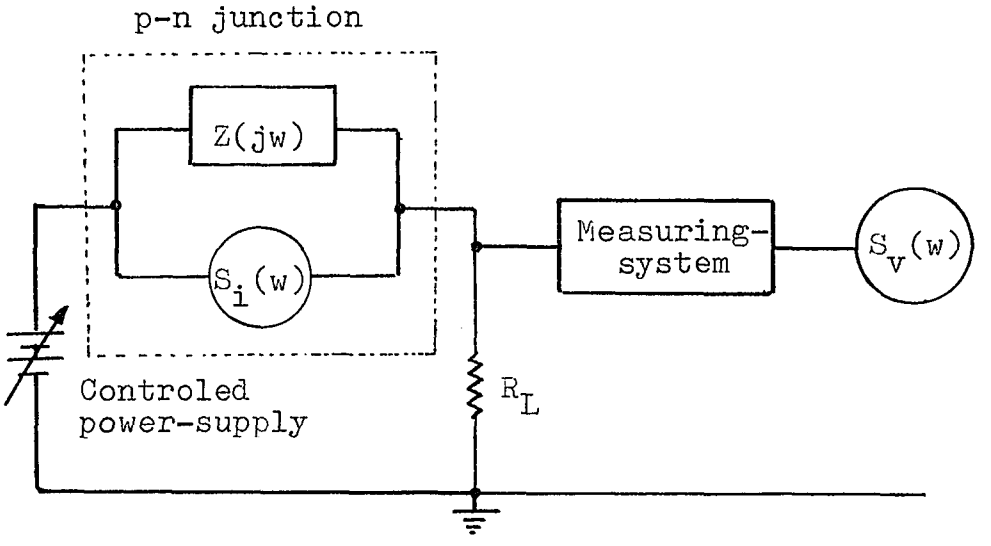

Fig. 1-2 Two factors involved in the determination of the noise-voltage spectral density, $S_v(w)$: $S_i(w)$, and H(jw) consists of Z(Jw), R_L, and the noise measuring system.

Accordingly, the author's task in the theoretical part of this research is then to determine $S_i(w)$ and $H(jw)$ for a given p-n junction configuration, and for a given reverse bias condition, especially at the avalanche breakdown knee.

It has been found that a very small percentage of units have shown significant discrepancies with respect to the theoretically predictable behavior, and this led the author to establish a hypothesis that the discrepancy is due to built-in instability mechanisms which eventually cause catastrophic destruction of the device. The validity of the hypothesis was examined from the life-test experiment, and found to have relatively high correlation.

The general content of this dissertation is the following:

In Chapter 2, the major physical noise generating mechanisms presently known to be associated with p-n junctions, such as Thermal-noise, Shot-noise, and 1/f-noise will be briefly reviewed and summarized. Experimental evidence that these noise mechanisms can not explain observed spectral densities under the breakdown mode will be presented.

In Chapter 3, the recent work by various investigators related to the small signal a-c impedance of a

p-n junction under breakdown condition will be summarized. It will be shown that the low-frequency approximation of a p-n junction impedance under the avalanche breakdown condition is expressed by the parallel combination of a voltage-dependent junction capacitance and a current-dependent multiplication zone conductance.

In Chapter 4, a theory will be proposed to explain experimentally observed noise-voltage spectral densities for the p-n junctions under breakdown condition. Simple geometrical configuration and uniform breakdown will be assumed in the derivation of $S_v(w)$. In the derivation of new theory, four factors are proposed as basic to the cause of the avalanche noise mechanism. They are:

(1) The number of primary carriers entering the carrier multiplication zone during the given time interval is a random process,

(2) Entry times of the primary carriers into the multiplication zone is a random process,

(3) Multiplication factor associated with the primary carriers is a random variable,

(4) The carrier transit times are statistically distributed.

To simplify these rather complicated multi-fold random processes, the author assumed that these four

random processes are independent of each other, stationary, ergodic, and Markovian. Further the noise current is approximated by an ensemble of triangular current pulses. After the autocorrelation function of the noise current, R(s), has been derived, the Wiener-Khintchine theorem was directly applied to obtain the noise-current spectral density, $S_i(w)$. $H(jw)H^*(jw)$ is computed from the series combination of low-frequency multiplication impedance (current-dependent) presented in Chapter 2, and external noise measuring circuit. The linear operation expressed by Eq.(1-1) then gives us the observed noise-voltage spectral density, $S_v(w)$. The new theoretical expression derived in this chapter can explain the noise-voltage spectral density observed in the majority of p-n junctions under avalanche breakdown condition. The theory presented in Chapter 4, however, fails to explain rather peculiar multi-peak phenomena in noise-voltage spectral density measured at 1 kHz when the avalanche current level was continuously increased.

In Chapter 5, the discrepancy between the theoretical results obtained in Chapter 4 and the experimentally observed multi-peak phenomena will be explained. The concept of local "hot-spot" will be introduced, and the effect of these hot-spots on observed noise-voltage spectral densities will be explained by multi-channel

approximation. An experimental verification of the two-channel model will be presented to show that the double-peak phenomenon is due to a hot-spot, and bulk channel.

In Chapter 6, the results of life-test performed at the N.C.E. Reliability Laboratory will be presented. The purpose of the life-test is to investigate the validity of using the noise-voltage spectral density as a prediction factor for the junction leakage degradation. Life-test data were accumulated and processed through an IBM 1620 digital computer for the correlation analysis. Three different types of diode have been chosen for life-test. The types and sample size are:

Life-test	Diode type*	Sample size
No.1	G315 (Zener-diode)	108
No.2	G321 (High-speed diode)	449
No.3	S2A (Rectifier)	200

In the last chapter, conclusions will be drawn from the theoretical results as well as from the facts obtained by life-test.

---

* Specification are listed in Chapter 6 (page 87-88).

Before we conclude the introduction, it may be worthwhile to mention briefly the mathematical background behind the theoretical work in this dissertation. As mentioned earlier, the essential part of the mathematical tool employed during the derivation of the noise current spectral density, in Chapter 4, is the Wiener-Khintchine theorem for which numerous excellent texts[4,19,20,21,28] are available. This theorem states that the spectral density and the autocorrelation function are Fourier transforms of each other, or

$$\begin{cases} S(w) = 2\int_{o}^{\infty} R(s)\cos(ws)\, ds \\ \\ R(s) = \int_{-\infty}^{\infty} S(w)\cos(ws)\, dw \end{cases} \qquad (1\text{-}2)^*$$

where R(s) is an autocorrelation function of a noise-current, I(t), which may be defined as the following:

$$R(s) = \lim_{T\to 0} \frac{1}{2T}\int_{-T}^{+T} I(t)I(t+s)\, dt \qquad (1\text{-}3)$$

---

* Many other expressions equivalent to Eq.(1-2) are available. The author followed the notation used in Dr. Russell's class in 1965 at N.C.E. The physical meaning of $S_v(w)$ is such that

$$\int_{o}^{\infty} S_v(w)\, dw = \overline{V_n^2(t)}$$

The R(s) defined as in Eq.(1-3) may be computed by the following method, provided that the joint probability $p(I(t)=x_1, I(t+s)=x_2; s)$ is known:

$$R(s) = \int_{-\infty}^{+\infty}\int_{-\infty}^{+\infty} x_1 x_2 p(x_1, x_2; s)\, dx_1 dx_2 \qquad (1\text{-}4)$$

Once the autocorrelation function of a p-n junction noise current has been found, it should be verified from the characteristics of autocorrelation function and its physical realization. The autocorrelation function derived in Chapter 4 was found to satisfy these requirements.

CHAPTER 2

SUMMARY OF RECENT PROGRESS IN NOISE THEORIES FOR p-n JUNCTIONS

2.1 Introduction

There are three basic types of noise commonly found in a p-n junction. They are Thermal-noise, Shot-noise, and 1/f-noise. It is the purpose of this chapter to review and summarize "up-to-date" theories associated with these three types of noise. The existing noise theories, however, can not explain drastic transition of noise spectral density around the breakdown knee.

The author will propose a new theory for the noise spectral density observed in a p-n junction under the avalanche breakdown condition in Chapter 4.

2.2 Thermal-noise

This is alternatively known as Johnson-noise.[17] Nyquist[29] showed that the mean-square voltage across a resistor of a-c resistance R in thermal equilibrium at temperature T is given by

$$S_v(w) = 4kTR \qquad (2\text{-}1)$$

where k is Boltzman's constant, 1.38×10^{-23} J/°K.

Notice that

$$\int_0^\infty S_v(w)dw = \int_0^\infty 4kTR\ dw = \overline{V_n^2(t)} \qquad (2\text{-}2)$$

does not converge. A quantum-mechanical correction to Nyquist's formula must be made to take account of the fact that even in the ground state at zero temperature there is a residual energy of ½hf. The most recent and complete expression for the thermal-noise voltage spectral density is rigorously derived by Ekstein and Rostoker[5] as

$$S_v(w) = 4hfR\left[\tfrac{1}{2} + \frac{1}{e^{hf/kT} - 1}\right] \qquad (2\text{-}3)$$

where $f=w/2\pi$, and h is Planck's constant, 6.625×10^{-34} J.sec. Under the usual condition such as $hf/kT \ll 1$, or $f \ll 2\times10^{10}T$ Hz, Eq.(2-3) reduces to Eq.(2-1). The author derived Eq.(2-3) with an assumption that the carriers are under harmonic oscillation at thermal equilibrium. This is shown in Appendix A. The derivation is somewhat simpler than Ekstein and Rostoker's approach.

Nyquist's formula relates the electrical manifestation of the thermal energy of the current carriers to the atoms of the material through the heat dissipative mechanism represented by R. This formula is of general nature, and applies to any heat dissipative medium which is in thermal equilibrium. Pure reactive elements do not in themselves

behave as thermal-noise sources since they are not heat-dissipative. An interesting application of this fact is in the field of parametric amplification in which signal amplication is accomplished by variable junction capacitance as a function of applied electric field. Practical p-n junctions, however, always possess a finite resistance in conjunction with depletion layer capacitance and this heat-dissipative resistance contributes thermal-noise.

The Nyquist's formula may be expressed in another way. If we consider a resistor as a source of noise power, the maximum available noise power from the resistor will be absorbed by a matched load, and the equivalent noise source power spectral density should be

$$S_p(w) = kT \qquad (2\text{-}4)$$

The classical thermal noise expression given by Eqs.(2-1) and (2-4) are well established both theoretically and experimentally. It is not surprising therefore that $S_p(w)$ is often used as a reference when specifying the spectral densities of other types of noise. In this connection, the concept of Noise-Temperature, Noise-Figure, and Equivalent Input Noise Temperature[3] have been introduced. Recent experimental results[47] show

that a film type resistor of approximately 60 ohms has flat spectral density up to 1-GHz and up to 1300 ^{o}C.

2.3 Shot-noise in p-n Junctions

Investigations of shot-noise in p-n junctions have been carried out by Montgomery and Clark,[26] Giacoletto,[9] Petritz,[31,32] and Van der Ziel.[41-45] The result of all these investigations of shot-noise shows frequency independence in the low-frequency region. The accepted formula for the current spectral density of shot-noise is

$$S_i(w) = 4kTG + 2q\bar{I}_o \qquad (2\text{-}5)$$

where k is Boltzman's constant, T is absolute temperature, q is the electronic charge, $\bar{I}_o$ is the d-c current, and G is the junction conductance given by

$$G = \left(\frac{q^2}{kT}\right)\left(\frac{D_p}{t_p}\right)^{1/2} p_n \mathrm{EXP}\left(\frac{qV_j}{kT}\right) \cdot \left\{\tfrac{1}{2}\left(1+w^2t_p^2\right)^{1/2}+\tfrac{1}{2}\right\}^{1/2} \qquad (2\text{-}6)$$

where D_p is the hole diffusion coefficient, t_p is the hole life-time, p_n is the equilibrium hole concentration, and V_j is the d-c voltage across the junction. The equivalent shot-noise current generator is placed in parallel with the junction. A derivation of Eq.(2-5) is shown in Appendix B, essentially following Van der Ziel's

approach.[44] Bennet[3] simplified the derivation by Van der Ziel with some "ad hoc" postulations. The first term in Eq. (2-5) will be recognized as the thermal-noise associated with the small signal admittance, and the second term is full shot-noise from the d-c component of current. The shot-noise is usually expressed in terms of equivalent noise resistance, R_{eq}, which is defined by

$$4kT\frac{1}{R_{eq}} = 4kTG+2qI_o \qquad (2-7)$$

Fig. 2-1 shows a possible way to measure the equivalent noise resistance, R_{eq}. If the diode under test is forward biased at ordinary current levels, the equivalent noise resistance of such diode will often be below the input noise resistance of the usual low-noise pre-amplifier. Hence, a suitable transformer must be used between the diode under test and the pre-amplifier.

Under the reverse biased condition, the transformer is not necessary, and the pre-amplifier may be directly connected to the blocking condenser because the noise equivalent resistance is considerably higher.

Shot-noise is caused by the randomness in the diffusion of the minority carriers, and the randomness in the recombination of minority carriers and majority carriers. In the transmission line analogy, the first

process corresponds to distributed noise emf's in series with the transmission line, and the second process corresponds to distributed noise-current generators in parallel with the transmission line*.

Figs. 2-2 and 2-3 show a typical broadband shot-noise** found in 1N3051*** diodes under forward and reverse bias conditions. One significant characteristic of shot-noise is that it increases as d-c current increases under ordinary bias condition. This fact, however, does not hold under avalanche breakdown condition, and will be discussed in detail in Chapter 4.

---

* See Appendix B.

** Broadband noise may be defined by $\left[\int_{1kHz}^{100kHz} S_i(w)dw\right]^{1/2}$.

** Quan-Tech Diode Noise Analyzer (Model-327) has been extensively used throughout this research for shot-noise measurements as well as 1/f-noise for various types of diode. Broadband shot-noise was measured by Model 327.

*** Zener-diode, V_Z=150 volts.

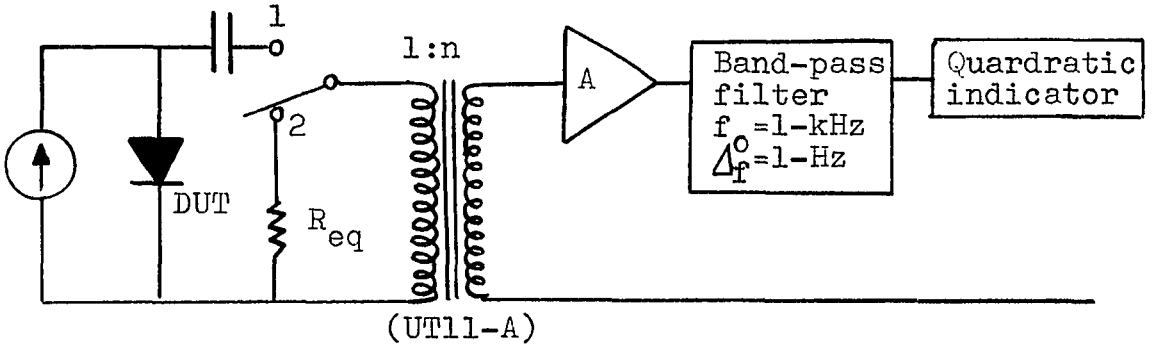

Fig. 2-1 A possible set-up to measure R_{eq} under forward-bias condition. If the switch is connected to contact 1, an indication is obtained at the indicator due to DUT noise, amplifier noise, and the resistive part of transformer impedance. Then the switch is connected to contact 2, and the purely ohmic resistance R_{eq} is adjusted until the same output indication is obtained. The determination of R_{eq} may be carried out with sufficient accuracy if

$$R_{eq}n^2 \geqq R_{eq\text{-}amp}+R_{T2}+R_{T1}n^2$$

where n is the transformer ratio, $R_{eq\text{-}amp}$ is the equivalent input noise resistance of amplifier. R_{T1} and R_{T2} represent the effective resistance of the primary and secondary winding of the transformer.

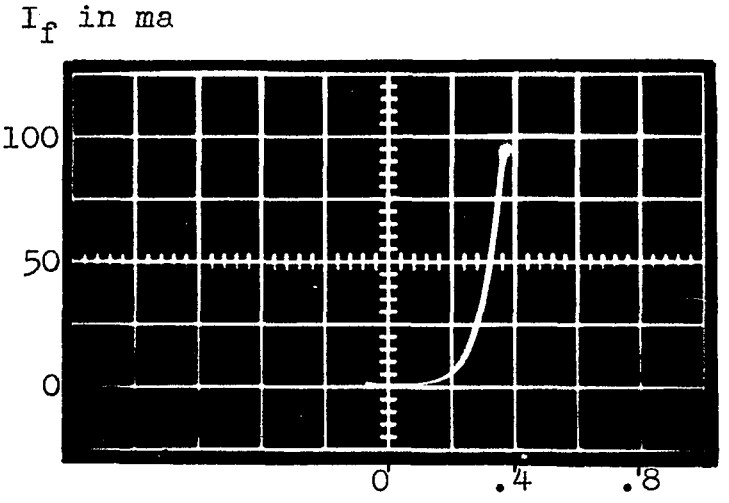

(a)

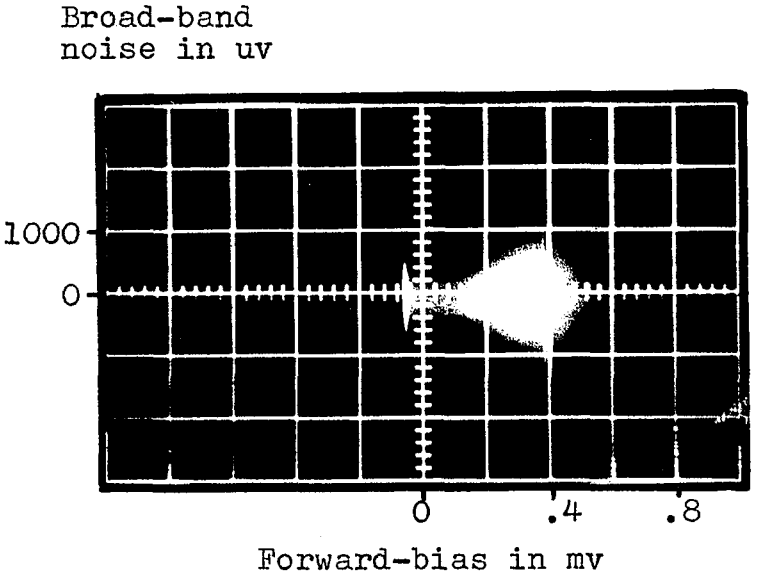

(b)

Fig. 2-2 (a) Forward-bias vs forward-current found in 1N3051,
(b) Broad-band noise vs forward-bias found in 1N3051.

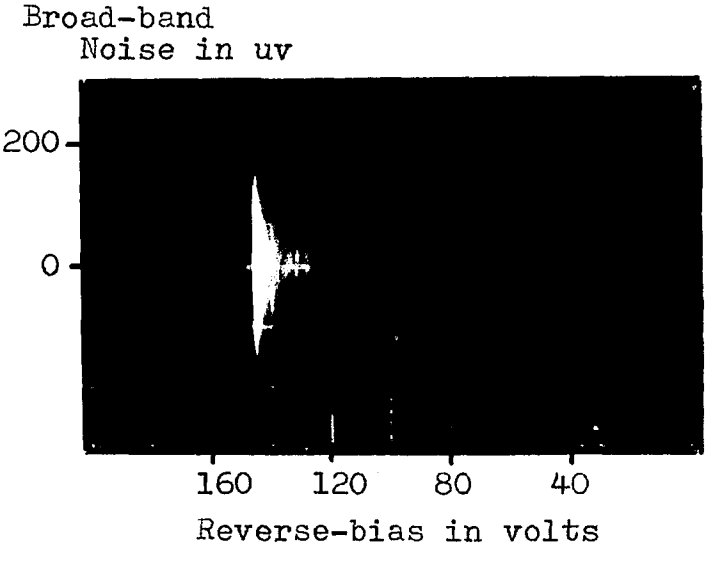

Fig. 2-3 A typical Broad-band noise vs reverse-bias found in 1N3051. The effect of shot-noise is significant.

2.4 1/f-noise in p-n Junctions[8]

At low-frequencies the shot-noise in a p-n junction is overshadowed by another type of noise, which is called by various names such as excess-noise, low-frequency noise, and 1/f-noise. The spectral density has the form

$$S_i(f) = c \frac{\bar{I}^b}{f^a} \qquad (2\text{-}8)$$

where b is in many cases approximately equal to two, and a is approximately unity* (the reson this noise is called as "1/f" noise).

---

* Note that if "a" were exactly equal to unity the mean total noise power in a band of frequencies from f_1 to f_2 would be given by

$$\int_{f_1}^{f_2} \frac{c\bar{I}^b}{f}\, df = c\bar{I}^b(\ln f_2 - \ln f_1)$$

This expression would give an infinite amount of noise power if the band extended either all the way down to zero frequency or all the way up to infinite frequency. Since the actual noise power remaines finite, the exact 1/f-law cannot hold except over a frequency band which is limited at both the low-frequency and high-frequency ends. It is, however, remarkable experimental fact that the 1/f law has been found to be very nearly satisfied over many frequency decades extending to a small fraction of Hz. If "a" is less than unity, the expression remaines finite for f_1 equal to zero but not for f_2 infinite. If

"a" is greater than unity, the expression remains finite for f_2 equal to infinity but not for f_1 to zero. Thus we see that allowing $a \neq 1$ in Eq. (2-8) still cannot give a law which is valid at both zero frequency and infinite frequency.

The value for "b" should be exactly two if 1/f-noise is due to the fluctuation of the carrier concentration dN about the mean $\overline{N}$, since the current fluctuation $dI = \overline{I} dN/\overline{N}$, and the total mean-square noise current fluctuation $\overline{dI^2}$ is

$$\overline{dI^2} = \overline{I^2}\,\overline{dN^2}/\,\overline{N^2} \qquad (2\text{-}9)$$

Thus $\overline{dI^2}$ is proportional to $\overline{I^2}$ provided that $\overline{dN^2}$ is independent of $\overline{I}$. It is the possibility that $\overline{dN^2}$ being dependent on $\overline{I}$ which explains why "b" is not exactly two.

Doubtless one of the difficulties in finding a physical model which yields experimentally observed 1/f characteristics is that 1/f type spectral density cannot include zero and infinite frequency. This problem is not unique to the p-n junction phenomena alone, but is manifested in Flicker-noise in vacuum tubes, and in Contact-noise between two metal contacts. This similarlity, however, suggests that there might be some common noise generating mechanism among these types of noise, and it has been suspected that the surface state is responsible for the 1/f type spectral density.

Although a precise model to explain 1/f-noise is not available at present, it is interesting to notice that 1/f type spectral density can be synthesized from the superposition of $c\overline{I^2}t_a/(1+w^2t_a^2)$ type spectral density* and a uniform distribution for the time constant t_a, that is, $p(t_a)=t_a^{-1}$. For the range of time constants from t_{a1} to t_{a2} we have

$$S_i(w) = \frac{c\overline{I^2}\int_{t_{a1}}^{t_{a2}} t_a^{-1}\left\{\frac{t_a}{(1+w^2t_a^2)}\right\}dt_a}{\int_{t_{a1}}^{t_{a2}} t_a^{-1}\,dt_a} \qquad (2\text{-}10)$$

and for a frequency range of $t_a^{-2}<w<t_a^{-1}$,

$$S_i(w) \approx \frac{c\overline{I^2}\pi}{2\ln(t_{a2}/t_{a1})}\frac{1}{w} \propto \frac{1}{f} \qquad (2\text{-}11)$$

Recently, it has been fairly well established, although not completely understood, that the electrical properties of a junction surface differ from those of the bulk (interior). This is to be expected, because the surface

---

* This spectral density is a characteristic of all linear physical processes governed by a simple exponential relaxation function.

represents an abrupt boundary for the outermost layer of atoms and should therefore disrupt the orderly energy distribution in the region. Even if the surface were absolutely perfect, that is, completely free from any atomic dissymmetry, it would be hard to imagine the carriers will behave the same at the surface as in the interior. Furthermore, from a practical view point, the surface is not perfect. Many theories have been proposed to explain surface phenomena such as absorbtion of chemical ions, perhaps water or gas molecules (depending on the kind of environment the surface is exposed to). According to Kingston,[18] and Bardeen,[2] there exist at the surface a number of energy states having energies that fall within the forbidden band gap of the semiconductor. Shockley[39,40] has shown that the surface energy states are related to surface life-time, t_s, such that

$$\frac{1}{t_{eff}} = \frac{1}{t_s} + \frac{1}{t_v} \qquad (2\text{-}12)$$

where t_{eff} is the effective life-time and t_v is the life-time of the bulk. Furthermore, the surface life-time has a statistical distribution, and this distribution has been suspected as a source of 1/f type spectral density by the reason given in Eqs. (2-11) and (2-12).

Fig. 2-4 shows a typical 1/f-noise found in a two-ampere-rated silicon diffused rectifier. $S_i(w)$ was found

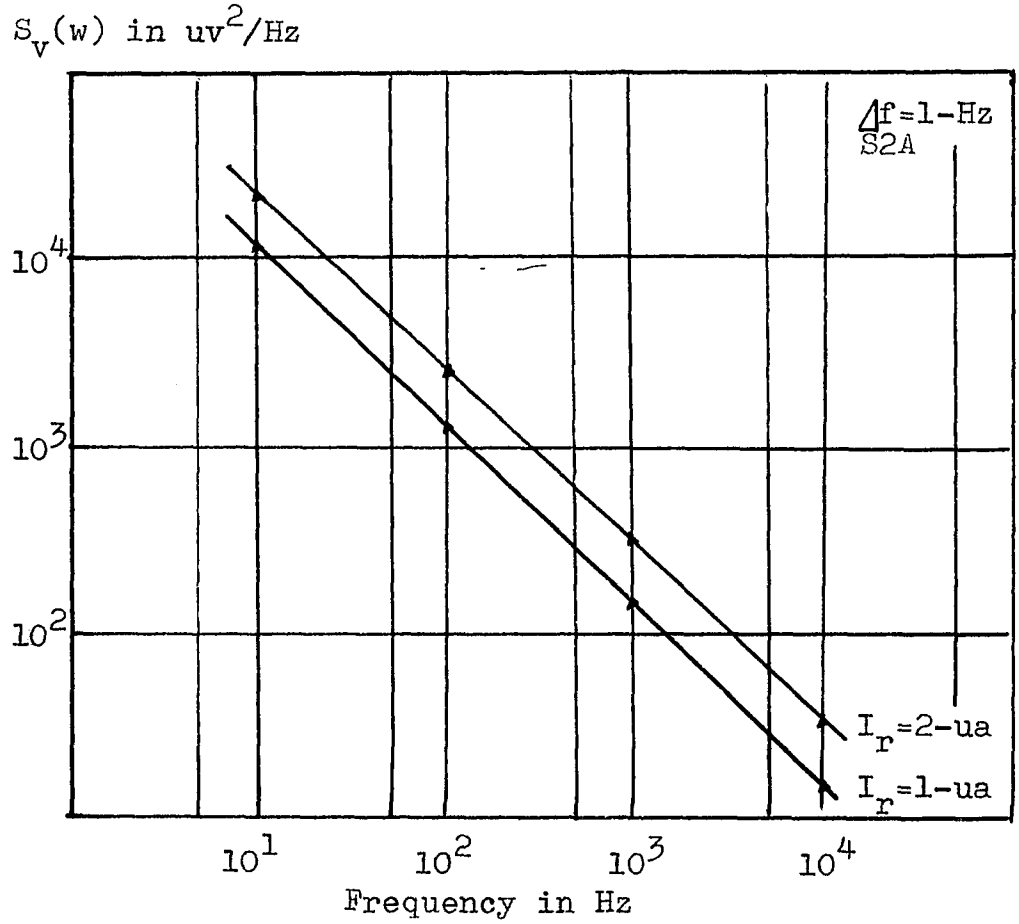

Fig. 2-4 A typical 1/f-noise found in S2A rectifier (two amperes rated diffused silicon rectifier). The inverse-proportionality does not hold under avalanche breakdown condition. See Fig. 4-1.

to be inversely proportional to frequency over a range of 10-Hz to more than 10-kHz for the tested unit.

CHAPTER 3

SUMMARY OF p-n JUNCTION IMPEDANCE UNDER THE AVALANCHE BREAKDOWN

3.1 Introduction

The small-signal a-c impedance of a p-n junction under the avalanche breakdown condition, Z(jw), plays a significant role in the derivation of the noise-voltage spectral density. Z(jw) has been derived by Reed,[35] Gilden and Hine,[10] Fisher,[7] and Misawa.[24] Their final formulas for Z(jw) are somewhat different depending on the approximations they have employed. Fisher's analysis is an improvement of Reed's model, and sufficiently realistic to predict most of the small signal characteristics shown by the computer analysis of Misawa. The final formulas of Gilden and Hine's model and Fisher's model will be presented in Section 3.2 and Section 3.3 respectively. It will be shown that their work is identical when frequency is low. Finally, the low-frequency impedance model as a combination of the junction capacitance and current-dependent junction conductance will be presented in Section 3-4.

3.2 Gilden and Hine's Impedance Model[10]

In their model, the space-charge wave approach has been used in the analysis leading directly to a simple equivalent circuit and a general expression for the small signal a-c impedance which includes the significant design and operating parameters. The assumption used in their derivation are:

(1) The n-region resistivity is much higher than the p-region resistivity, so that the depletion layer is spread mainly into the n-region. This provides a highly unsymmetrical p-n junction and the electrical field is linear from x=0 to x=W_n where W_n is approximately the length of depletion layer under the assumption (Refer to Fig. 3-1),

(2) The reverse current consists mainly of minority holes that diffuse from the n-region to p-region through the depletion layer,

(3) Actual carrier multiplication occurs in a thin portion of depletion layer rather than across the entire layer. This assumption is necessary becuase the minority carriers in the n-region, which are holes, have to drift some finite length, l_d, before they encounter a sufficiently large electric field to start carrier multiplication. The depletion layer is subdivided into l_d and l_a which may be called the drift zone and the avalanche zone respectively.

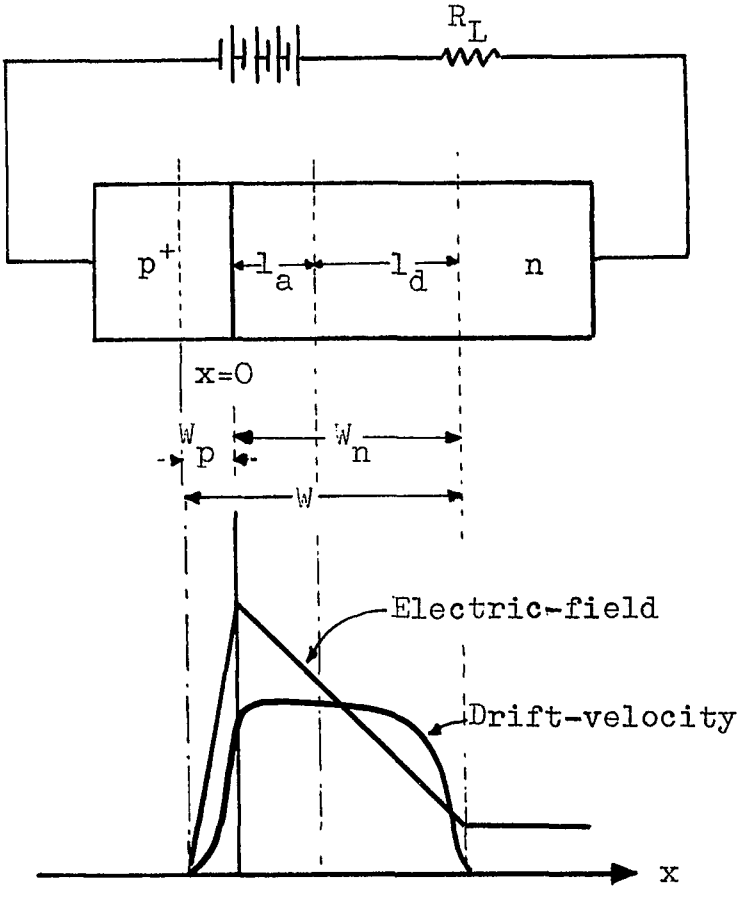

Fig. 3-1 Junction configuration investigated by Gilden and Hines, and Fisher in deriving p-n junction impedance, Z(jw), under the breakdown mode.

With these assumptions, Gilden and Hine have obtained a formula for the impedance of a p-n junction under the avalanche breakdown condition as follows:

$$Z(jw) = R_s + \frac{l_d^2}{2v_d \mathcal{G} A}\left\{\frac{1}{1-\frac{w^2}{w_a^2}}\right\}\left\{\frac{(1-\cos\theta)}{\frac{\theta^2}{2}}\right\} + \frac{1}{jwC_j}\left\{(1-\theta^{-1}\sin\theta)+\frac{\theta^{-1}\sin\theta+(l_a/l_d)}{1-\frac{w_a^2}{w^2}}\right\} \qquad (3\text{-}1)^*$$

where

$w=2\pi f$

R_s is a parasitic series resistance of inactive zone.

l_a is the width of avalanche zone.

l_d is the width of drift zone.

$W_n=l_a+l_d$ is the width of n-side depletion layer.

v_d is the saturation drift velocity.

$\mathcal{G}$ is the dielectric constant of depletion layer.

A is the area of p-n junction.

$w_a=2\bar{u}_i l_a \bar{I}/\mathcal{G}A\bar{t}_a$ is the avalanche frequency.

$\bar{u}_i$ is the average ionization coefficient (assumed equal for holes and electrons).

$\bar{t}_a$ is the transit time at avalanche zone.

---

* This is a correct version. Gilden and Hine's original Eq.(19) contains an error, apparently typographical.

$\bar{I}_o$ is the breakdown current.

$\theta = w\bar{t}_d$ is the transit angle.

C_j is the junction capacitance.

Eq. (3-1) can be further simplified for the small tansition angle θ* Noticing $2(1-\cos\theta)/\theta^2$ are approximated by one for values of θ less than $\frac{1}{4}\pi$, i.e., w less than $\frac{1}{4}\pi v_d/l_d$, we obtain

$$Z(jw) = R_s + \frac{l_d^2}{v_d \epsilon A}\left\{\frac{1}{1-\frac{w^2}{w_a^2}}\right\} + \frac{1}{jwC_j}\left\{\frac{1}{1-\frac{w_a^2}{w^2}}\right\} \qquad (3\text{-}2)$$

where $C_j = \epsilon A/(l_d+l_a)$, the depletion layer capacitance. The last term is reactive and corresponds to a parallel resonant circuit which includes the diode capacitance and shunt inductance. The second term is an active resistance which becomes negative for $w>w_a$. The first term is a parasitic series resistance of the n-region.

---

* In their report "w_a" is $2\pi(7 \text{ to } 20)\times10^9$ radians/sec. With n-type material of approximately 0.2 ohms-cm resistivity, and under reverse bias on the order of 30-40 volts, a depletion layer is found to be order of 1-micron thick, and $\bar{t}_d > 1.2\times10^{-11}$ sec.

3.3 Fisher's Impedance Model[7]

In his model, unequal electron and hole ionization rates and saturation drift velocities are considered. His final result for the impedance expression is, again with reference to Fig. 3-1,

$$Z(jw) = R_s + \frac{1}{jwC_j}\left\{1 - \frac{(W_p/W)F(w\bar{t}_p)+(W_n/W)F(w\bar{t}_n)}{1-\frac{w^2}{w_a^2}}\right\} \tag{3-3}$$

where

W is the width of depletion layer.

W_p is the width of p-side depletion layer.

W_n is the width of n-side depletion layer.

C_j is the junction capacitance.

$F(w\bar{t}_p)=\theta_p^{-1}\sin\theta_p - j\theta_p^{-1}(1-\cos\theta_p)$

$F(w\bar{t}_n)=\theta_n^{-1}\sin\theta_n - j\theta_n^{-1}(1-\cos\theta_n)$

w_a is the avalanche frequency.

R_s is a parasitic series resistance of inactive zone.

Eq. (3-3) can be further simplified for the small transit angles θ_p and θ_n, noticing $F(w\bar{t}_p)=1-\frac{1}{2}j\theta_p$ and $F(w\bar{t}_n)=1-\frac{1}{2}j\theta_n$,

$$Z(jw) = R_s + \frac{1}{jwC_j}\left[1 - \frac{1-jw\left\{(W_p/W)\frac{1}{2}\bar{t}_p+(W_n/W)\frac{1}{2}t_n\right\}}{1-\frac{w^2}{w_a^2}}\right] \tag{3-4}$$

3.4 Low-frequency Approximation of p-n Junction Impedance Under Avalanche Breakdown Condition

Although the final results of a p-n junction impedancedance under the avalanche breakdown condition derived by Gilden and Hine appear to be different from those of Fisher, the differences are due to the approximations employed. At sufficiently low-frequencies ($w \ll w_a$), they are essentially identical and explain experimentally observed small-signal a-c impedance behavior. Eqs. (3-2) and (3-3) are reduced respectively as the following:

$$Z(jw)_{\text{low-frequency}} \approx \frac{l_d^2}{2v_d \mathcal{C} A} \approx \frac{l_d V_b}{2v_d \bar{t}_d \bar{I}_o} \qquad (3\text{-}5)$$

(Gilden and Hine's model)

$$Z(jw)_{\text{low-frequency}} \approx \frac{W_n \bar{t}_n}{2WC_j} \qquad (3\text{-}6)$$

(Fisher's model)

Noticing $C_j = \mathcal{C}A/l_d = \bar{I}_o \bar{t}_n / V_b$, and $W_n = W$ (this is the case when the p-side is highly doped compared with the n-side), one can see that Eq. (3-5) and Eq. (3-6) are almost identical. The author will use the impedance model described in Eq.(3-5) when deriving the noise-voltage spectral density $S_v(w)$ in Chapter 4.

CHAPTER 4

NOISE-VOLTAGE SPECTRAL DENSITY IN p-n JUNCTIONS UNDER UNIFORM AVALANCHE BREAKDOWN

4.1 Introduction

Existing noise theories for thermal, shot, and 1/f noises which have been reviewed briefly in Chapter 2 fail to explain the drastic transition of the noise-voltage spectral density, $S_v(w)$, around avalanche breakdown knee. According to the author's experiments, the noise-voltage spectral density observed in a p-n junction under the avalanche breakdown condition tends to be "white" (all the way down to 10-Hz and up to 100-kHz) as reverse breakdown current increases. This is shown in Fig. 4-1. Furthermore, $S_v(w)$ is approximately inversely proportional to breakdown current after reaching its peak, as shown in Figs. 4-9 through 4-15.

These facts are obviously contradictory to the shot-noise or 1/f-noise type spectral density. To make the problem more complicated, some p-n junctions display one or more rather peculiar multiple peaks of spectral density as shown in Figs. 4-10 and 4-11.

The purpose of this chapter is to investigate the noise-voltage spectral density found in a p-n junction

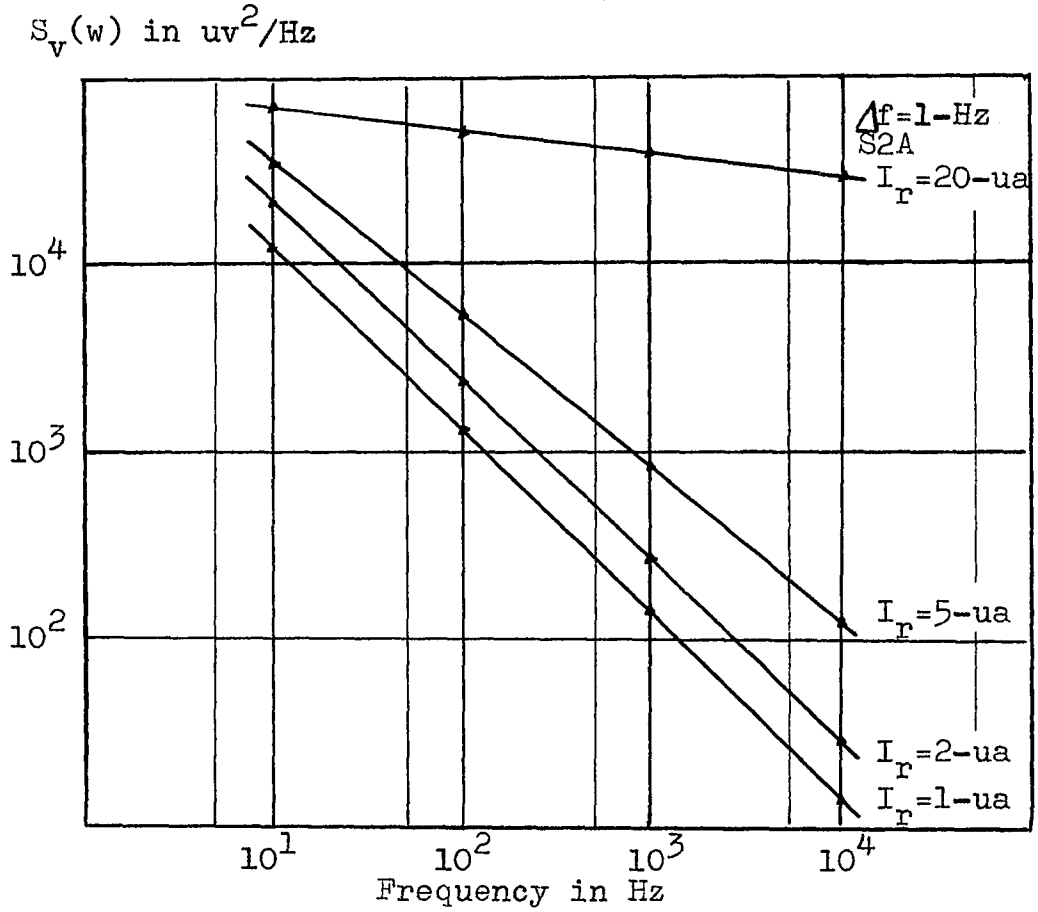

Fig. 4-1 $S_v(w)$ tends toward "white" as I_r increases. This fact indicates that new noise generating mechanism may be involved over 1/f-noise. Haitz (Ref.14,15) also reported the transition of $S_v(w)$.

under uniform breakdown condition. The junction will be assumed to be microplasma free*.

In chapter 1, we have stated that for the linear system

$$S_v(w) = H(jw)H^*(jw)S_i(w) \qquad (4\text{-}1)$$

where $S_i(w)$ is the noise-current spectral density which represents the noise generating mechanism in a p-n junction under given bias condition, and given junction configuration. $H(jw)$ is a transfer characteristic which consists of the junction impedance, and external circuit including the noise measuring system. $S_v(w)$ is than the noise-voltage spectral density which may be observed experimentally. Accordingly, our aim is to determine $S_i(w)$ and $H(jw)$ under the avalanche breakdown condition. $S_i(w)$ will be derived in Section 4.2 using the Wiener-Khintchine theorem as well as Carlson's theorem. It has been found that the probability distribution, and the mean-square of the number of carriers emerging from the carrier multiplication zone play a significant role in the derivation of $S_i(w)$. These stochastic processes will be analyzed in Section 4.3. Having the analytical expressions

---

* The multi-channel effect due to the microplasmic breakdown path will be investigated in Chapter 5 to explain multiple peaks phenomenon of $S_v(w)$.

of $S_i(w)$ and $H(jw)$, the final object $S_v(w)$ will be computed by the linear operation given by Eq. (4-1).

The theoretical result in this chapter can explain the noise-voltage spectral density commonly found in the majority of p-n junctions. Some units have, however, shown significant discrepancy from theoretical prediction with respect to the behavior of $S_v(w)$, and this will be discussed in detail in Chapter 5.

4.2 Current-Spectral Density of Noise Source in the Multiplication Zone

We now seek an expression for the noise-current spectral density of the noise source in the multiplication zone, $S_i(w)$. Four factors are suspected to cause the noise. They are:

(1) The number of carriers, K, entering the multiplication zone during the time interval of (-T,+T) is a random variable. If we consider $\overline{k}=E(K)/2T$ as the average number of carriers entering the multiplication zone during the time interval of 2T, the probability distribution of K for given 2T may be expressed by the Poisson distribution[6]

$$p(K,2T) = \frac{(\overline{k}\cdot 2T)^K}{K!} \text{EXP}(-\overline{k}\cdot 2T) \qquad (4\text{-}2)$$

The assumption that $\overline{k}$ is constant for all time intervals

means that the random process in question is stationary,

(2) Entry times of primary carriers (minority holes in n-region) into the multiplication zone, t_k, are a random variable. If the number of the primary carriers entering the multiplication zone during the time interval of 2T is Poisson type as stated in Eq. (4-2), it can be shown* that the entry times have an uniform distribution

$$p(t_k) = \begin{cases} \frac{1}{2T} & \text{when } -T \le t_k \le +T \\ 0 & \text{otherwise} \end{cases} \qquad (4\text{-}3)$$

(3) A primary carrier having entered the multiplication zone at time t_k produces an avalanche with a total number of carriers, M_k, emerging from the multiplication zone. Although the average of M_k, $E(M_k)$, will be a constant in a steady avalanche, not all primary carriers in the multiplication zone encounter the same number of ionization events. What we know is that M_k will be an integer having the value of 0, 1, 2, ..., m. If we can assume that the probability of ionization by a given primary carrier is a constant (again we are assuming a stationary random process), then $p(M_k)$ also is a Poisson type. We will, however, proceed to determine $S_i(w)$ without specifying $p(M_k)$ for the time being (The determination of

---

* Appendix C. $p(1,t_1;1,t_2;.1,t_K/K,2T)=\frac{K!}{(2T)^K}\prod_{k=1}^{K}(2T)_k$.

$p(M_k)$ is one of the major problems in deriving $S_i(w)$, and will be discussed in detail in Section 4.3),

(4) The carrier transit times, t_{as}, as well as the ionization time delays, t_{ds}, each associated with M_k random ionization events, have statistical distribution (See Fig. 4-2).

In order to study these rather complicated random processes, let us define $i_o(t)$ as the current pulse observed at the end of the multiplication zone (x=0 in Fig. 3-1) due to a primary carrier which enters the multiplication zone at time t=0 without encountering any ionization (M_k=1). This $i_o(t)$ may be obtained from the Poisson equation

$$\nabla^2 V = -\frac{\rho}{\epsilon} \qquad (4\text{-}4)$$

where ϵ is the permittivity, ρ is the space-charge density of the depletion layer, and V is the potential at the distance from x=0. Under the avalanche condition, the electric field is high enough that we may neglect the effect of space-charge* The Laplace equation then

---

* This may be an over simplification. Strictly speaking $\nabla^2 V=-qN_d/\epsilon$ and $V=-qN_d x^2/2\epsilon$ for the step-junction, and $\nabla^2 V=-qax$ and $V=qax^3/6\epsilon$ for the graded-junction where N_d is the donor impurity concetration, and "a" is the grade-constant in atoms/cm^4. The solution of Laplace equation gives us $V=V_j x/d$ where V_j is the voltage drop across

the junction depletion layer whose width is d. This simplification was, however, necessary to obtain rather simple form of $i_o(t)$ to compute the autocorrelation function later.

---

applies, and the current pulse induced at the external circuit due to the motion of a carrier is found to be*

$$i_o(t) = \begin{cases} \frac{2q}{t_a^2}t & \text{for } 0 \le t \le t_a \\ 0 & \text{otherwise} \end{cases} \qquad (4\text{-}5)$$

where $t_a=(2m/qV_j)^{1/2}d$ is the carrier transit time across the depletion layer. "m" is the effective mass of the carrier, and V_j is the voltage drop across the depletion layer.

The multiplication process due to random ionization which may be characterized by the statistical distribution of the carrier transit times, t_{a1}, t_{a2},....., t_{aM_k} each associated with the ionization time delays, t_{d1}, t_{d2},....., t_{dM_k} for the given ionization events M_k is an (M_k^2+1)-fold random process. This (M_k^2+1)-fold joint-probability, $p(t_{d1},t_{a1};.....;t_{dM_k},t_{aM_k}/M_k)$ is not determined at present. M_k random ionizations due to a primary carrier will produce a current pulse train, $i_{M_k}(t)$, at the external circuit as the following:

---

* Appendix D

$$i_{M_k}(t) = \sum_{s=1}^{M_k} \frac{2q}{t_{as}^2}(t-t_{ds})G(t_{ds},t_{ds}+t_{as}) \qquad (4\text{-}6)$$

where $G(t_{ds},t_{ds}+t_{as})$ is the Gate-function. $i_{M_k}(t)$ is illustrated in Fig. 4-2. In spite of its appearence, $i_{M_k}(t)$ expressed in Eq. (4-6) may not be evaluated* unless (M_k^2+1)-fold joint-probability, $p(t_{d1},t_{a1};..;t_{dM_k},t_{aM_k}/M_k)$, is specified. To overcome this difficulty, the author will approximate $i_{M_k}(t)$ as the following:

$$i_{M_k}(t) = M_k i(t) \qquad (4\text{-}7)$$

where i(t) is identical to $i_o(t)$ except t_a in Eq. (4-5) should be replaced by the average of carrier transit times, $E(t_{as})$ or $\bar{t}_{as}$**. Notice that we are essentially

---

* With some constraint, $i_{M_k}(t)$ may be evaluated assuming the probability distributions $p(t_{ds}/M_k)$ and $p(t_{as}/M_k)$ are statistically independent. See Appendix E.

** Recent study by Ryder[36] and Phillips[33] indicates that the carrier drift velocity reaches a finite saturation velocity approximately 8×10^6 cm/sec if applied electric field is greater than 1.5×10^4 volts/cm for the n-type silicon at 300 ^oK as shown in Fig. 4-4. In this case it can be assumed that $t_{a1}>t_{a2}>t_{a3}\ ...\ >t_{aM_k}$ due to a finite saturation velocity, and height of current train due to multiplication process should increases since the area of each current pulse should be same as q, the electronic charge, 1.6×10^{-16} coulomb.

** The author wishes to acknowledge a suggestion from Dr. Y.W. Lee of Massachusetts Institute of Technology.

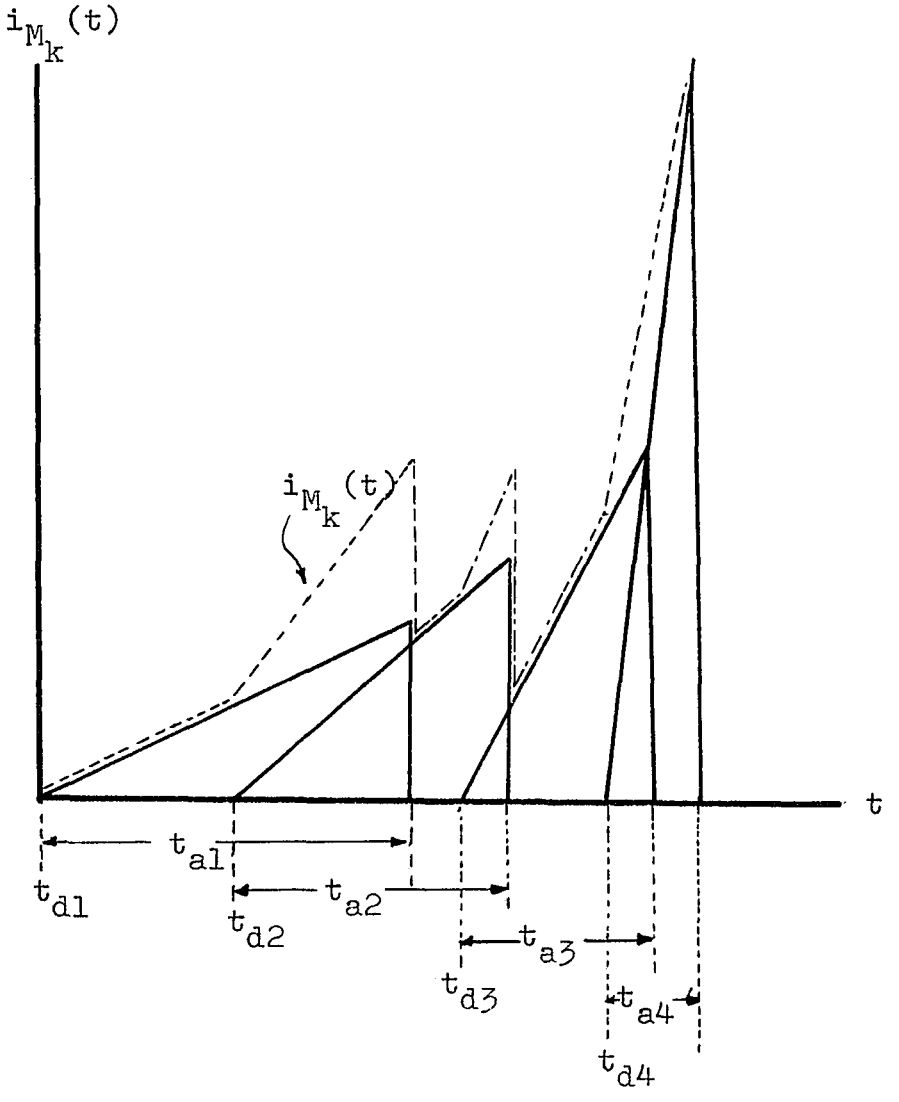

Fig. 4-2 Illustration for the construction of $i_{M_k}(t)$ assuming $M_k=4$. t_{as} are the carrier transit times, and t_{ds} are the ionization time delays.

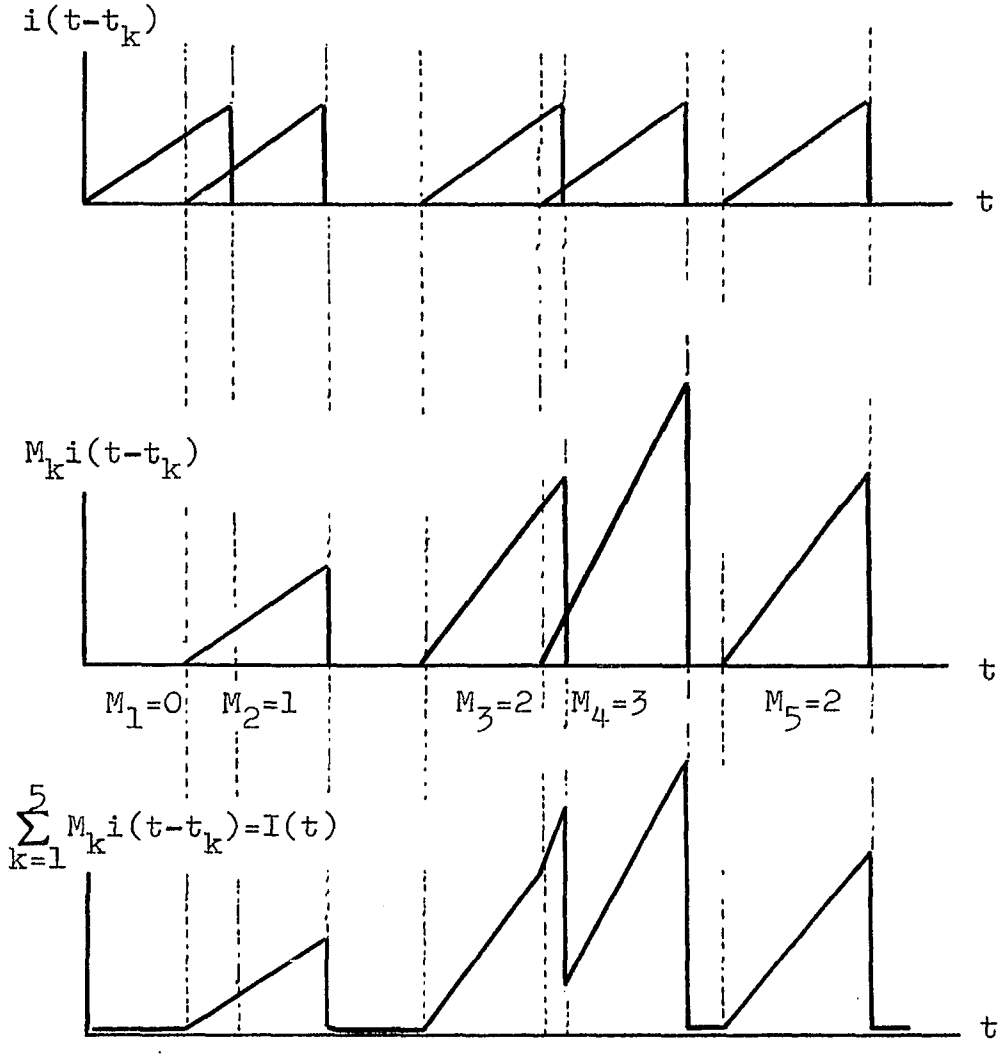

Fig. 4-3 Illustration for the construction of $I(t)$ as a summation of $M_k i(t-t_k)$ assuming $k=5$, $M_1=0$, $M_2=1$, $M_3=2$, $M_4=3$, and $M_5=2$.

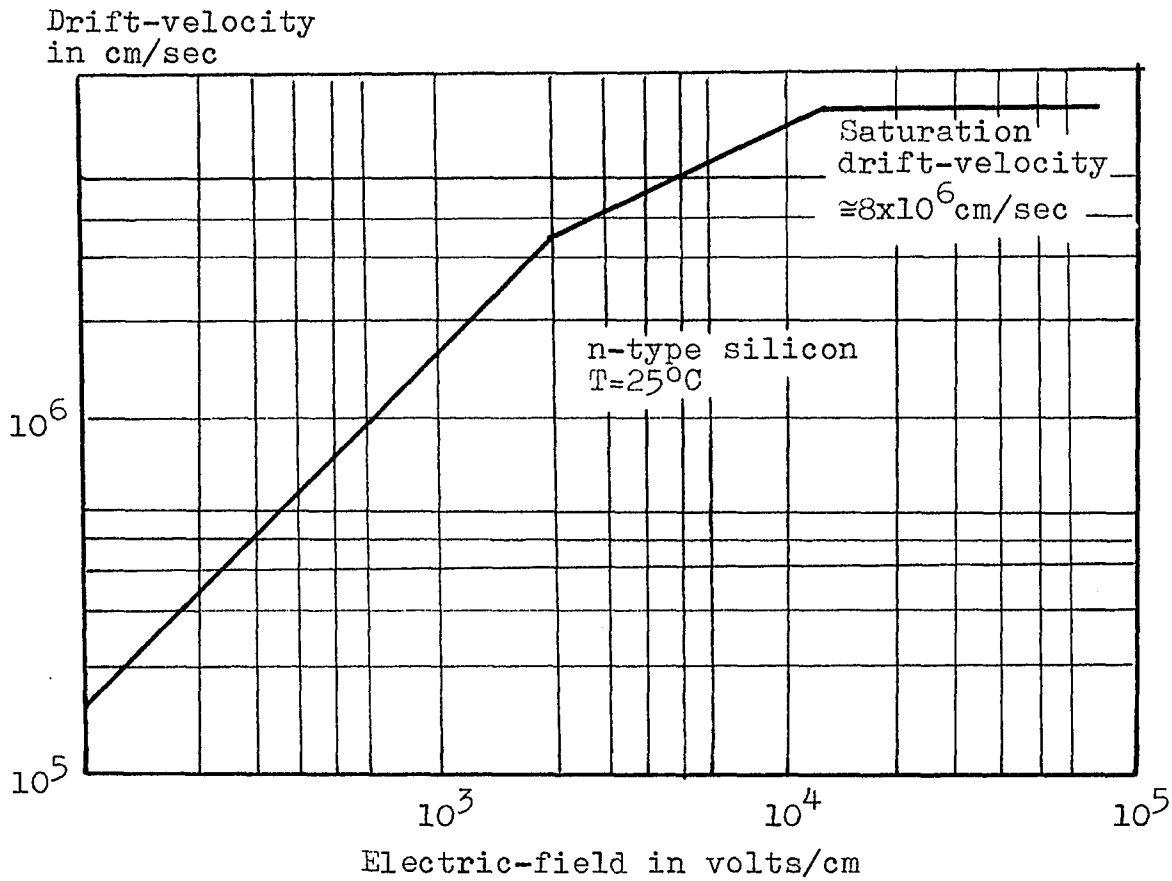

Fig. 4-4 Drift-velocity as a function of electric-field (After E.J. Ryder, Ref. 36).

approximating M_k current pulses by an equivalent triangular pulse.

With these approximations, we now can write for the multiplication current, I(t), due to the primary carriers successively entering the multiplication zone at the entry times, t_1, t_2,....,t_k as the following:

$$I(t) = \sum_{k=1}^{K} M_k i(t-t_k) \qquad (4-8)$$

where K is the number of carriers entering the multiplication zone during the time interval of (-T,+T). I(t) as a summation of the current pulses $i(t-t_k)$ associated with the multiplication factor M_k is illustrated in Fig 4.3.

The noise-current spectral density, $S_i(w)$, will be obtained from the Wiener-Khintchine theorem once the autocorrelation function of the multiplication current I(t) expressed in Eq. (4-8) is known. From the definition of the autocorrelation function, R(s), we have

$$R(s) = E\left[\sum_{k=1}^{K} M_k i(t-t_k) \sum_{j=1}^{K} M_j i(t-t_j+s) \right] \qquad (4-9)$$

Since M_k and t_k are statistically independent random variables

$$R(s) = E\left[\sum_{k=1}^{K} \sum_{j=1}^{K} E(M_k \cdot M_j) \cdot i(t-t_k) i(t-t_j+s) \right] \qquad (4-10)$$

Furthermore, we have the relation

$$E(M_k \cdot M_j) = E(M_k^2) + E(M_k \cdot M_j)_{k \neq j} \tag{4-11}$$

Substituting the above relation into Eq. (4-10),

$$R(s) = E(M_k^2) \cdot E\left[\sum_{k=1}^{K} i(t-t_k)i(t-t_k+s)\right] + E(M_k \cdot M_j)_{k \neq j} \cdot E\left[\sum_{\substack{k=1 \\ (k \neq j)}}^{K} \sum_{j=1}^{K} i(t-t_k)i(t-t_j+s)\right] \tag{4-12}$$

By adding and subtracting $E(M_k \cdot M_j)_{k \neq j}$ times $E\left[\sum_{k=1}^{K} i(t-t_k)i(t-t_k+s)\right]$ to Eq. (4-12),

$$R(s) = \left\{E(M_k^2) - E(M_k \cdot M_j)_{k \neq j}\right\} \cdot E\left[\sum_{k=1}^{K} i(t-t_k)i(t-t_k+s)\right] + E(M_k \cdot M_j) \cdot E\left[\sum_{k=1}^{K} \sum_{\substack{j=1 \\ \text{(including } k=j\text{)}}}^{K} i(t-t_k)i(t-t_j+s)\right] \tag{4-13}$$

To evaluate R(s) term by term, let us define

$$R(s) \equiv \overline{A} \cdot B(s) + \overline{C} \cdot D(s) \tag{4-14}$$

where

$$\overline{A} \equiv E(M_k^2) - E(M_k \cdot M_j)_{k \neq j}$$

$$\overline{C} \equiv E(M_k \cdot M_j)_{k \neq j}$$

$$B(s) \equiv E\left[\sum_{k=1}^{K} i(t-t_k)i(t-t_k+s)\right]$$

$$D(s) \equiv E\left[\sum_{k=1}^{K}\sum_{j=1}^{K} i(t-t_k)i(t-t_k+s)\right] \qquad (4\text{-}15)$$

B(s) is now a (K+1)-fold random variable consisting of K entry times, t_k, and K itself. Thus

$$\begin{aligned} B(s) &= E\left[\sum_{k=1}^{K} i(t-t_k)i(t-t_k+s)\right] \\ &= \int_{-\infty}^{+\infty}\int_{-\infty}^{+\infty}\cdots\int_{-\infty}^{+\infty}\sum_{k=1}^{K} i(t-t_k)i(t-t_k+s)\cdot p(t_1,t_2,..,t_k,K) \\ &\qquad \cdot dt_1 dt_2 \ldots dt_k dK \\ &= \int_{-\infty}^{+\infty}\int_{-\infty}^{+\infty}\cdots\int_{-\infty}^{+\infty}\sum_{k=1}^{K} i(t-t_k)i(t-t_k+s)\cdot p(t_1,t_2,..,t_k/K)\cdot p(K) \\ &\qquad \cdot dK dt_1 dt_2 \ldots dt_k \\ &= \int_{-\infty}^{+\infty} p(K)dK \int_{-\infty}^{+\infty}\cdots\int_{-\infty}^{+\infty}\sum_{k=1}^{K} i(t-t_k)i(t-t_k+s)\cdot p(t_1)\cdot p(t_2)\cdot\cdot p(t_k) \\ &\qquad \cdot dt_1 dt_2 \ldots dt_k \end{aligned} \qquad (4\text{-}16)$$

We have assumed an uniform distribution for the entry times, t_k, as stated in Eq. (4-3). Thus B(s) can be further simplified as the following:

$$\begin{aligned} B(s) &= \int_{-\infty}^{+\infty} p(K)dK\left[\sum_{k=1}^{K}\int_{-T}^{+T}\frac{dt_1}{2T}\int_{-T}^{+T}\cdots\cdots\int_{-T}^{+T}\frac{dt_k}{2T}\, i(t-t_k)i(t-t_k+s)\right] \\ &= \int_{-\infty}^{+\infty} p(K)dK\left[\sum_{k=1}^{K}\frac{1}{2T}\int_{-T}^{+T} i(t-t_k)dt_k\right] \end{aligned} \qquad (4\text{-}17)$$

All current pulses due to single carriers have the same pulse shape for various t_k if $M_k=1$, i.e.,

$$i(t-t_k)i(t-t_k+s) = i(t)i(t+s) \quad \ldots \quad \text{for all } t_k \tag{4-18}$$

Substituting the above relation into Eq. (4-17), we have

$$B(s) = \int_{-\infty}^{+\infty} p(K)dK \frac{1}{2T} \cdot K \cdot \int_{-\infty}^{+\infty} i(t)i(t+s)dt$$

$$= \frac{E(K)}{2T} \int_{-\infty}^{+\infty} i(t)i(t+s)dt \tag{4-19}$$

and

$$D(s) = E\left[\sum_{k=1}^{K}\sum_{j=1}^{K} i(t-t_k)i(t-t_k+s)\right]$$

$$= \int_{-\infty}^{+\infty} \int_{-\infty}^{+\infty}\left[\sum_{k=1}^{K}\sum_{j=1}^{K} i(t-t_k)i(t-t_j+s)\right]$$

$$\cdot p(t_1,t_2,t_3,\ldots,t_k,K)dt_1dt_2dt_3\ldots dt_kdK \tag{4-20}$$

as done before in deriving Eqs. (4-16) and (4-17), the (K+1)-fold joint probability density may be decomposed into product form because of the statistical independence of K and t_k:

$$D(s) = \int_{-\infty}^{+\infty} p(K)dK\left[\sum_{k=1}^{K}\sum_{j=1}^{K} \int_{-T}^{+T}\frac{dt_1}{2T}\int_{-T}^{+T}\ldots\int_{-T}^{+T}\frac{dt_k}{2T} i(t-t_k)i(t-t_j)\right] \tag{4-21}$$

The K^2 terms of the double summation in this equation may be formed into two groups: the K terms for which k=j and

(K^2-K) terms for which $k \neq j$.

When $k=j$, the K-fold integral over the various t_k becomes

$$K\int_{-T}^{+T}\frac{dt_1}{2T}\int_{-T}^{+T}\cdots\cdots\int_{-T}^{+T}\frac{dt_k}{2T}\, i(t-t_k)i(t-t_k+s)$$

$$= \frac{1}{2T}\int_{-\infty}^{+\infty} i(t)i(t+s)dt \qquad (4\text{-}22)$$

When $k \neq j$,

$$(K^2-K)\int_{-T}^{+T}\frac{dt_1}{2T}\int_{-T}^{+T}\cdots\cdots\int_{-T}^{+T}\frac{dt_k}{2T}\, i(t-t_k)i(t-t_j+s)$$

$$= \frac{(K^2-K)}{2T}\int_{-T}^{+T} i(t-t_k)dt_k \frac{1}{2T}\int_{-T}^{+T} i(t-t_j+s)dt_j$$

$$= (K^2-K)\left[\frac{1}{2T}\int_{-T}^{+T} i(t-t_k)dt\right]^2 = (K^2-K)\left(\frac{q}{2T}\right)^2 \qquad (4\text{-}23)$$

since the area under the triangular current pulse expressed by Eq. (4-5) is q. Substituting Eqs. (4-19) and (4-21) into Eq. (4-14), we have

$$R(s) = \left\{E(M_k^2)-E(M_k\cdot M_j)_{k\neq j}\right\}\int_{-\infty}^{+\infty}\frac{E(K)}{2T}\, i(t)i(t+s)dt$$

$$+ E(M_k\cdot M_j)_{k\neq j}\left[\frac{E(K)}{2T}\int_{-\infty}^{+\infty} i(t)i(t+s)dt + E(K^2-K)\left(\frac{q}{2T}\right)^2\right]$$

$$= E(M_k^2)\frac{E(K)}{2T}\int_{-\infty}^{+\infty} i(t)i(t+s)dt + E(M_k\cdot M_j)_{k\neq j}E(K^2-K)\left(\frac{q}{2T}\right)^2$$

(4-24)

Since $i(t)$ is $2qt/\bar{t}_{as}^2$ when $0 \le t \le \bar{t}_{as}$, and zero otherwise,

$$\int_{-\infty}^{+\infty} i(t)i(t+s)dt = \frac{4q^2}{\bar{t}_{as}^4}\int_0^{\bar{t}_{as}-s} t(t+s)dt$$

$$= \frac{4q^2}{\bar{t}_{as}^4}\left\{\frac{\bar{t}_{as}^3}{3} - \frac{\bar{t}_{as}^2}{2}s + \frac{1}{6}s^3\right\} \qquad (4\text{-}25)$$

Substituting Eq. (4-25) into Eq. (4-24), we have

$$R(s) = E(M_k^2)\frac{E(K)}{2\bar{T}}\frac{4q^2}{\bar{t}_{as}^4}\left\{\frac{\bar{t}_{as}^3}{3} - \frac{\bar{t}_{as}^2}{2}s + \frac{1}{6}s^3\right\}$$

$$+\left\{E(M_k \cdot M_j)_{k\neq j}E(K^2-K)\left(\frac{q}{2\bar{T}}\right)^2\right\} \qquad (4\text{-}26)$$

Now the noise-current spectral density due to the multiplication process, $S_i(w)$, can be obtained by taking the Fourier-transform of the autocorrelation function, $R(s)$ expressed in Eq. (4-26) by the Wiener-Khintchine theorem. The result is*

$$S_i(w) = 2\int_0^{\infty} R(s)\cos(ws)ds$$

$$= E(M_k^2)\frac{E(K)}{2\bar{T}}\frac{4q^2}{(w\bar{t}_{as})^4}\left\{(w\bar{t}_{as})^2 + 2(1-\cos w\bar{t}_{as} - w\bar{t}_{as}\sin w\bar{t}_{as})\right\}$$

$$+\left\{E(M_k \cdot M_j)_{k\neq j}E(K^2-K)\left(\frac{q}{2\bar{T}}\right)^2\right\}\delta(w) \qquad (4\text{-}27)$$

---

*Appendix F.

The impulse in the second term, $\delta(w)$, is due to the average component of multiplication current. Notice the first term of Eq. (4-27) approaches $E(M_k^2)\frac{E(K)}{2T}q^2$ when $w\bar{t}_{as}$ approaches zero* Eq.(4-26) and Eq. (4-27) are plotted in Fig. 4-5 and Fig. 4-6 respectively.

As stated earlier, the average number of primary carriers entering the multiplication zone during the time interval of 2T, E(K)/2T, was considered to be constant, which assumes the random process in question is stationary. Then $E(K)q^2/2T$ is considered to be $q\bar{I}_s$ where $\bar{I}_s$ is the saturation current. The noise source whose noise-current spectral density is expressed by Eq. (4-27) is located across the p-n junction impedance, Z(jw), which has been reviewed in Chapter 3. To employ the low-frequency impedance model expressed by Eq. (3-5) or Eq. (3-6), if we restrict ourselves to the frequency range of interest 30-Hz to 100-kHz, $S_i(w)$ expressed in Eq. (4-27) may be reduced to

$$S_i(w)\Big|_{\text{low-frequency}} = E(M_k^2)q^2\bar{I}_s \qquad (4\text{-}28)$$

where $E(M_k^2)$ is the mean-square of the number of carriers emerging from the multiplication zone. This $E(M_k^2)$ will be discussed in the next section.

---

* $\lim_{x\to 0} x^{-4}\left\{x^2+2(1-\cos x-x\sin x)\right\}=\frac{1}{4}$. This is computed for x up to 10 in Table 4-1.

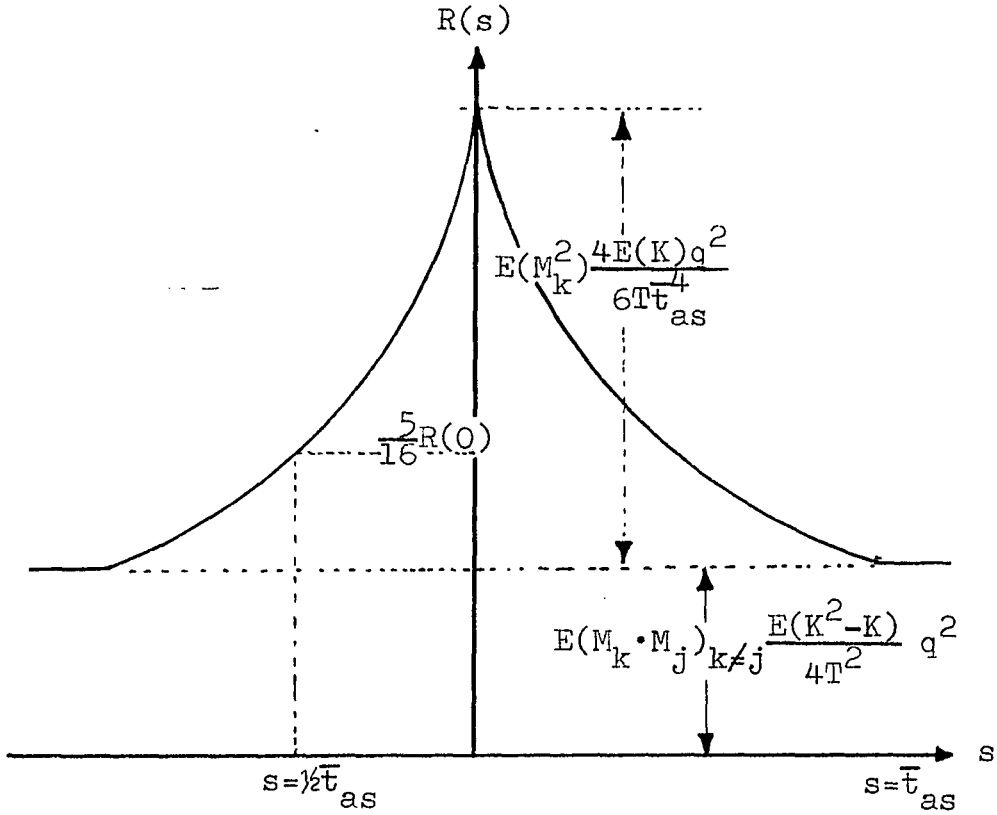

Fig. 4-5 Autocorrelation function R(s) expressed in Eq. (4-26). Notice $4q^2/3\bar{t}_{as}$ is the total area of $i^2(t)$.

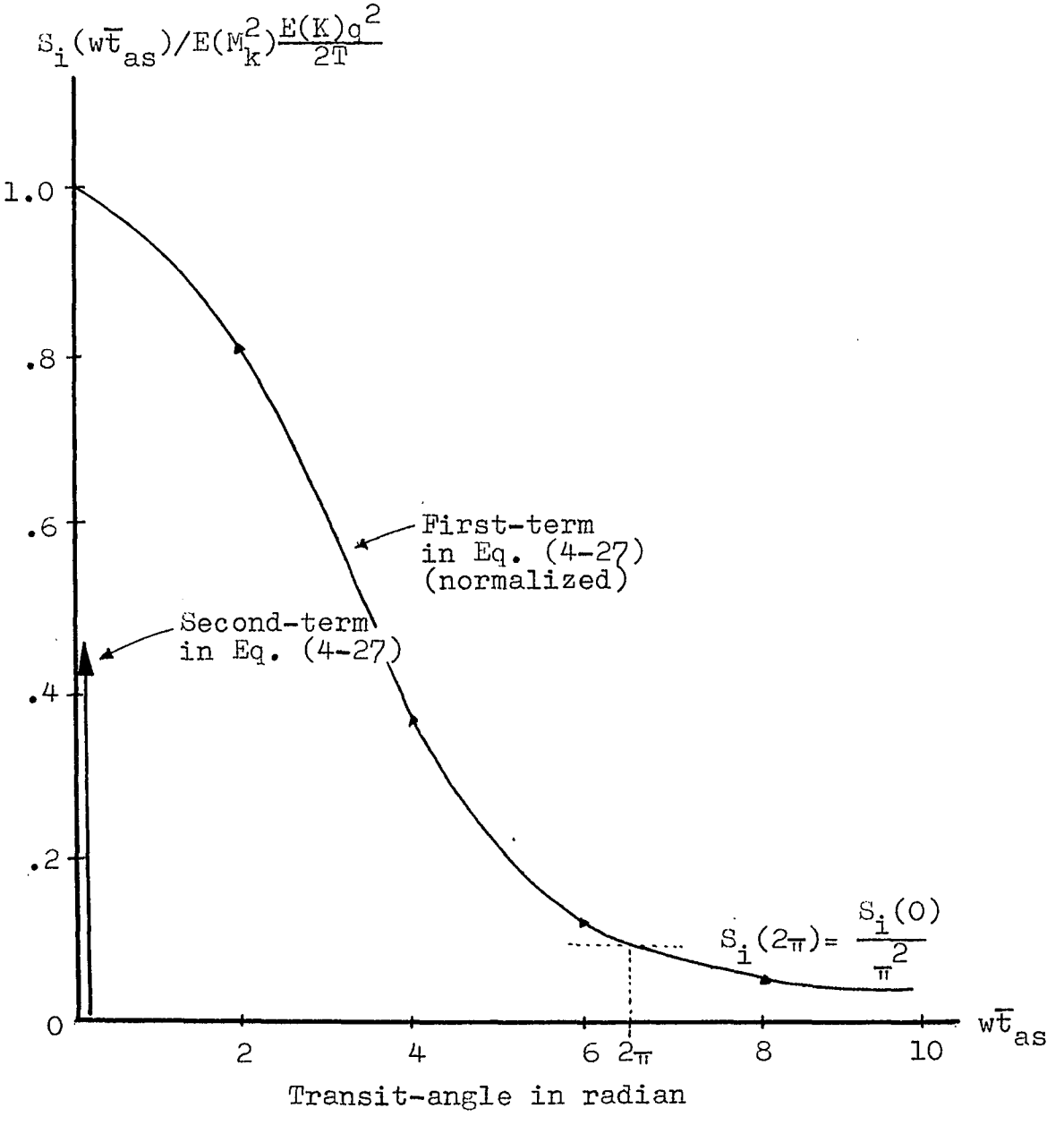

Fig. 4-6 Noise-current spectral density, $S_i(w\bar{t}_{as})$, (normalized) expressed in Eq. (4-27). Notice that the noise-current spectral density is plotted with respect to the transit-angle $w\bar{t}_{as}$, where $\bar{t}_{as}=E(t_{as})$.

Table 4-1 Computation of the first term (normalized) in Eq. (4-27)

```
      X=0.5
1     Y=4.*(X**2.+2.*(1.-COS(X)-X*SIN(X)))/X**4.
      PUNCH,X,Y
      X=X+0.5
      IF(X-15.)1,1,2
2     CONTINUE
      END
```

Transit-angle, $\overline{wt}_{as}$	$S_i(\overline{wt}_{as})$ (normalized)
.50000000	.94518581
1.0000000	.94419800
1.5000000	.87378800
2.0000000	.79827567
2.5000000	.70247617
3.0000000	.59941196
3.5000000	.49525834
4.0000000	.39628581
4.5000000	.30711987
5.0000000	.23061289
5.5000000	.16870510
6.0000000	.12169854
6.5000000	8.8505507E-02
7.0000000	6.7128672E-02
7.5000000	5.4960980E-02
8.0000000	4.9241699E-02
8.5000000	4.7415385E-02
9.0000000	4.7191074E-02
9.5000000	4.6987417E-02
10.000000	4.5823621E-02
10.500000	4.3333913E-02
11.000000	3.9639852E-02
11.500000	3.5088711E-02
12.000000	3.0322094E-02
12.500000	2.5871255E-02
13.000000	2.2164466E-02
13.500000	1.9431514E-02
14.000000	1.7692682E-02
14.500000	1.6814945E-02

4.3 Probability Distribution and the Mean-Square of the Number of Carriers Emerging from the Multiplication Zone

The calculation of $E(M_k^2)$ is rather mathematically complicated because the emergence times of individual carriers from the multiplication zone are not independent. The following assumptions will be employed to approach the problem:

(1) The multiplication carriers due to a primary carrier moving through the multiplication zone reach a finite saturation velocity which is independent of the number of ionization events,

(2) The space-charge created by the ionization does not affect the ionization coefficient,

(3) The ionization coefficients of holes and electrons are equal, and remain constant throughout the multiplication zone.

With these assumptions, each ionization event produced by a primary carrier is considered to be an independent random process. The probability that a primary carrier will produce M_k ionization events is then given by the Poisson-distribution,

$$p(M_k) = \frac{(\overline{M}_k)^{M_k}}{M_k!}\text{EXP}(-\overline{M}_k) \qquad (4\text{-}29)$$

where $\overline{M}_k$ is the average number of ionization events

produced by a primary carrier in the multiplication zone*. Once we have $p(M_k)$, $E(M_k^2)$ may be found in the usual manner**

$$E(M_k^2) = \sum_{M_k=0}^{\infty} M_k^2 p(M_k)$$

$$= \overline{M}_k^2 + \overline{M}_k = \overline{M}_k(\overline{M}_k+1) \qquad (4\text{-}30)$$

** Appendix G.

* McKay[22] has shown that $\overline{I}_o = \overline{M}_k \overline{I}_s$ where $\overline{I}_o$ is the circuit current, and $\overline{I}_s$ is the saturation current. He also has shown that

$$\overline{M}_k = \left[1 - \int_{x=0}^{x=d} u_i(E)dx \right]^{-1}$$

where $u_i(E)$ is the ionization coefficient which is a function of the electric field E. Experimental plots of $u_i(E)$ for Silicon and Germanium[33] are available, and are given by an approximation (empirical relation),

$$u_i(E) = 6.25 \times 10^{-34} E^7 \text{ cm}^{-1} \quad \text{for Germanium}$$

$$u_i(E) = 1.65 \times 10^{-24} E^5 \text{ cm}^{-1} \quad \text{for Silicon}$$

Miller[23] has given the following empirical relation for $\overline{M}_k$:

$$M_k = \frac{1}{1 - (\frac{V}{V_b})^n}$$

where V is the voltage across the multiplication zone and V_b is the breakdown voltage of a p-n junction. The values of "n" are as follows:

	n-type	p-type
Silicon	3	6
Germanium	4	2

Substituting Eq. (4-30) into Eq. (4-27), we have

$$S_i(w) = (\overline{M}_k+1)\overline{I}_o \frac{4q}{(w\overline{t}_{as})^4}\left\{(w\overline{t}_{as})^2+2(1-\cos w\overline{t}_{as}-w\overline{t}_{as}\sin w\overline{t}_{as})\right\}$$

$$+\left\{E(M_k \cdot M_j)_{k\neq j}E(K^2-K)(\frac{q}{2T})^2\delta(w)\right\} \qquad (4-31)$$

and for low-frequency range, let us say f=1-kHz,

$$S_i(w)\Big|_{\substack{w=2\pi\times10^3 \\ \text{radian}}} = (\overline{M}_k+1)q\overline{I}_o \qquad (4-32)$$

Now the noise source due to the multiplication process, whose noise-current spectral density is expressed by either Eq. (4-31) or Eq. (4-32), is located across the current-dependent junction impedance Z(w) as shon in Fig. 4-7.

$$Z(jw) = \frac{1}{jwC_j}\left\{1 - \frac{1-jw(W_p\bar{t}_p/2W + W_n\bar{t}_n/2W)}{1-\frac{w^2}{w_a^2}}\right\}$$

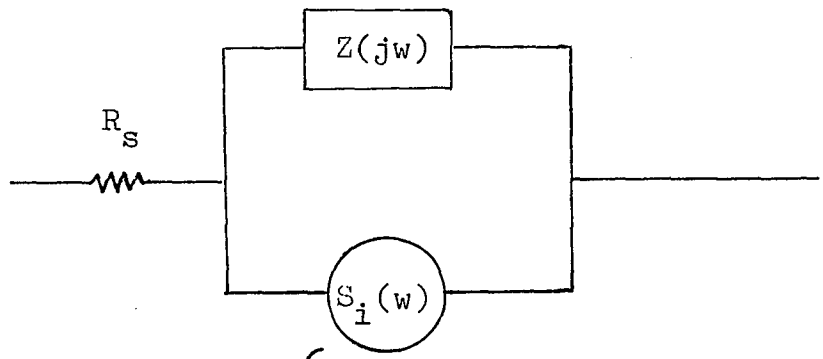

$$S_i(w) = \frac{V_b}{n(V_b-V)}\,4q\bar{I}_o\left\{\frac{(w\bar{t}_{as})^2+2(1-\cos w\bar{t}_{as}-w\bar{t}_{as}\sin w\bar{t}_{as})}{(w\bar{t}_{as})^4}\right\}$$

Fig. 4-7 Noise equivalent circuit for a p-n junction under the avalanche breakdown condition.

4.4 Determination of the Noise Voltage Spectral Density

Fig. 4-8-a shows a circuit configuration to obtain the noise-voltage spectral density, $S_v(w)$, across an external current-limiting resistor R_L. If the input impedance of the noise measuring device is large enough so that the noise current is limited only by a d-c current-limiting resistor R_L, the transfer characteristic H(jw) (in this case transfer impedance) will be given by (See Fig. 4-8-b),

$$H(jw) = \frac{Z(jw)\cdot R_L}{R_s + R_L + Z(jw)}$$

$$= \frac{Z(jw)}{1 + \frac{R_s}{R_L} + \frac{Z(jw)}{R_L}} \qquad (4\text{-}33)$$

From the practical viewpoint, it is reasonable to assume $R_L \gg R_s$, and $R_L \gg Z(jw)$, under the avalanche breakdown condition. In this case, H(jw) may be approximated by the junction impedance Z(jw). $S_v(w)$ may be interpreted as the open-circuit noise-voltage spectral density.

As we have stated earlier in Eq. (4-1), $S_v(w)$ now can be obtained from the linear operation

$$S_v(w) = H(jw)H^*(jw)S_i(w) \qquad (4\text{-}34)$$

Substituting Eq. (4-31) and Eq. (4-33) into above equation,

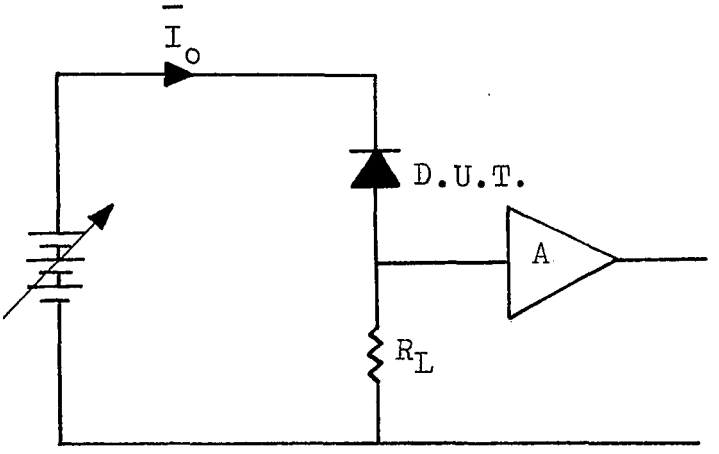

(a)

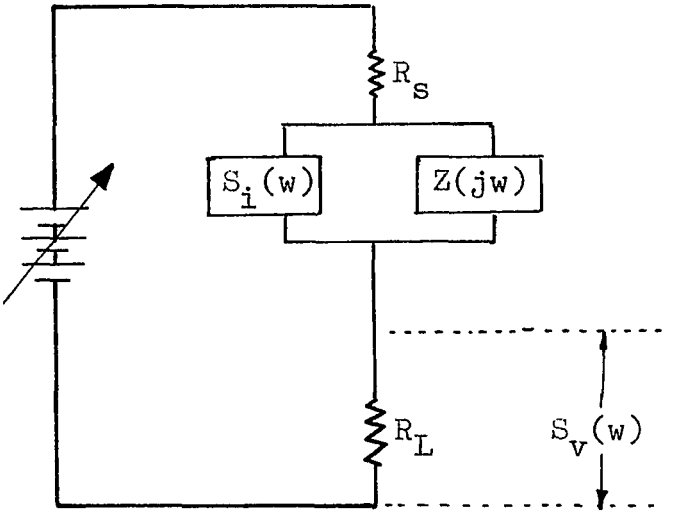

(b)

Fig. 4-8 Circuit configuration to derive $S_v(w)$. (a) Actual test set-up, (b) The p-n junction is replaced by R_s, $S_i(w)$, and $Z(jw)$.

we have complete expression for $S_v(w)$ as follows:

$$S_v(w) = \left[\frac{\left\{ 1 - \frac{1-jw\left(\frac{W_p \bar{t}_p}{2W} + \frac{W_n \bar{t}_n}{2W}\right)}{1 - \frac{w^2}{w_a^2}} \right\} \frac{1}{jwC_j}}{1+\frac{R_s}{R_L}+\frac{1}{jwC_j R_L}\left\{1- \frac{1-jw\left(\frac{W_p \bar{t}_p}{2W} + \frac{W_n \bar{t}_n}{2W}\right)}{1 - \frac{w^2}{w_a^2}}\right\}} \right]^2$$

$$\cdot \left[(\bar{M}_k+1)\bar{I}_o \frac{4q}{(w\bar{t}_{as})^4} \left\{ (w\bar{t}_{as})^2 + 2(1-\cos w\bar{t}_{as} - wt_{as}\sin w\bar{t}_{as}) \right\} \right.$$

$$\left. + E(M_k \cdot M_j)_{k\neq j} E(K^2-K)\left(\frac{q}{2\bar{T}}\right)^2 \delta(w) \right] \qquad (4\text{-}35)$$

If we restrict ourselves to the frequency range of interest, 30-Hz to 100-kHz (which wasthe range of the noise spectrum analyzer, Quan-Tech Model-303), and if we assume that $R_L \gg R_s$ and $R_L \gg Z(jw)$, we have

$$H(jw) \approx Z(jw) \approx \frac{l_d V_b}{2v_d \bar{t}_d \bar{I}_o} \qquad (4\text{-}36)$$

and

$$S_i(w) \approx (\bar{M}_k+1) q\bar{I}_o = \left\{ \frac{1}{1 - \int_o^d u_i(E)dx} + 1 \right\} q\bar{I}_o \qquad (4\text{-}37)$$

Around the breakdown knee $\int_0^d u_i(E)dx \ll 1$, and Eq. (4-37) may be further approximated by $2q\bar{I}_o$. Under this condition, Eq. (4-35) may be reduced to

$$S_v(w)\Big|_{\text{low-frequency}} = H(jw)H^*(jw)S_i(jw)\Big|_{\text{low-frequency}}$$

$$= \left[H(jw)\right]^2 S_i(w)\Big|_{\text{low-frequency}}$$

$$= \frac{kV_b^2}{\bar{I}_o} \qquad (4\text{-}38)$$

where $k=\frac{1}{2}ql_d^2/v_d^2\bar{\tau}_d^2$ in ampere/Hz. The author will call this "k" the spectral proportionality constant. V_b is the breakdown voltage, and $\bar{I}_o$ is the reverse breakdown current (average of I(t)).

Examination of Eq. (4-38) reveals two important facts. They are:

(1) If one unit has higher breakdown voltage, V_b, than another unit, S_v(1-kHz) should be higher*, provided that the spectral proportionality constant is the same for both units,

(2) S_v(1-kHz) should decrease as $\bar{I}_o$ increases. These two facts that are so clearly broughtout by Eq. (4-38) were not predicted by any existing noise theories.

---

* When two G315 are connected in series, S_v(1-kHz) approximately doubles at the given current level.

Fig. 4-9 through Fig. 4-15 are typical S_v(1-kHz) obtained experimentally from G315 diodes. An experimental set-up to obtain these figures is shown in Fig. 4-16.

These S_v(1-kHz) plots, in general, follow the theoretical prediction, $S_v(1\text{-kHz}) \propto \bar{I}_o^{-1}$, given by Eq. (4-38). Notice, however, that Fig. 4-10 and Fig. 4-11 show a significant discrepancy from the theory, namely multiple-peak phenomenon of S_v(1-kHz). This phenomenon has been found to be crucial in reliability-prediction for a p-n junction, and will be analyzed in the next chapter.

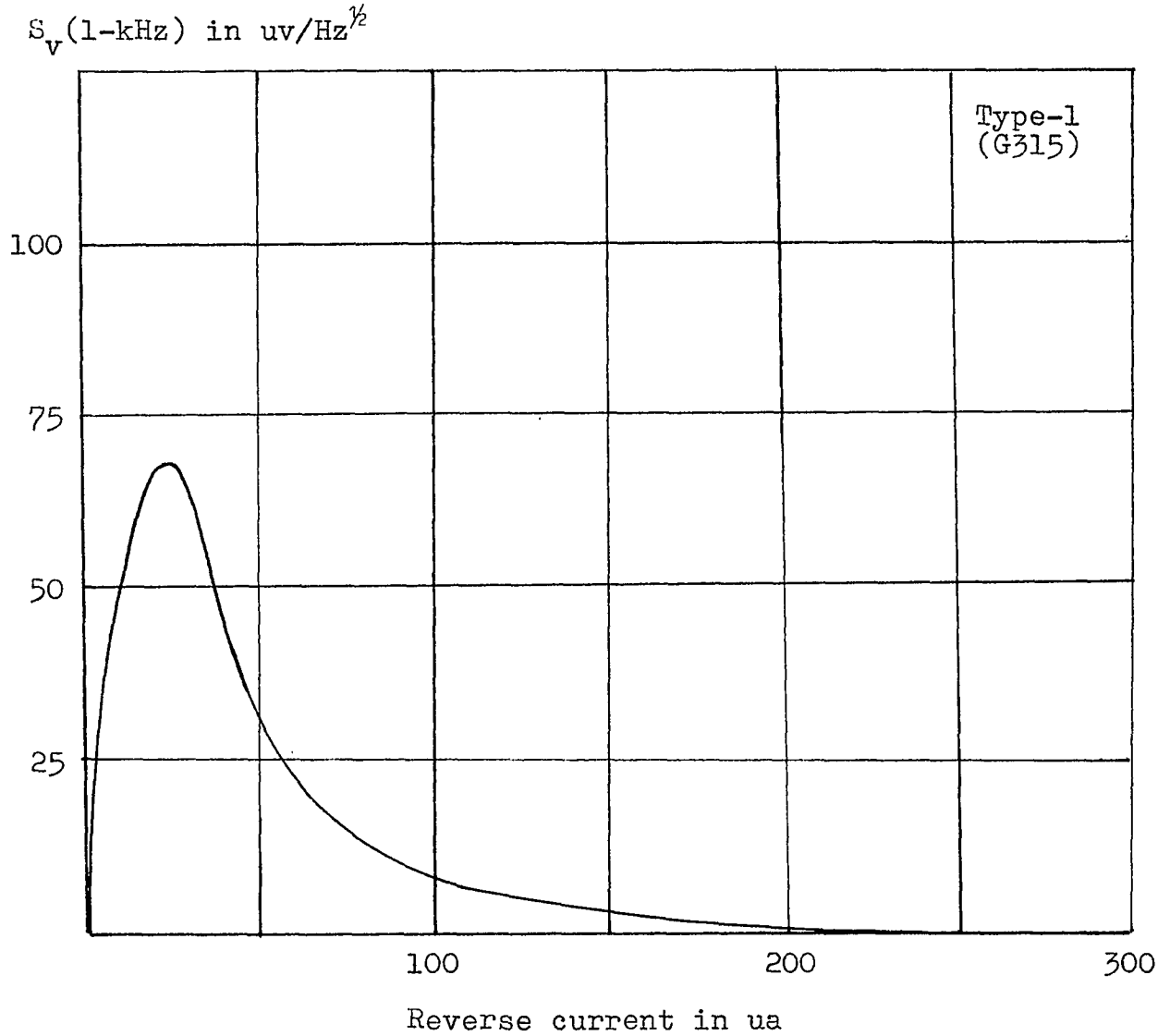

Fig. 4-9 Type-1. S_v(1-kHz) is characterized by one peak. The vast majority of p-n junction belong to this type-1. Notice the effect of shot-noise is disappearing after S_v(1-kHz) reaching the peak, then following the theoretical prediction expressed by Eq. (4-38).

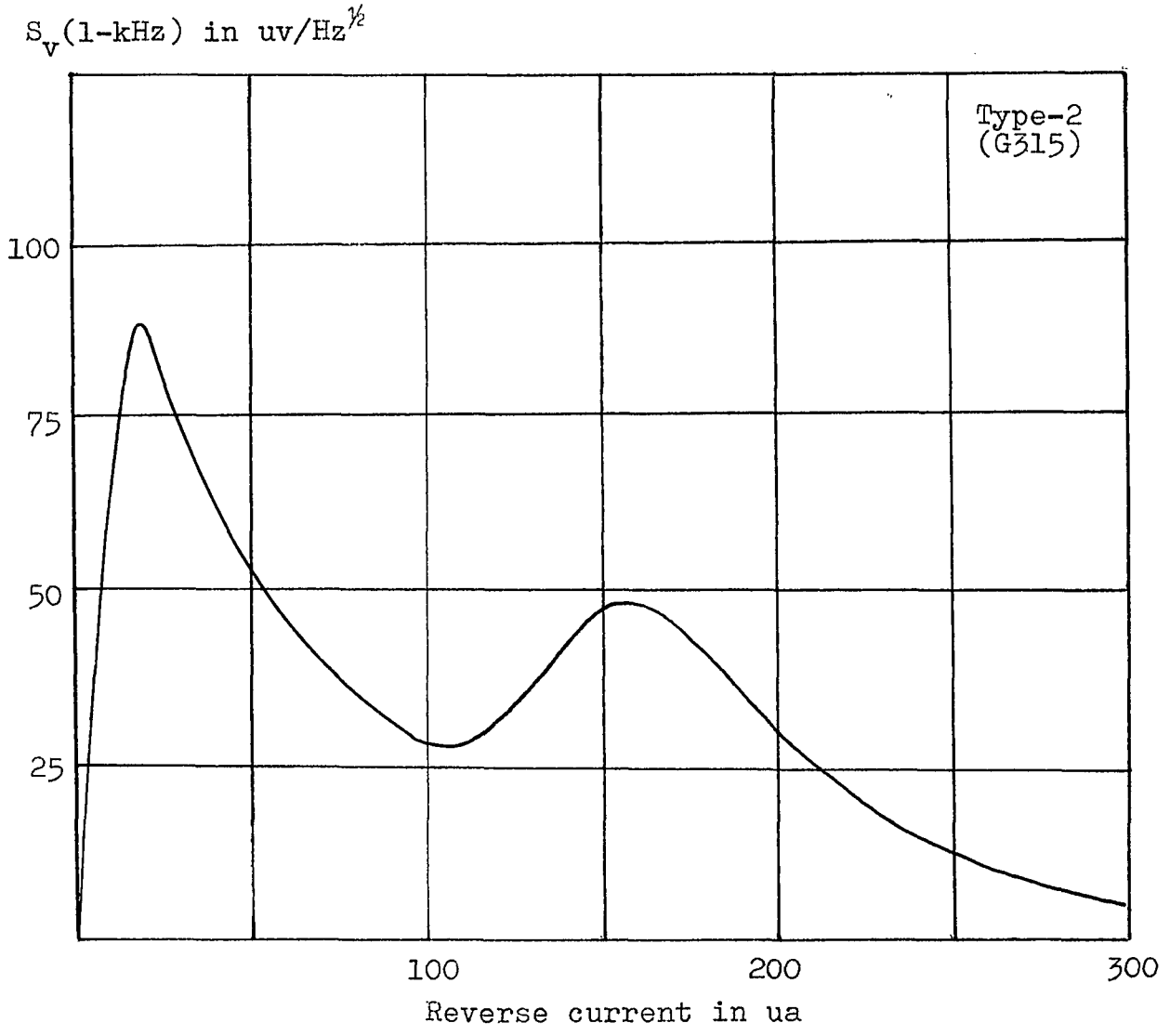

Fig. 4-10 Type-2. S_v(1-kHz) is characterized by two peaks. Life-test shows that this type degrades more rapidly than other type. 35 units out of 200 units tested belong to Type-2.

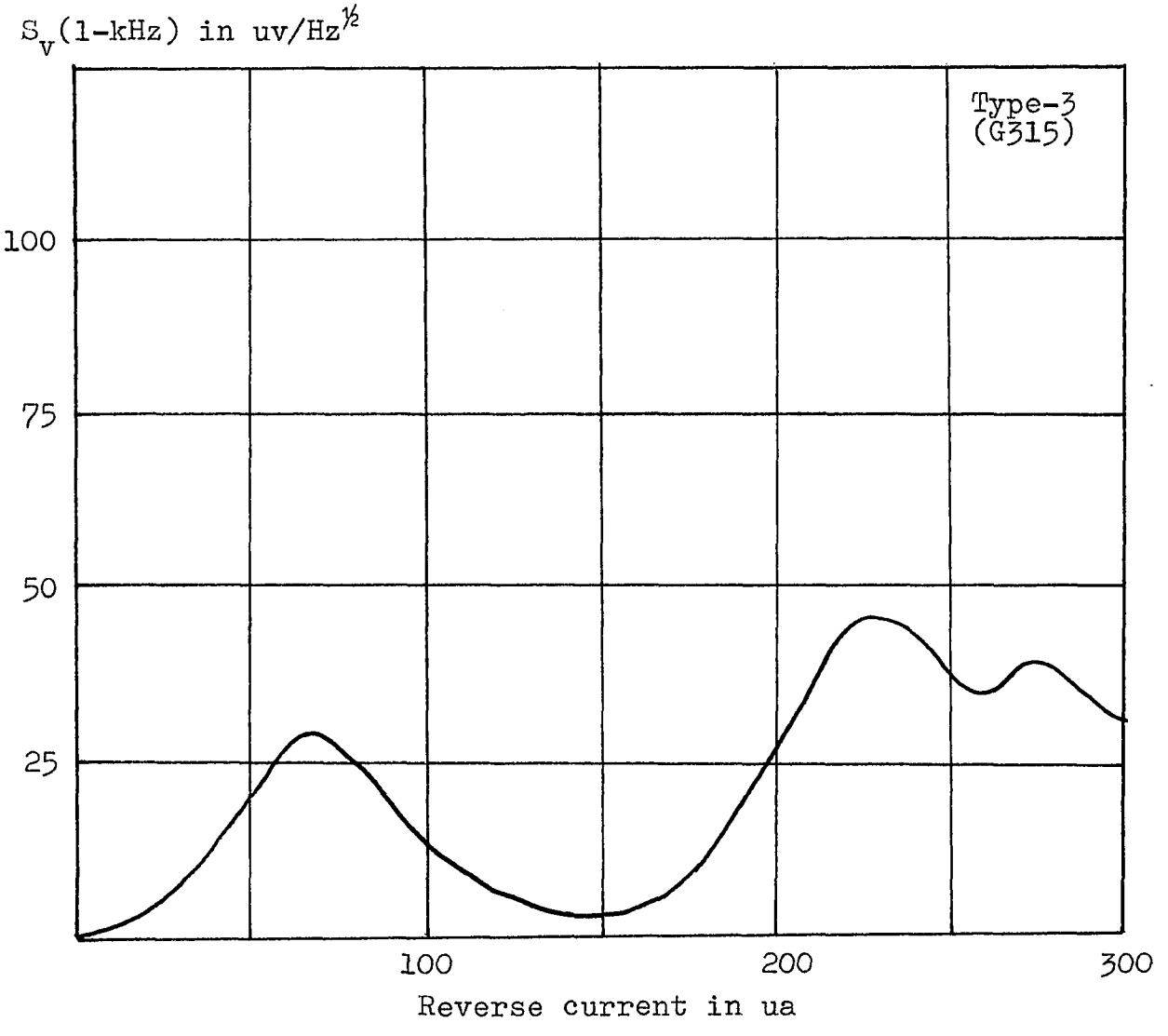

Fig. 4-11 Type-3. Only one unit among 200 units tested has shown this type. S_v(1-kHz) is characterized by 3 peaks.

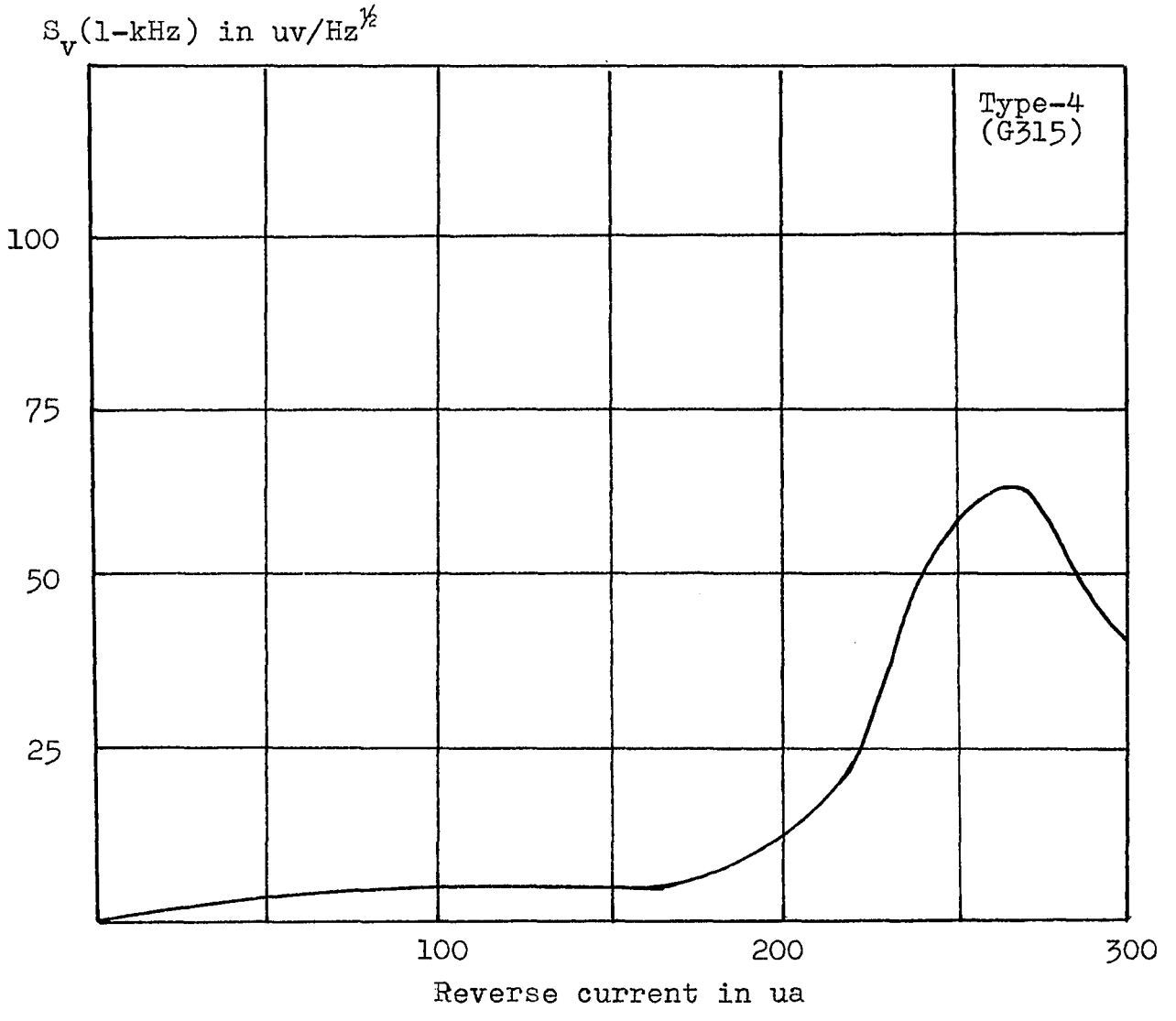

Fig. 4-12 Type-4. S_v(1kHz) is characterized by I_r(1-st peak)-shift to larger value. This type came from higher a-c impedance units. 9 units among 200 units tested have shown this type.

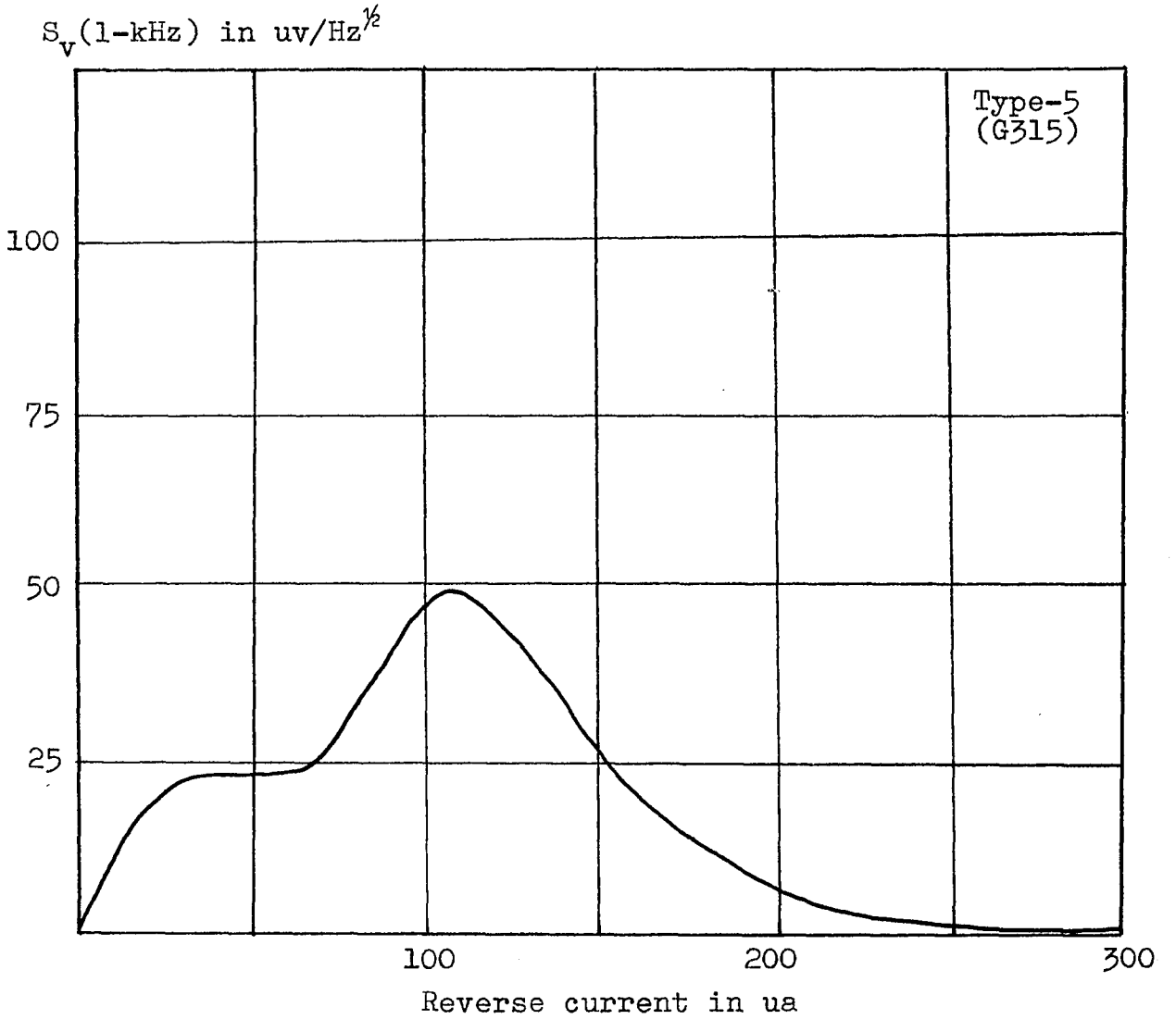

Fig. 4-13 Type-5. S_v(1-kHz) is characterized by the plateau before peak. 8 units among 200 units tested have shown this type.

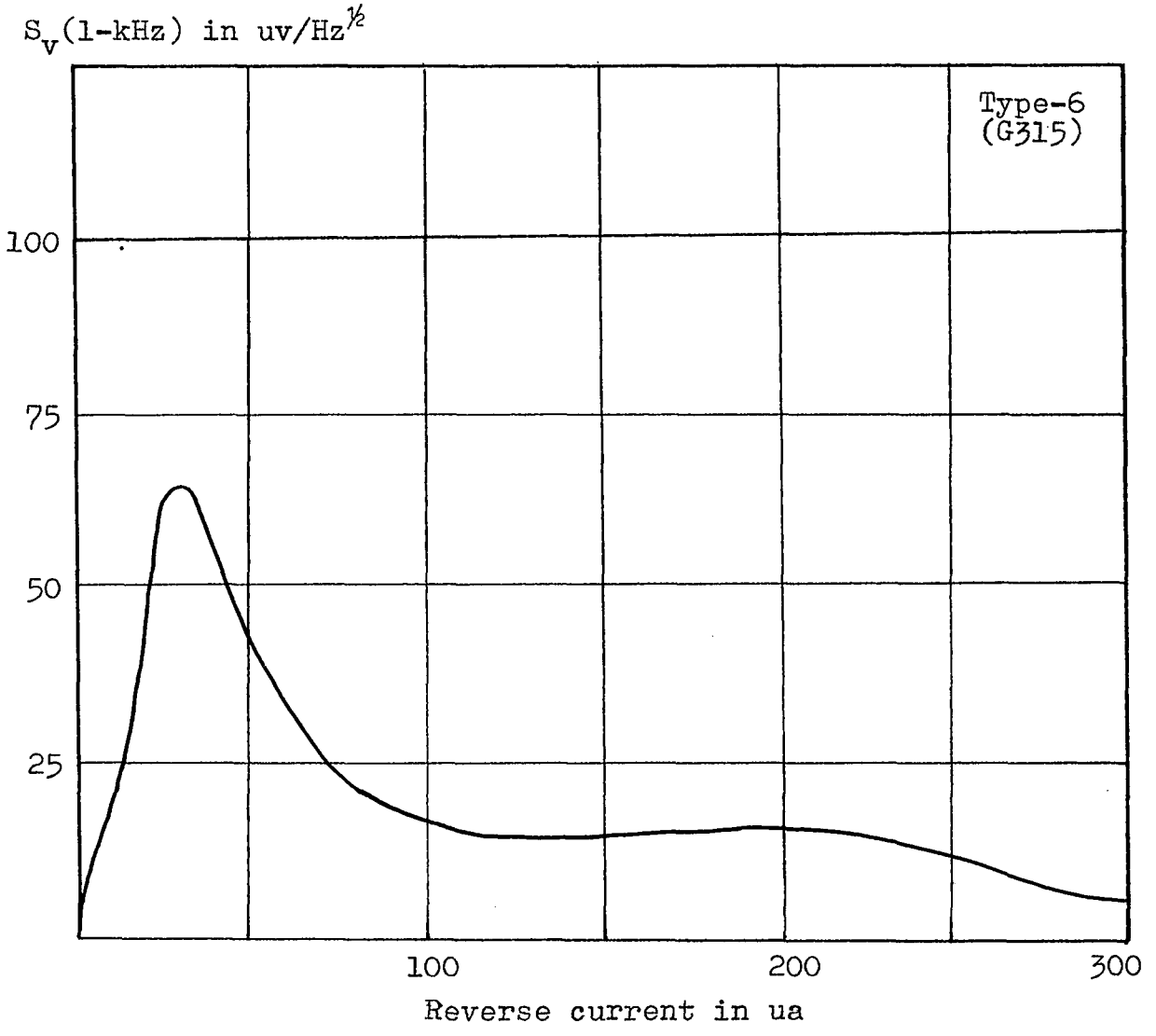

Fig. 4-14 Type-6. S_v(1-kHz) is characterized by the plateau after peak. 4 units among 200 units tested have shown this type.

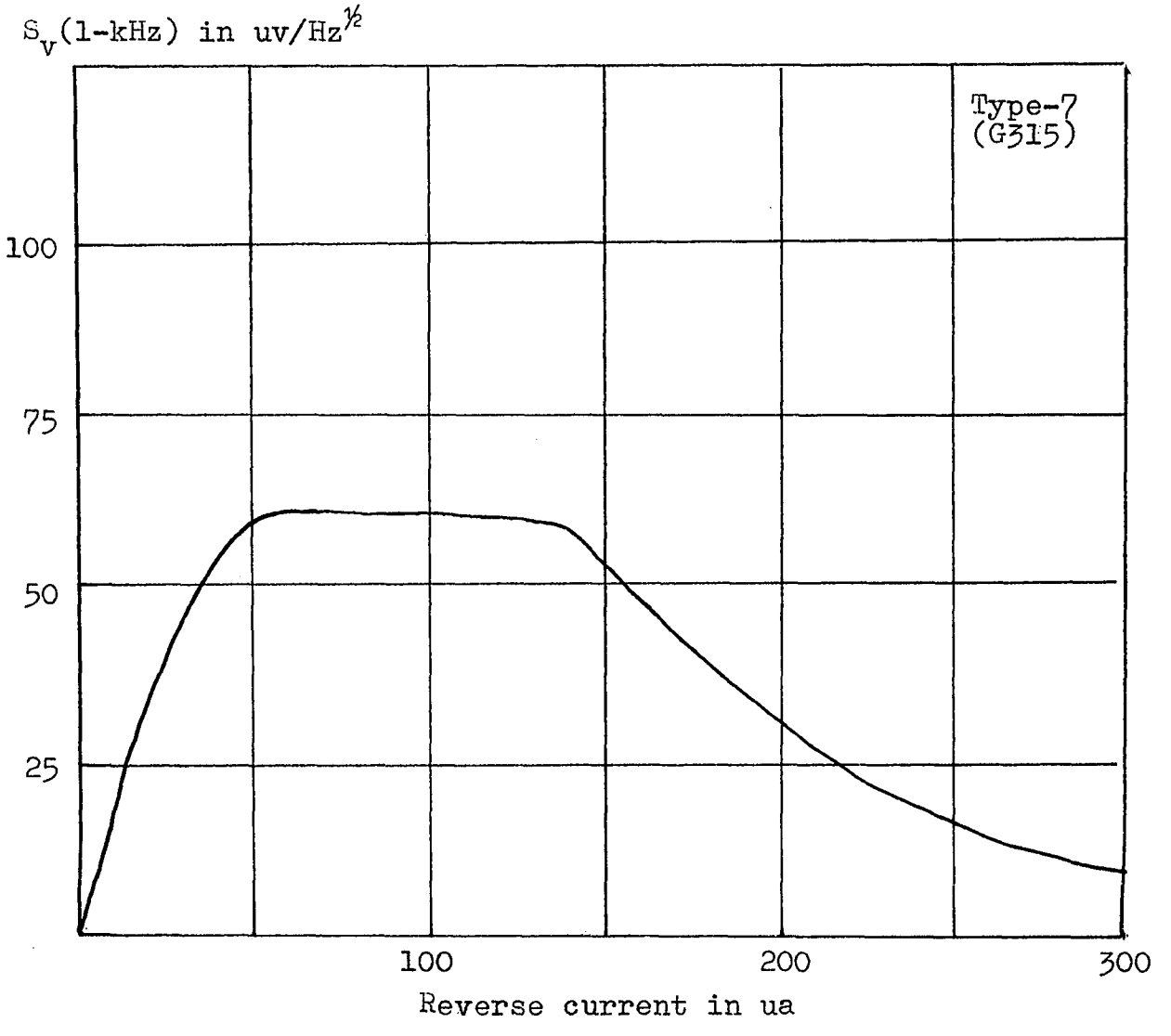

Fig. 4-15 Type-7. S_v(1-kHz) is characterized by the flat top. 5 units out of 200 units tested have shown this type.

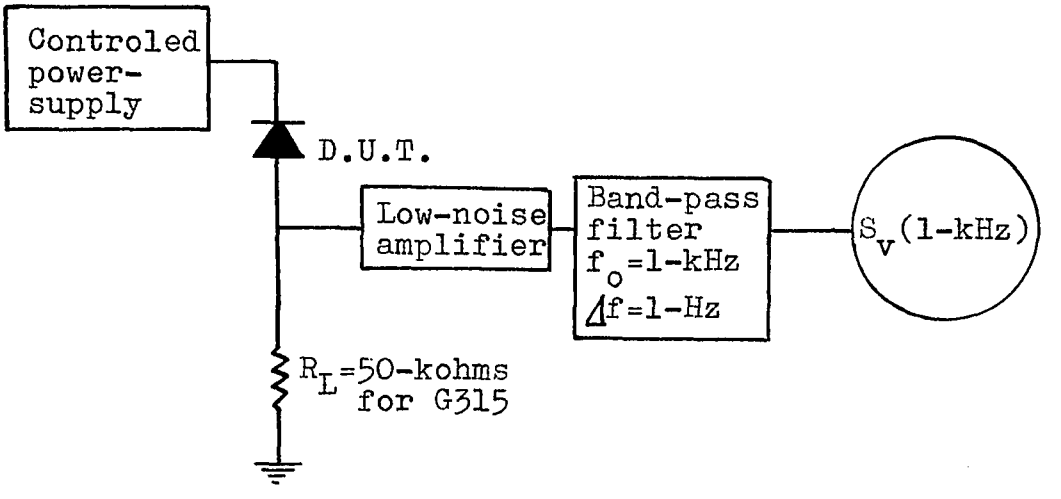

Fig. 4-16 An experimental set-up to obtain S_v(1-kHz) plots shown in Fig. 4-9 through Fig. 4-15.

CHAPTER 5

EXPLANATION OF MULTIPLE-PEAK PHENOMENON OF NOISE-VOLTAGE SPECTRAL DENSITY

5.1 Introduction

In Chapter 4, we have derived an open-circuit noise-voltage spectral density $S_v(w)$. It was also shown that $S_v(w)$ can be approximated for low-frequncies as the following:

$$S_v(w)\Big|_{\text{low-frequency}} = \frac{kV_b^2}{\bar{I}_o} \qquad (5\text{-}1)$$

where

V_b is the breakdown voltage of a p-n junction.

$\bar{I}_o$ is the average breakdown current, $\overline{I(t)}$.

k is the spectral proportionality constant.

Although S_v(1-kHz) observed in the majority of practical p-n junctions, in general, follows the theoretical prediction expressed in Eq. (5-1), some units show a significant discrepancy from the theory as shown in Figs. 4-10 and 4-11, namely multiple-peak phenomenon. It is the purpose of this chapter to explain the multiple-peak phenomenon.

Göetzberger[11,12] and Newman[27] reported that most practical junctions have small, light emitting regions of lower breakdown voltage, so-called microplasmas. They

also have shown that the number of microplasmas increase with increasing applied voltage. Based on their experimental proof, the practical junctions may be simulated by multiple breakdown channels whose series resistance R_s and breakdown voltage V_b are different. This multiple breakdown channel concept will be employed to explain observed multiple-peak phenomenon of $S_v(w)$.

5.2 Noise-Voltage Spectral Density due to Multiple-breakdown Channels

Supposing a p-n junction can be subdivided into n breakdown channels whose series resistances are R_{s1}, R_{s2}, ..., and R_{sn}, each associated with breakdown voltages of V_{b1}, V_{b2}, ..., V_{bn} as shown in Fig. 5-1-a. If the branch currents for the channels are designated as I_1, I_2, ..., I_n, the total circuit current, I_o, is

$$I_o = \sum_{j=1}^{n} I_j \tag{5-2}$$

and

$$R_{sj}I_{sj} + V_{bj} = R_{s(j+1)}I_{s(J+1)} + V_{b(j+1)} \tag{5-3}$$

which gives

$$I_j = \frac{D_j}{D} \tag{5-4}$$

where

$$D \equiv \begin{vmatrix} 1 & 1 & 1 & \cdots\cdots\cdots & 1 \\ R_{s1} & -R_{s2} & 0 & \cdots\cdots\cdots & 0 \\ 0 & +R_{s2} & -R_{s3} & \cdots\cdots\cdots & 0 \\ \cdot & & & & \\ \cdot & & & & \\ \cdot & & & & \\ 0 & 0 & 0 & \cdots +R_{s,n-1} & -R_{s,n} \end{vmatrix} \qquad (5\text{-}5)$$

and D_j is the same as D except that the j-th column is replaced by I_o, $(V_{b2}-V_{b1})$, ..., and $(V_{bn}-V_{b,n-1})$. These I_j, each associated with the series resistance R_j and the breakdown voltage V_{bj}, will produce an equivalent noise source, S_{vj}, for each channel as shown in Fig. 5-1-b,

$$S_{vj} = \frac{k_j V_{bj}^2}{I_j^2} \qquad (5\text{-}6)$$

Once the S_{vj} are known, the noise-voltage spectral density across the external current limiting resistor R_L due to the multiple breakdown channel effect, $S_{v\sum j}$, is

$$S_{v\sum j} = \sum_{j=1}^{n} S_{vj}\left\{\frac{R_L//(G-G_j)^{-1}}{R_{sj}+R_L//(G-G_j)^{-1}}\right\}^2 \qquad (5\text{-}7)$$

where $G=\sum_{j=1}^{n} R_{sj}^{-1}$ and $G_j=R_j^{-1}$. "//" denotes "in prallel with." Obviously this $S_{v\sum j}$ is a function of I_j, R_{sj}, V_{bj}, and k_j. It is rather complicated to compute $S_{v\sum j}$ quantitatively unless the value of these variables are known. These variables may be, furthermore, related to each other.

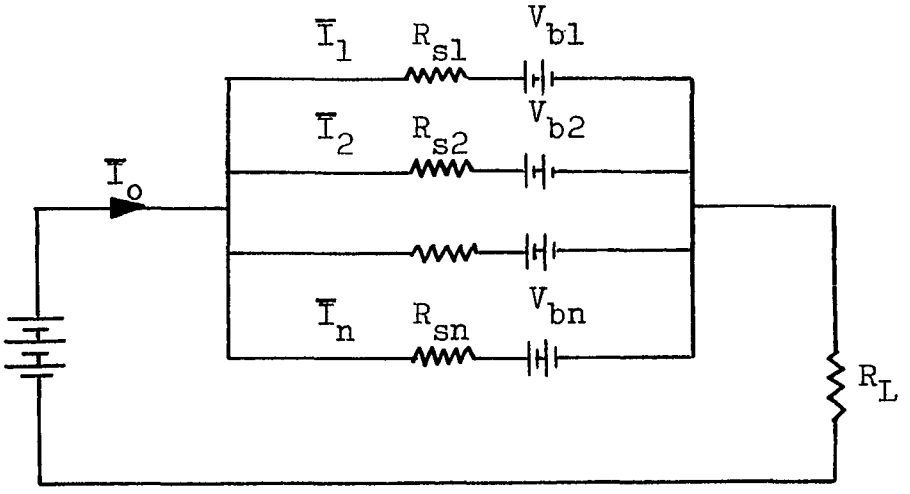

(a)

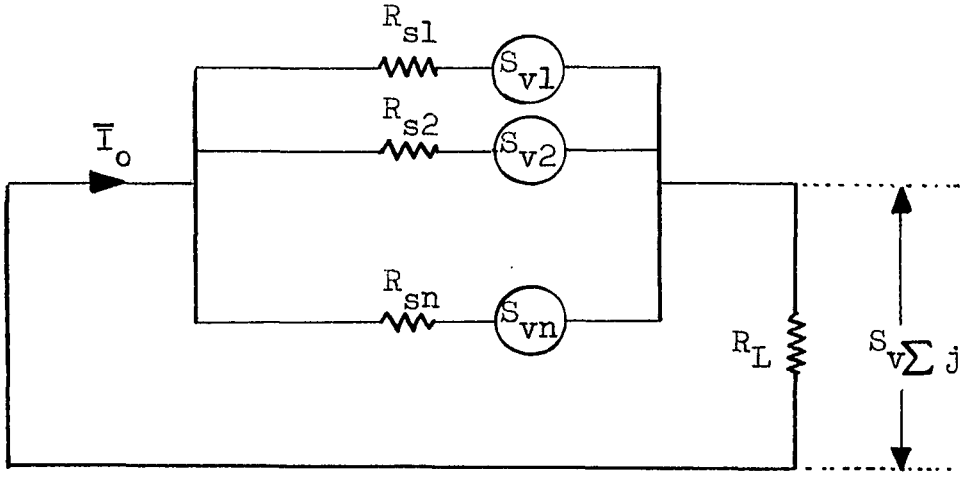

(b)

Fig. 5-1 (a) Simulation of multi-breakdown channels by R_{sj}, V_{bj}, and $\bar{I}_j$,
(b) Noise equivalent circuit of multi-breakdown channels.

5.3 Two-channel Model

To simplify the evaluation of $S_v \sum_j$ expressed in Eq. (5-7), let us assume:

(1) The junction under consideration has one normal channel through the bulk, and another one which is microplasma channel. The microplasma channel will consist of a series resistance R_{s2}, breakdown voltage V_{b2}, and the spectral proportionality constant k_2. The rest of the bulk properties will be represented by R_{s1}, V_{b1}, and k_1 respectively.

(2) The breakdown voltage of a microplasma channel will be considered to be lower than the breakdown voltage of the bulk channel, i.e., $V_{b1} > V_{b2}$.

With these assumptions, n=2. Eqs. (5-3) and (5-4) may be rewitten as follows (See Fig. 5-2-a):

$$I_o = I_1 + I_2 \tag{5-8}$$

$$R_{s1}I_1 + V_{b1} = R_{s2}I_2 + V_{b2} \tag{5-9}$$

which gives

$$I_1 = \frac{(V_{b2}-V_{b1}) + R_{s2}I_o}{R_{s2} + R_{s1}} \tag{5-10}$$

and

$$I_2 = \frac{(V_{b1}-V_{b2}) + R_{s1}I_o}{R_{s1} + R_{s2}} \tag{5-11}$$

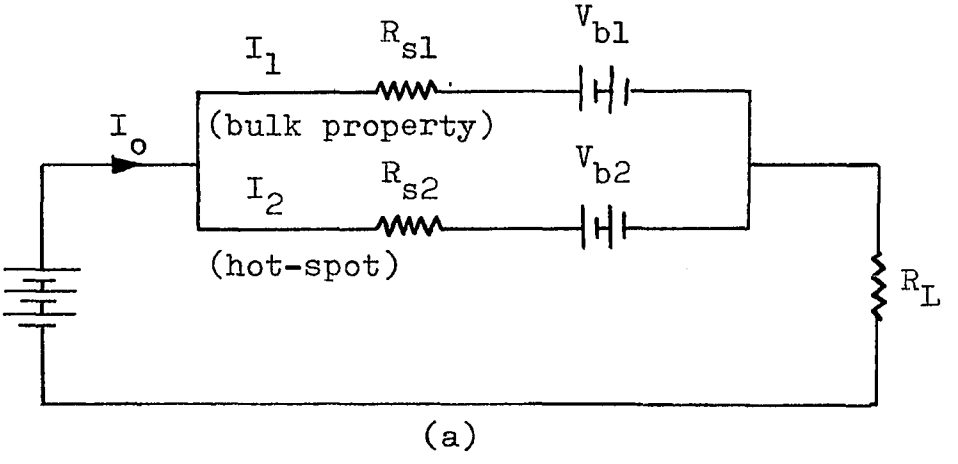

(a)

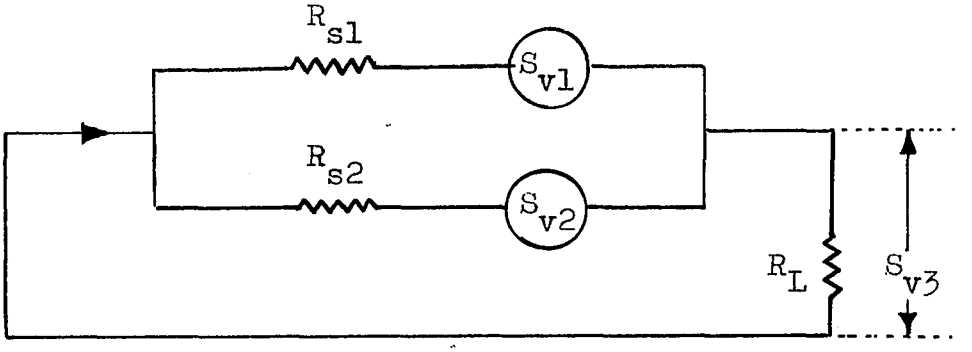

(b)

Fig. 5-2 (a) Simulation of two-channel model,
(b) Noise equivalent circuit of two-channel model.

These V_{b1}, I_1, V_{b2}, and I_2 in the uniform bulk breakdown channel and a microplasmic breakdown channel produce two separate noise sources whose noise-voltage spectral density S_{v1} and S_{v2} are given by

$$S_{v1} = \frac{k_1 V_{b1}^2 (R_{s1}+R_{s2})}{(V_{b2}-V_{b1})+R_{s2}I_o} \tag{5-12}$$

and

$$S_{v2} = \frac{k_2 V_{b2}^2 (R_{s1}+R_{s2})}{(V_{b1}-V_{b2})+R_{s1}I_o} \tag{5-13}$$

With reference to Fig. 5-2-b, the noise-voltage spectral density S_{v3} across the current-limiting resistance R_L is now expressed by

$$S_{v3} = S_{v1}\left\{\frac{R_{s2}//R_L}{R_{s1}+(R_{s2}//R_L)}\right\}^2 + S_{v2}\left\{\frac{R_{s1}//R_L}{R_{s2}+(R_{s1}//R_L)}\right\}^2 \tag{5-14}$$

where "//" denotes "in parallel with".

In a practical case, R_{s1} and R_{s2} are at most a few hundred ohms, and R_L will be at least a few thousand ohms. Under these circumstance $R_{s1}//R_L \cong R_{s1}$, and $R_{s2}//R_L \cong R_{s2}$. Thus, Eq. (5-14) may be reduced to

$$S_{v3} = S_{v1}\left\{\frac{R_{s2}}{R_{s1}+R_{s2}}\right\}^2 + S_{v2}\left\{\frac{R_{s1}}{R_{s1}+R_{s2}}\right\}^2$$

$$= \frac{S_{v1}R_{s2}^2 + S_{v2}R_{s1}^2}{(R_{s1}+R_{s2})^2} \tag{5-15}$$

Substituting Eq. (5-12) and Eq. (5-13) into Eq. (5-15) and letting $V_{b1}-V_{b2}=\Delta V_b$, we have

$$S_{v3} = \frac{k_1}{(R_{s1}+R_{s2})}\left\{\frac{V_{b1}^2 R_{s2}^2}{\Delta V_b + R_{s2} I_o} + \frac{(k_2/k_1)V_{b1}^2(1+(\Delta V_b/V_{b1}))^2 R_{s1}^2}{-\Delta V_b + R_{s1} I_o}\right\} \tag{5-16}$$

Assuming $\Delta V_b/V_{b1} \ll 1$, and $k_2/k_1=1$,

$$S_{v3} = \frac{k_1 V_{b1}^2}{(R_{s1}+R_{s2})}\left\{\frac{-R_{s2}^2\Delta V_b + R_{s2}^2 R_{s1} I_o + \Delta V_b R_{s1}^2 + R_{s2} R_{s1}^2 I_o}{R_{s1} R_{s2} I_o^2 + \Delta V_b (R_{s1}-R_{s2}) I_o - (\Delta V_b)^2}\right\} \tag{5-17}$$

By rearranging, we have

$$S_{v3} = \frac{k_1 V_{b1}^2}{I_o}\left[\frac{1}{1 - \left\{\dfrac{(\Delta V_b)^2}{R_{s1} R_{s2} I_o^2 + (R_{s1}-R_{s2})(\Delta V_b) I_o}\right\}}\right] \tag{5-18}$$

Examination of Eq. (5-18) reveals some interesting facts. They are:

(1) As a special case, if we let ΔV_b be zero (which means uniform breakdown without microplasmic breakdown channel), Eq. (5-18) is reduced to Eq. (5-1) as it should be:

$$S_{v3}\Big|_{\Delta V_b=0} = \frac{k_1 V_{b1}^2}{I_o} \tag{5-19}$$

The first factor in Eq. (5-18) is the theoretical minimum of the noise-voltage spectral density, and may be observed if no microplasmic breakdown channel exists.

(2) The second factor in Eq. (5-18) is greater than one provided that $R_{s1}R_{s2}I_o$ is greater than $(R_{s1}-R_{s2})\Delta V_b$. The second factor in Eq. (5-18), under the stated condition, must be responsible for excess noise level over the theoretical minimum. It should be mentioned that the condition $R_{s1}R_{s2}I_o > (R_{s1}-R_{s2})\Delta V_b$ may not be replaced by the condition $R_{s1} > R_{s2}$ even though it makes automatically the second factor greater than one. We have no prior knowledge about the magnitude of R_{s1} and R_{s2}.

(3) By taking a partial derivative of the second factor in Eq. (5-18) with respect to external circuit current I_o, one may obtain the local peak condition:

$$\frac{\partial}{\partial I_o}\left\{\frac{\Delta V_b^2}{R_{s1}R_{s2}I_o^2+(R_{s1}-R_{s2})\Delta V_b I_o}\right\}^{-1} = 0 \qquad (5\text{-}20)$$

which is satisfied by

$$I_o = \frac{\Delta V_b(R_{s2}-R_{s1})}{2R_{s1}R_{s2}} \qquad (5\text{-}21)$$

(4) The difference between R_{s1} and R_{s2} alone does not cause excess noise, since the second factor is zero

regardless of the difference between R_{s1} and R_{s2} if ΔV_b is zero,

(5) As the breakdown current I_o approaches infinity, the second factor approaches one. This fact indicates that the excess noise over the theoretical minimum disappears as the breakdown currenet I_o approaches infinity,

(6) Supposing $R_{s1}=R_{s2}$ in Eq. (5-18), we have

$$S_{v3}\Big|_{R_{s1}=R_{s2}} = \frac{k_1 V_{b1}^2}{I_o}\left\{\frac{1}{1-(\frac{\Delta V_b}{R_{s1}I_o})^2}\right\} \qquad (5\text{-}22)$$

S_{v3} expressed by Eq. (5-22) may be interpreted as the noise-voltage spectral density observed in a p-n junction when there is a microplasmic breakdown channel with lower breakdown voltage with respect to the breakdown voltage of bulk, and equal series resistance. It is rather interesting to notice that we can simulate the situation using two diodes whose series resistance are equal. The difference in breakdown voltage, ΔV_b, may be supplied by external means as shown in Fig. 5-3. Eq. (5-22) indicates that the noise-voltage spectral density across R_L may be controled by changing ΔV_b. Experimental results are shown in Fig. 5-4.

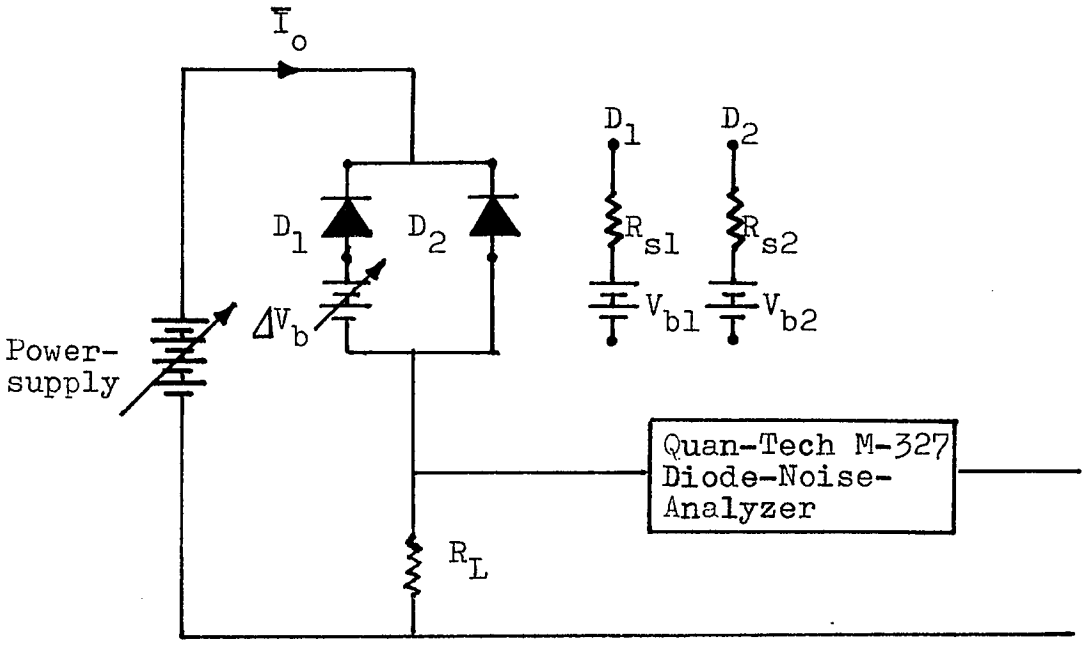

Fig. 5-3 An experimental set-up to verify Eq. (5-22). Artificial external voltage ΔV_b is inserted in series with D_1 to simulate the difference in breakdown voltages of two channels. Two diode should be selected for the same series resistance, $R_{s1}=R_{s2}$, to satisfy the assumption.

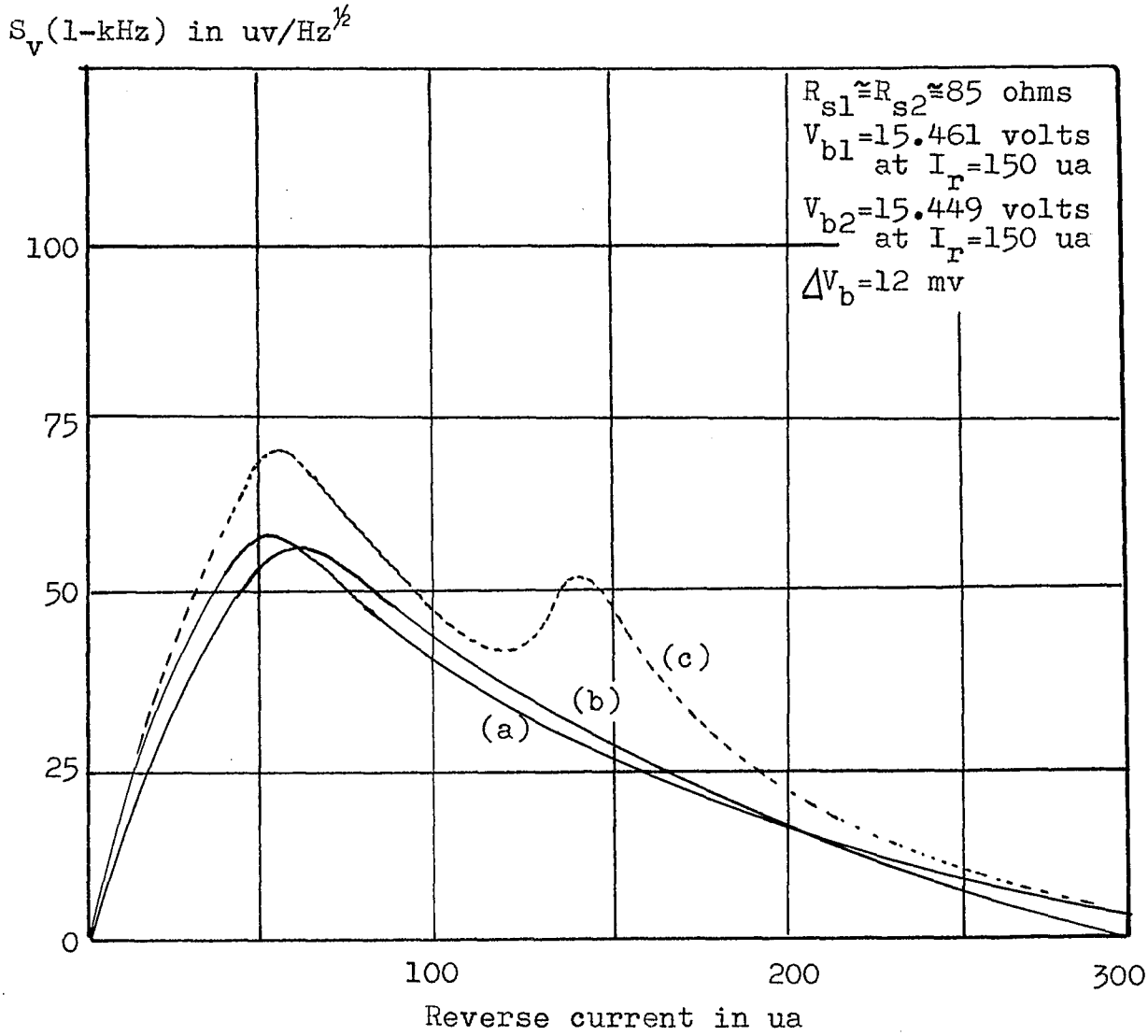

Fig. 5-4 Effect of ΔV_b on S_v(1-kHz). Two G315 are selected for $R_{s1} \cong R_{s2}$ from a batch. (a), and (b) are individual S_v(1-kHz) plots. (c) is obtained when ΔV_b=12 mv as shown in Fig. 5-3.

CHAPTER 6

CORRELATION FOUND BETWEEN MULTIPLE-PEAK PHENOMENON AND DEGRADATION OF REVERSE CHARACTERISTIC

6.1 Introduction

In the previous chapter, it was shown that the multiple-peak phenomenon of the noise-voltage spectral density in a p-n junction under breakdown conditions is due to microplasmic breakdown channels. These microplasmic channels may contribute, at least partially, to the degradation of the reverse characteristic, since each low breakdown channel should suffer a much higher local current density compared to the rest of the bulk. Under certain conditions, the local high current density in a microplasmic channel may even lead to the ultimate destruction of the device as time goes on.

A microplasmic breakdown channel could be, therefore, considered as a "built-in" instability mechanism. Fortunately, we now have a powerful method of detecting these troublesome microplasmic breakdown channels by means of S_v(1-kHz)-analysis.

It is the purpose of this chapter to present the results obtained from a series of life-test experiments performed to investigate whether the behavior of S_v(1-kHz)

(hence the existence of microplasmic channels) is related to the degradation of the reverse characteristic. If there is a high correlation between the behavior of S_v(1-kHz) and the degradation of the reverse characteristic, the former may be chosen as the prediction parameter for the degradation of the reverse characteristic.

Three different types of diodes were tested for 1000 hours life-test under specified test conditions. Type of diode tested, and sample-size are as follows:

Life-test No.	Type of diode*	Sample-size
Life-test No.1	G315	108
Life-test No.2	G321	449
Life-test No.3	S2A	200

*The specifications of G315, G321, and S2A are as follows:

G315

Zener-diode.
Nominal Zener Voltage: 15 volts at 8.5 ma.
Zener Impedance: 16 ohms at 8.5 ma.
700 ohms (max) at 250 ua.
Maximum Zener Current: 20 ma. at 55°C.
Temperature Coefficient: 0.070%/°C.

G321

Very high-speed, and high-reliability siganal-diode.
Silicon, Planar-epitaxial construction.
V_f(max): 0.85 volts at 20 ma.
I_r(max): 0.1 ua. at 50 volts reverse-bias and 20°C.
V_b(min): -50 volts.

C_j: 4×10^{-12} farads at zero-bias.
t_{rr}: 4×10^{-9} seconds ($I_f = I_r = 10$ ma, recovery to 0.1 ua).
P(max): 250 mw.
I_f(max): 200 ma., d-c steady state.

S2A

Two-ampere rated diffused silicon rectifier.
Epoxi-encapsulation.
V_b(min): -200 volts.

6.2 Life-test No.1 (G315)

G321 is a Zener-diode which has a nominal breakdown voltage of 15 volts. The units were classified into seven types as Type-1 through Type-7 according to their spectral behavior as shown in Fig. 4-9 through Fig. 4-15 respectively.

Before the life-test, twelve parameters, shown in Table 6-1, were measured. The average value and standard-deviation of these twelve parameters for each of the seven types are given in Table 6-2.

During life-test No.1, the Zener-current of 10 ma was maintained for 1000 hours at room temperature. The change in Zener-voltage at 100-ua, 200-ua, and 300-ua levels was monitored at time intervals of 100 hours. The life-test data is shown in Appendix I. After the life-test was done, the percent-degradation at the given Zener-current levels was calculated as follows:

$$\%\text{-Degradation} = \frac{V_r(T_o,I_r)-V_r(T_{1000},I_r)}{V_r(T_{1000},I_r)} \times 100 \qquad (6\text{-}1)$$

where $V_r(T_o,I_r)$ is the initail Zener-voltage at the specified Zener-current I_r, and $V_r(T_{1000},I_r)$ is the Zener-voltage at the same Zener-current I_r after the 1000-hour life-test was done. This percentage-degradation at given

Zener-current level I_r is an indication of the deterioration of the reverse characteristic during the life-test period.

The data accumulated during the life-test period were processed by digital computer to obtain multi-correlation coefficient, R_{xy}, between the twelve parameters listed in Table 6-1 and the percentage-degradation at 100-ua, 200-ua, and 300 ua levels. The computer program written for this purpose is shown in Appendix H. The result obtained from the multi-correlation program is summarized for each current level in Table 6-4, Table 6-5, and Table 6-6 respectively.

From life-test No.1, we have reached the following conclusions:

(1) The majority of units (80%) belong to either Type-1 or Type-2,

(2) Comparison of Type-1 and Type-2 indicates that units with a second-peak in S_v(1-kHz) show much higher percentage degradation. From this fact, we may choose S_v(1-kHz) measured at the second-peak (parameter 9 in Table 6-1) as a prediction factor for the percentage-degradation,

(4) Although Type-4 through Type-7 are susceptable to percentage-degradation, R_{xy} values can not be adquately interpreted since sample-size are two small

for these Types,

(4) Type-7 shows almost perfect correlation between a-c small-signal impedance and percentage-degradation.

Table 6-1 Twelve parameters measured before the life-test No.1

Parameter*	Description
1. $S_v(1\text{-kHz})_{100}$	Noise-voltage spectral density at 1-kHz, and at I_r=100-ua.
2. $S_v(1\text{-kHz})_{200}$	" " " at I_r=200-ua.
3. $S_v(1\text{-kHz})_{300}$	" " " at I_r=300-ua.
4. $S_v(10\text{-Hz})_{100}$	Noise-voltage spectral density at 10-Hz, and at I_r=100-ua.
5. $S_v(10\text{-Hz})_{200}$	" " " at I_r=200-ua.
6. $S_v(10\text{-Hz})_{300}$	" " " at I_r=300-ua.
7. $S_v(1\text{-kHz})_{1\text{-st peak}}$	Noise-voltage spectral density at the first peak.
8. I_r(1-st)	I_r to observe $S_v(1\text{-kHz})_{1\text{-st peak}}$
9. $S_v(1\text{-kHz})_{2\text{-nd peak}}$	Noise-voltage spectral density at the second peak
10. I_r(2-nd)	I_r to observe $S_v(1\text{-kHz})_{2\text{-nd peak}}$
11. $Z_j(1\text{-kHz})_{200}$	a-c impedance at 1-kHz and I_r=200-ua.
12. $Z_j(1\text{-kHz})_{300}$	" " " I_r=300-ua.

* Parameters 1, 2, 3, 4, 5, 6, 7, and 9 are measured in $uV/Hz^{1/2}$. Parameters 8 and 10 are measured in ua. Parameters 11 and 12 are measured in ohms.

Table 6-2 Classification of G315 by S_v(1-kHz)

Type	Characteristic of S_v(1-kHz)	No. of units	Average %-DEG*	Unit number
1	Fig. 4-9	46 (42.6%)	2	1,3,5,8,10,12,14, 15,16,19,20,21,22, 27,31,32,34,35,36, 38,42,43,44,47,48, 49,53,56,61,63,64, 67,69,74,77,79,85, 86,87,90,91,93,96, 102,105,107.
2	Fig. 4-10	35 (32.4%)	21	6,7,11,13,17,18,23, 24,25,26,37,40,46, 50,51,52,55,59,60, 62,65,68,70,71,73, 80,83,92,94,95,99, 101,104,106,108
3	Fig. 4-11	1 (0.9%)	**	98.
4	Fig. 4-12	9 (8.3%)	20	2,29,39,45,58,81, 82,84,97.
5	Fig. 4-13	8 (7.4%)	25	33,57,66,72,75,88, 89,103.
6	Fig. 4-14	4 (3.7%)	25	4,9,41,54
7	Fig. 4-15	5 (4.6%)	12	28,30,76,78,100

* Average percent-degradation calculated at I_p=200-ua.
** Type-3 is deleted because of its small sample-size.

Table 6-3 Average value and Standard-deviation* the parameters listed in Table 6-1

Parameter	Type-1	Type-2	Type-4	Type-5	Type-6	Type-7
1. $S_v(1\text{-kHz})_{100}$	67 (72)	90 (91)	61 (69)	60 (42)	21 (16)	57 (34)
2. $S_v(1\text{-kHz})_{200}$	16 (31)	52 (75)	25 (25)	30 (28)	3 (2)	16 (20)
3. $S_v(1\text{-kHz})_{300}$	2 (3)	6 (16)	8 (14)	1 (1)	3 (4)	3 (2)
4. $S_v(10\text{-Hz})_{100}$	105 (109)	103 (70)	113 (87)	113 (120)	43 (17)	58 (71)
5. $S_v(10\text{-Hz})_{200}$	78 (89)	95 (75)	113 (82)	118 (131)	26 (14)	76 (67)
6. $S_v(10\text{-Hz})_{300}$	72 (94)	68 (74)	92 (97)	62 (71)	30 (24)	62 (55)
7. $S_v(1\text{-kHz})_{1\text{-st peak}}$	108 (140)	130 (101)	199 (167)	147 (74)	51 (43)	81 (83)
8. $I_r(1\text{-st})$	63 (56)	43 (25)	114 (64)	121 (57)	31 (7)	80 (44)
9. $S_v(1\text{-kHz})_{2\text{-nd peak}}$	-	137 (99)	-	-	-	-
10. $I_r(2\text{-nd})$	-	126 (45)	-	-	-	-
11. $Z_j(1\text{-kHz})_{200}$	94 (51)	102 (54)	138 (147)	95 (64)	59 (39)	112 (41)
12. $Z_j(1\text{-kHz})_{300}$	53 (28)	58 (36)	103 (152)	60 (44)	38 (21)	57 (21)

* Figures in parenthesis indicate Standatd-deviation

Table 6-4 R_{xy} between the parameters in Table 6-1 and percent-degradation at I_r=100 ua.

Type	Characteristic of S_v(1-kHz)	No. of units in %	Parameters 1	2	3	4	5	6	7	8	9	10	11	12
1	Fig. 4-9	42.6	8	5	9	2	0	1	25	4	-	-	3	2
2	Fig. 4-10	32.4	47	29	6	16	20	26	28	2	43	1	22	27
3	Fig. 4-11	0.9	*	*	*	*	*	*	*	*	*	*	*	*
4	Fig. 4-12	8.4	5	42	6	11	20	24	14	33	-	-	2	2
5	Fig. 4-13	7.4	36	14	9	20	33	40	5	36	-	-	44	30
6	Fig. 4-14	3.7	24	8	42	51	39	40	51	0	-	-	27	27
7	Fig. 4-15	4.6	5	17	40	29	20	17	18	13	-	-	88	89

*Type-3 is deleted from the correlation analysis since only one unit among 108 units tested (0.9%) has shown this characteristic.

Table 6-5 R_{xy} between the parameters in Table 6-1 and percent-degradation at I_r=200 ua.

Type	Characteristic of S_v(1-kHz)	No. of units in %	Parameters 1	2	3	4	5	6	7	8	9	10	11	12
1	Fig. 4-9	42.6	7	0	11	4	10	13	2	10	-	-	9	3
2	Fig. 4-10	32.4	45	28	11	16	20	27	24	3	41	1	23	28
3	Fig. 4-11	0.9	*	*	*	*	*	*	*	*	*	*	*	*
4	Fig. 4-12	8.4	1	38	5	6	14	28	9	34	-	-	7	7
5	Fig. 4-13	7.4	32	4	7	9	20	30	4	41	-	-	26	11
6	Fig. 4-14	3.7	24	8	42	51	39	40	51	0	-	-	27	27
7	Fig. 4-15	4.6	0	21	47	27	16	13	14	20	-	-	91	92

*Type-3 is deleted from the correlation analysis since only one unit among 108 units tested (0.9%) has shown this characteristic.

Table 6-6 R_{xy} between the parameters in Table 6-1 and percent-degradation at I_r=300 ua.

Type	Characteristic of S_v(1kHz)	No. of units in %	Parameters 1	2	3	4	5	6	7	8	9	10	11	12
1	Fig. 4-9	42.6	11	7	14	10	12	15	6	5	-	-	10	2
2	Fig. 4-10	32.4	42	26	12	14	19	26	21	4	41	0	22	27
3	Fig. 4-11	0.9	*	*	*	*	*	*	*	*	*	*	*	*
4	Fig. 4-12	8.4	2	35	2	5	11	33	5	36	-	-	11	11
5	Fig. 4-13	7.4	29	10	12	1	9	16	1	39	-	-	23	9
6	Fig. 4-14	3.7	28	2	36	45	35	34	55	6	-	-	30	29
7	Fig. 4-15	4.6	3	17	47	24	17	12	16	17	-	-	91	93

*Type-3 is deleted from the correlation analysis since only one unit among 108 units tested (0.9%) has shown this characteristic.

6.3 Life-test No. 2 (G321)

The G321, high speed signal diode used in the life-test No.2, is rated for a maximum breakdown voltage of 50 volts at 0.1-ua. Actual life-test was performed by the manufacturer for 1000 hours with time intervals of 250 hours. According to the manufacturer's life-test report, one out of 500 units failed. The author selected 10 units of relatively low degradation (0 to 1.8%) and 10 units of relatively high degradation (-17.2 to 37%) as shown in Table 6-7, and tested S_v(1-kHz) for each of these 20 units. None of them showed multiple-peak phenomenon of the noise-voltage spectral density (the manufacturer claims that G321 is designed to be a high reliability unit).

Four parameters, listed in Table 6-8, were correlated, and R_{xy} are shown in Table 6-9. The correlation analysis indicates that the initial leakage (I_r(0) in Table 6-8) has the highest correlation with respect to percent-degradation (92%). S_v(1-kHz) is rather insensitive as a prediction factor for percent-degradation for G321.

The following conclusions are obtained from the life-test No.2:

(1) If a unit is designed for high reliability unit (as the manufacturer claims), the multiple-peak phenomenon can not be observed,

(2) The initial leakage is highly correlated with percent-degradation for G321,

(3) S_v(1kHz) were measured after life-test was done. This fact may be a reason why R_{xy} between S_v(1-kHz) and percent-degradation shows such low correlation.

Table 6-7 Typical high, and low percentage-degradation units selected from G321

Low percentage-degradation units

Sample No.	Percentage-degradation	S_v(1-kHz)*$_{10\text{-ua}}$
517	0.0	20
519	0.6	7
530	0.7	12
534	1.2	20
536	0.0	17
552	1.3	9
558	1.1	16
562	1.8	12
586	0.7	4
769	0.0	6

High percentage-degradation units

Sample No.	Percentage-degradation	S_v(1kHz)$_{10\text{-ua}}$
467	9.8	8
494	6.1	12
612	14.4	23
686	-17.2	12
783	15.7	24
784	37.7	40
812	24.8	18
833	37.2	17
834	32.8	5
900	23.1	37

*S_v(1-kHz) is measured at I_r=10 ua in uv/Hz$^{\frac{1}{2}}$.

Table 6-8 Four parameters measured in life-test No.2

Parameter	Description	Average	Standard-deviation
1. $I_r(0)$	Initial leakage current at V_b=50 volts.	18.41 (na)	6.53
2. $I_r(1000)$	Leakage current at V_b=50 volts after 1000-hour life-test.	19.05 (na)	6.80
3. S_v(1-kHz)*	Noise-voltage spectral density measured at I_r=10 ua after 1000-hour life-test.	16.61 ($uv/Hz^{1/2}$)	23.10
4. Percent-degradation	$\frac{I_r(1000)-I_r(0)}{I_r(0)\times 10^{-2}}$	4.44 (%)	12.24

* Notice these S_v(1kHz) were measured after life-test was performed.

Table 6-9 R_{xy} among the four parameters listed in Table 6-8

	$I_r(1000)$	S_v(1-kHz)*	%-DEG**
$I_r(0)$	92%	22%	12%
$I_r(1000)$	-	14%	9%
S_v(1-kHz)*	-	-	5%

** Percentage-degradation

6.4 Life-test No.3 (S2A)

Two hundred units of S2A, diffused silicon rectifiers used in life-test No.3, were rated for I_f=2 amperes and V_b=200 volts at I_r=100x10^{-6} amperes.

When the author was performing life-test No.3, the multiple-peak phenomenon of the noise-voltage spectral density was not known, and S_v(1-kHz) were measured at three discrete current levels (I_r=1-ua, 10-ua, and 100-ua) rather than continuous monitoring conditions. The author regrets that much valuable information, such as multiple-peak phenomenon of the noise-voltage spectral density, was lost in life-test No.3.

Thirteen parameters, listed in Table 6-10, were measured before life-test No.3 was performed. The average and the standard-deviation of these thirteen parameters are shown in Table 6-11.

During the life-test period, 200 volts of reverse-bias alone was applied at room temperature, and the variation of the thirteen parameters listed in Table 6-11 was monitored with time intervals of 100 hours for 1000 hours. The life-test data is shown in Appendix K.

Table 6-12 shows R_{xy} between the thirteen parameters and percentage-degradation. Fig. 6-1 shows the variation of some parameters as time goes on.

The following conclusions are obtained from the life-test No.3:

(1) Stress-factor, which is defined as the ratio of the life-test voltage (200 volts) over the breakdown voltage measured at the specified reverse current level (10-ua), has been found to have almost no correlation (2%) with respect to percent-degradation,

(2) The noise-voltage spectral density measured at 1-kHz and I_r=10-ua showed the highest correlation (16%) with respect to percent-degradation.

Table 6-10 Thirteen parameters measured before life-test No.3

Parameter	Description
1. V_b(1-ua)	Reverse-bias at I_r=1-ua.
2. $S_v(10\text{-Hz})_{1\text{-ua}}$	Noise-voltage spectral density at 10-Hz and I_r=1-ua.
3. $S_v(1\text{-kHz})_{1\text{-ua}}$	Noise-voltage spectral density at 1kHz and I_r=1-ua.
4. $r_{1\text{-ua}}$	Ratio of the parameters 2 and 3.
5. $E.N.F^*_{1\text{-ua}}$	Excess noise figure at 1-ua. $= \frac{S_v(1\text{-kHz})_{1\text{-ua}} \times 10^4}{V_b(1\text{-ua})^2}$
6. V_b(10-ua)	Reverse-bias at I_r=10-ua.
7. $S_v(10\text{-Hz})_{10\text{-ua}}$	Noise-voltage spectral density at 10-Hz and I_r=10-ua.
8. $S_v(1\text{-kHz})_{10\text{-ua}}$	Noise-voltage spectral density at 1-kHz and I_r=10-ua.
9. $r_{10\text{-ua}}$	Ratio of the parameters 7 and 8.
10. $E.N.F_{10\text{-ua}}$	Excess noise figure at 10-ua. $= \frac{S_v(1\text{-kHz})_{10\text{-ua}} \times 10^4}{V_b(10\text{-ua})^2}$
11. Z_j(10-ua)	Differential impedance $= \frac{V_b(10\text{-ua}) - V_b(1\text{-ua})}{9 \times 10^{-6}}$
12. $I_r(V_b$=200v)	I_r at 200 volts reverse-bias.
13. Stress-factor	200 volts/V_b(10-ua).

* Excess noise figure is defined in accordance with Eq. (5-1). ENF is a measure of an excess noise over the theoretical minimum .

Table 6-11 Average and Standard-deviation of the thirteen parameters listed in Table 6-10

Parameter	Average	Standard-deviation
1. V_b(1-ua)	210.16 volts	66.66
2. S_v(10-Hz)$_{1\text{-ua}}$	54.41 uv/Hz$^{1/2}$	147.93
3. S_v(1-kHz)$_{1\text{-ua}}$	9.36 uv/Hz$^{1/2}$	14.68
4. $r_{1\text{-ua}}$	6.38	5.26
5. E.N.F.$_{1\text{-ua}}$	0.00	0.03
6. V_b(10-ua)	257.97 volts	62.49
7. S_v(10-Hz)$_{10\text{-ua}}$	149.86 uv/Hz$^{1/2}$	332.41
8. S_v(1-kHz)$_{10\text{-ua}}$	49.00 uv/Hz$^{1/2}$	91.35
9. $r_{10\text{-ua}}$	4.10	3.67
10. E.N.F.$_{10\text{-ua}}$	0.15	0.95
11. Z_j(10-ua)	5.31×10^6 ohms	6.33×10^6
12. I_r(V_b=200v)	19.32×10^{-6} amperes	60.78
13. Stress factor	1.56	1.41

Table 6-12 R_{xy} between the thirteen parameters listed in Table 6-10 and percentage-degradation

Parameter	R_{xy}
1. V_b(1-ua)	3 %
2. S_v(10-Hz)$_{1\text{-ua}}$	13 %
3. S_v(1-kHz)$_{1\text{-ua}}$	12 %
4. $r_{1\text{-ua}}$	6 %
5. E.N.F.$_{1\text{-ua}}$	12 %
6. V_b(10-ua)	2 %
7. S_v(10-Hz)$_{10\text{-ua}}$	14 %
8. S_v(1-kHz)$_{10\text{-ua}}$	16 %
9. $r_{10\text{-ua}}$	9 %
10. E.N.F.$_{10\text{-ua}}$	12 %
11. Z_j(10-ua)	1 %
12. I_r(V_b=200v)	5 %
13. Stress factor	2 %

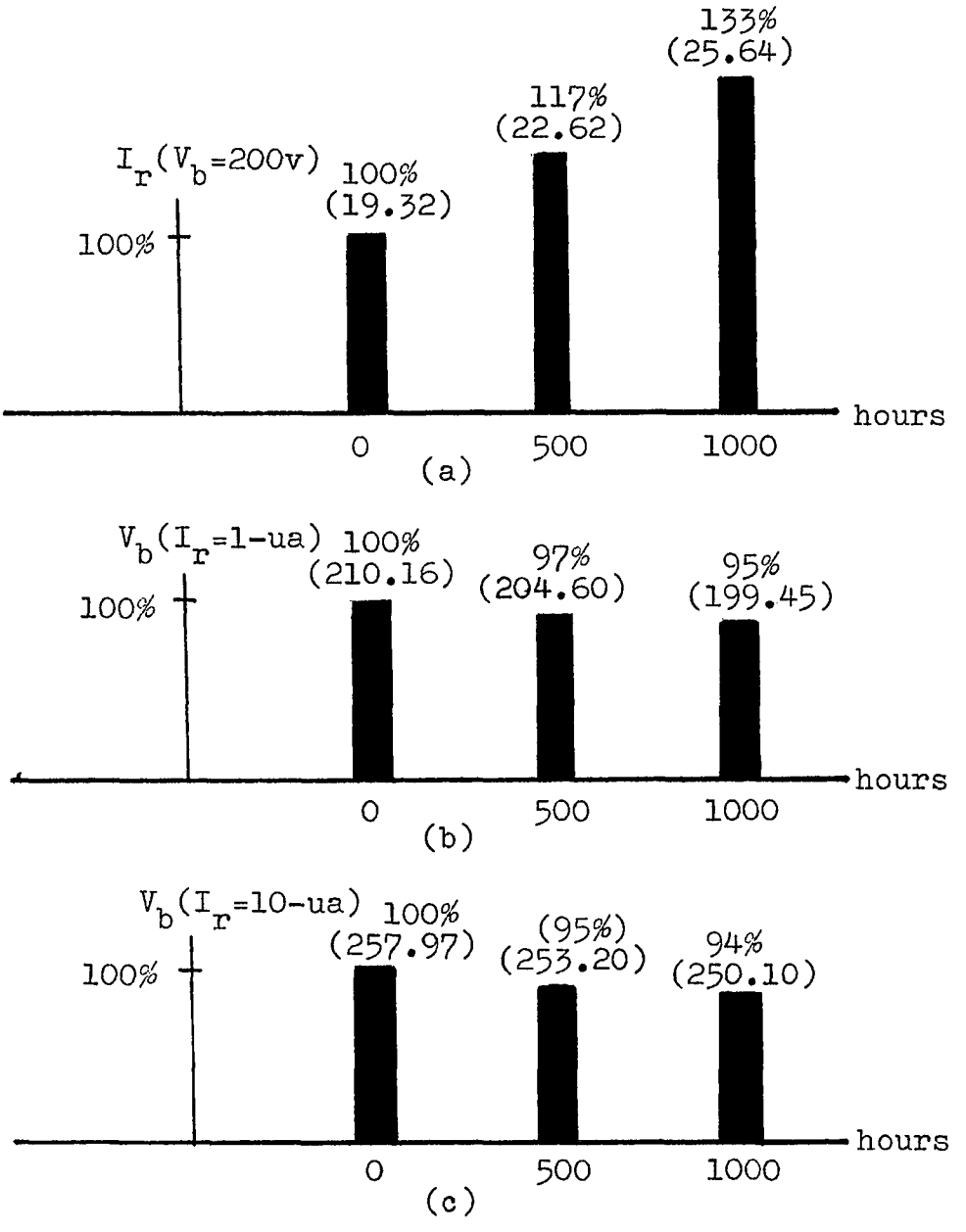

Fig. 6-1 The variation of some parameters during 1000-hours life-test period. (a) Leakage measured at V_b=200 volts, (b) Breakdown voltage measured at I_r=1-ua, and (c) Breakdown voltage measured at I_r=10-ua.

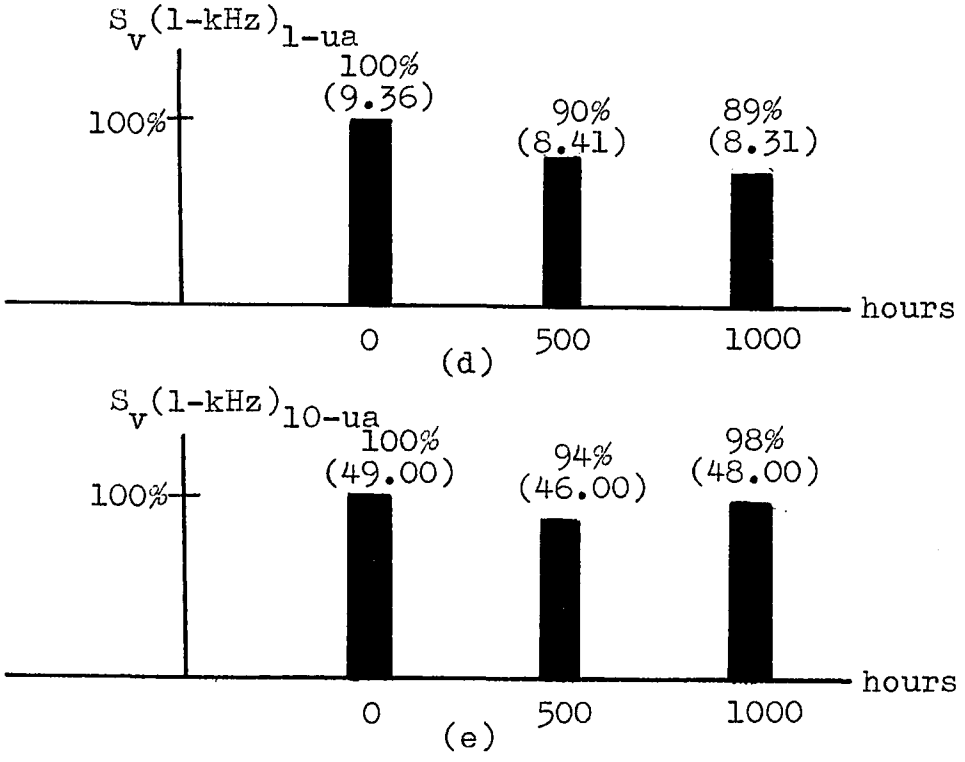

Fig. 6-1 Continued:
(d) S_v(1-kHz) measured at I_r=1-ua,
(e) S_v(1-kHz) measured at I_r=10-ua.

CHAPTER 7

CONCLUSIONS AND RECOMMENDATION

Conclusions

(1) Existing noise theories such as thermal-noise, shot-noise, and 1/f-noise are not adquate to explain the noise-voltage spectral density, $S_v(w)$, observed in a p-n junction under the avalanche breakdown conditions.

(2) Four factors which are considered to be the main stochastic processes involved in $S_v(w)$ were analyzed. They are:

(a) The number of carriers, K, entering the multiplication zone during the time interval of 2T is a random variable. The probability distribution of K was treated as Poisson type, assuming the average number of carriers entering the multiplication zone during the time interval of 2T is constant. This implies that the random process in question is stationary,

(b) The entry time of each primary carrier into the multiplication zone, t_k, is a random variable. The probability distribution of t_k was shown to be an uniform distribution under the assumption that the probability distribution of K is Poisson type,

(c) A primary carrier having entered the multiplication zone at time t_k produces an avalanche with a

total number of carriers M_k emerging from the multiplication zone. The mean-square of the fluctuation of M_k, $E(M_k^2)$, plays a significant role in the derivation of $S_v(w)$. Assuming the probability distribution of M_k is also a Poisson type, $E(M_k^2)$ was found to be $E(M_k)\{E(M_k)+1\}$,

(d) The carrier transit times, t_{as}, as well as the ionization time delays, t_{ds}, each associated with M_k random ionization events, have statistical distribution. To obtain an analytical expression of $S_v(w)$, t_{ds} was replaced by $E(t_{ds})$.

(3) The noise-current pulses, I(t), due to the above mentioned rather complicated multi-fold random process was approximated by

$$I(t) = \sum_{k=1}^{K} M_k i(t-t_k) \qquad (7\text{-}1)$$

where

$$i(t) = \frac{2q}{\bar{t}_{as}^2}\, t$$

between $0 \le t \le \bar{t}_{as}$, and otherwise zero.

(4) The noise-current spectral density, $S_i(w)$, was derived from the autocorrelation function of the noise-current pulses, R(s), by the Wiener-Khintchine theorem. The R(s) and $S_i(w)$ were found to be:

$$R(s) = E(M_k^2)\frac{E(K)}{2T}\frac{4q^2}{\bar{t}_{as}^4}\left\{\frac{\bar{t}_{as}^3}{3} - \frac{\bar{t}_{as}^2}{2}s + \frac{1}{6}s^3\right\}$$

$$+E(M_k \cdot M_j)_{k\neq j}\frac{E(K^2-K)}{4T^2}q^2 \qquad (7\text{-}2)$$

and

$$S_i(w) = E(M_k^2)\frac{E(K)}{2T}\frac{4q^2}{(w\bar{t}_{as})^4}\left\{(w\bar{t}_{as})^2+2(1-\cos w\bar{t}_{as}\right.$$

$$\left.-(w\bar{t}_{as})\sin w\bar{t}_{as})\right\} + E(M_k \cdot M_j)_{k\neq j}\frac{E(K^2-K)}{4T^2}q^2\delta(w)$$

(7-3)

(5) The noise-voltage spectral density, $S_v(w)$, was determined from the linear operation

$$S_v(w) = H(jw)H^*(jw)S_i(w) \qquad (7\text{-}4)$$

where $H(jw)$ is a transfer impedance given by

$$H(jw) = \frac{Z(jw)}{1 + \frac{R_s}{R_L} + \frac{Z(jw)}{R_L}} \qquad (7\text{-}5)$$

and $Z(jw)$, R_s, R_L, and $H^*(jw)$ denote the junction impedance, the series resistance, the d-c current limiting resistance, and the complex conjugate of $H(jw)$.

(6) If we restrict ourselves to the frequency range of interest, 30-Hz to 100-kHz, $S_v(w)$ can be simplified

as follows:

$$S_v(w)\Big|_{\text{low-frequency}} = \frac{kV_b^2}{I_r} \qquad (7\text{-}6)$$

where k is the spectral proportionality constant, V_b is the breakdown voltage, and I_r is the breakdown current.

(7) Although the noise-voltage spectral density found in the majority of p-n junctions under the avalanche breakdown conditions follows the theoretical prediction, $S_v(1\text{-kHz}) \alpha I_r^{-1}$, some units have shown the multiple-peak phenomenon at different current levels. It was shown that the multiple-peak phenomenon is due to microplasmic breakdown channels.

(8) The life-test experiments indicate that the units whose noise-voltage spectral density measured at 1-kHz have multiple-peak phenomenon are relatively highly correlated with respect to the percentage-degradation.

Recommendation

Since the multiple-peaks phenomenon was found to be highly correlated with respect to the percentage-degradation, one should be able to eliminate unreliable units from the batch by inspecting the units for multiple-peak phenomenon. Consequently, one can increase the reliability of those remaining p-n junction devices which successfully pass this screening test.

APPENDIX A

Quantum Mechanical Consideration of Thermal Noise

A rigorous derivation of Eq. (2-3) has been carried out by Ekstein and Rostoker.[5] The author will show here a simplified derivation of Eq. (2-3) assuming that the carriers are under the harmonic oscillation at thermal equilibrium. The harmonic oscillator of mass m, and compliance k has an equation of motion given by

$$\frac{d^2x}{dt^2} = -\frac{k}{m}x \qquad \text{(A-1)}$$

The resonance frequency, f, is given by

$$f = \frac{1}{2\pi}(k/m)^{1/2} \qquad \text{(A-2)}$$

or

$$k = f^2(2\pi)^2 m \qquad \text{(A-3)}$$

The potential energy is given by

$$V(x) = \tfrac{1}{2}kx^2 = 2\pi^2 mf^2x^2 \qquad \text{(A-4)}$$

If we substitute Eq. (A-4) into the Schrödinger Equation,

$$\frac{d^2\phi}{dx^2} + \frac{2m}{\hbar^2}(E - 2\pi^2 mf^2x^2)\phi = 0 \qquad \text{(A-5)}$$

where $\hbar = h/2\pi$.

If we substitute

$$s = (2\pi mf/\hbar)^{1/2} x \tag{A-6}$$

into Eq. (A-5), it becomes

$$\frac{d^2\phi}{ds^2} + (C-s^2) = 0 \tag{A-7}$$

where

$$C = 2E/hf \tag{A-8}$$

To lead Eq. (A-7) into Hermit differential equation, let substitute

$$\phi = e^{-\frac{1}{2}s^2} H \tag{A-9}$$

into Eq. (A-7). H must satisfy Eq. (A-7) such way that ϕ approaches zero as s approaches to infinity. Substitution of Eq. (A-9) into (A-7) leads

$$\frac{d^2H}{ds^2} - 2s\frac{dH}{ds} + (C-1)H = 0 \tag{A-10}$$

This can be solved by a series solution

$$H = \sum_{r=0}^{\infty} A_r s^r \tag{A-11}$$

Substitution of Eq. (A-11) into (A-10) gives

$$\sum_{r=0}^{oo} (r+1)(r+2)A_{r+2}+(C-1-2r)\ s^r = 0 \tag{A-12}$$

or

$$A_{r+2} = \frac{2r+1-C}{(r+1)(r+2)}A_r \tag{A-13}$$

H to remain finite, it is necessary to stipulate $A_{r+2}=0$ when $A_r \neq 0$, which leads

$$\frac{2r+1-C}{(r+1)(r+2)} = 0 \qquad \text{(A-14)}$$

or

$$C = 2r+1 = \frac{2E}{hf}$$

or

$$E = hf(r+\tfrac{1}{2}) \quad \text{for } r=0, 1, 2, \ldots \qquad \text{(A-15)}$$

This result shows that the energy state is a half multiple of hf. This is differ from old Bohr's theory which states that the quantized energy level were rhf (This Bohr's theory was wrong). This result can explain the fact that even in the ground-state at the absolute zero temperature there is a residual zero-point energy, $E_o = \frac{1}{2}hf$.

Let consider the energy level given in Eq. (A-15) is some integer multiple m of the energy hf plus zero temperature residual energy ½hf. The number of oscillators having the energy mhf is given by the Boltzman distribution law,

$$N_m = N_o e^{-mhf/kT} \qquad \text{(A-16)}$$

where N_o is the number of oscillators per unit volume at m=0 level. The energy contributed by the N_m oscillators is given by

$$(mhf)(N_m) = mhfN_o e^{-mhf/kT} \qquad \text{(A-17)}$$

Therefore the average energy $\bar{E}$ of an oscillator is

$$\bar{E} = \frac{\sum_{m=0}^{\infty} mhfN_o e^{-mhf/kT}}{\sum_{m=0}^{\infty} N_o e^{-mhf/kT}} + \tfrac{1}{2}hf$$

$$= \frac{0+hfe^{-hf/kT}+2hfe^{-2hf/kT}+\cdots}{1+e^{-hf/kT}+e^{-2hf/kT}+\cdots\cdots\cdots} + \tfrac{1}{2}hf$$

$$= \frac{hf}{e^{-hf/kT}-1} + \tfrac{1}{2}hf$$

$$= hf\left(\tfrac{1}{2} + \frac{1}{e^{-hf/kT}-1}\right) \qquad \text{(A-18)}$$

Notice Eq. (A-18) approaches kT when $hf \ll kT$.

APPENDIX B

Shot-noise in p-n Junctions

Investigations of Shot-noise in p-n junctions have been carried out by Montgomery and Clark,[26] Giacoletto,[9] Petritz,[31,32] and Van der Ziel.[41-45]

A derivation of Eq. (2-5) will be shown here essentially following Van der Ziel's procedure[44] employing transmission line analogy. Bennet[3] simplified the derivation by Van der Ziel, with some "ad hoc" postulates.

Let consider the one dimensional diffusion of minority carriers injected into p-n junction. We will assume the drift of minority carriers be negligible in comparison with diffusion in forward biased condition. We have the diffusion equations[30,33]

$$\frac{\partial p}{\partial t} = -(p-p_n)/t_p - (1/e)\frac{\partial i_p}{\partial x} \qquad \text{(B-1)}$$

$$i_p = -eD_p\frac{\partial p}{\partial x} \qquad \text{(B-2)}$$

where D_p is the hole (minority carrier in n-region) diffusion coefficients, t_p is the hole life-time, e is the electronic charge, i_p is the hole current, p_n is the equilibrium hole concentration, and p is the actual hole

concentration (both per unit length). Introducing the excess hole concentration

$$p' = p - p_n \tag{B-3}$$

we can write Eq. (B-1) and Eq. (B-2) as

$$\begin{cases} \dfrac{\partial p'}{\partial x} = -(1/eD_p)i_p & \text{(B-4)} \\ \text{and} \\ \dfrac{\partial i_p}{\partial x} = (e/t_p)p' - e\dfrac{\partial p'}{\partial t} & \text{(B-5)} \end{cases}$$

Now let consider a transmission line with negligible distributed self-inductance shown in Fig. B-1. The differential equation for the given transmission line is

$$\begin{cases} \dfrac{\partial E}{ox} = -RE & \text{(B-6)} \\ \dfrac{\partial I}{\partial x} = -GE - C\dfrac{\partial E}{ot} & \text{(B-7)} \end{cases}$$

where E is the voltage, I is the current, R, G, and C are resistance, conductance, and capacitance per unit length. Comparing Eqs. (B-4), (B-5), (B-6), and (B-7), one will see the following correspondense.

$$\begin{array}{l} E \cdots\cdots p' \\ I \cdots\cdots i_p \\ R \cdots\cdots \cdots (1/eD_p) \\ G \cdots\cdots e/t_p \\ C \cdots\cdots e \end{array} \tag{B-8}$$

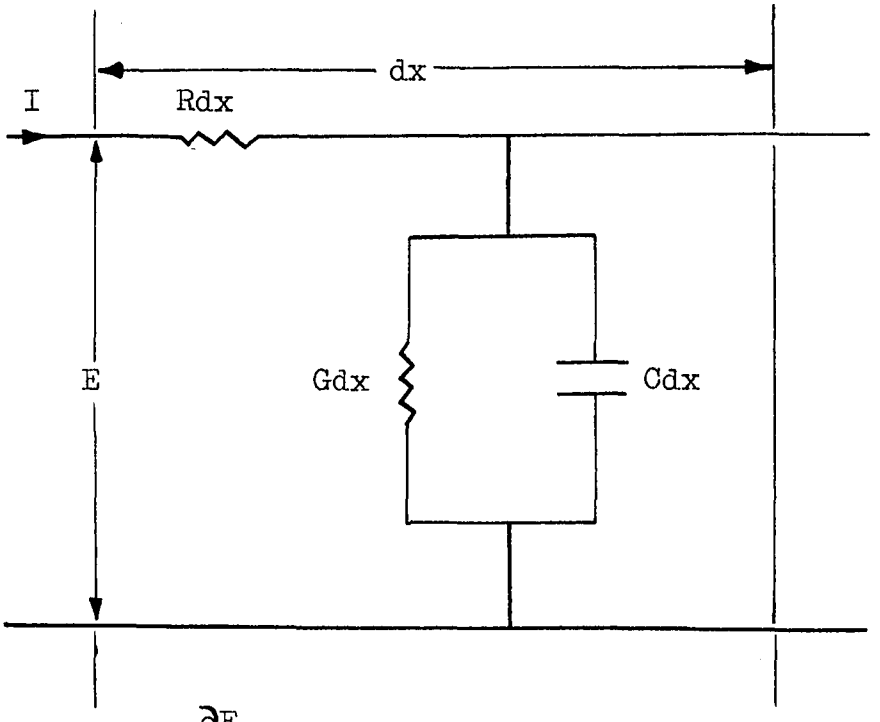

$$\frac{\partial E}{\partial x} = -RI$$

$$\frac{\partial I}{\partial x} = -GE - C\frac{\partial E}{\partial t}$$

$$Z_o = Z(jw)^{1/2}/Y(jw)^{1/2}$$

$$r = Z(jw)^{1/2} \cdot Y(jw)^{1/2}$$

Fig. B-1 Transmission line without self-inductance.

To solve the problem of hole flow in n-type material, we solve the corresponding transmission line problem by standard methods and then translate back to the original p-n junction problem. Two important quantities in the transmission line problem are[34] the characteristic-impedance, $Z_o=R^{1/2}/(G+jwC)^{1/2}$, and the propagation-constant, $r=R^{1/2}(G+jwC)^{1/2}$. In diffusion problem the corresponding quantities are

$$Z_o = \left\{e^2 D_p(1+jwt_p)/t_p\right\}^{-1/2} \qquad \text{(B-9)}$$

$$r = \left\{(1+jwt_p)/D_p t_p\right\}^{1/2} \qquad \text{(B-10)}$$

which may be defined as characteristic-impedance and propagation-constant of the semiconductor.

In p-n junctions, the current is considered to be carried by holes and n-region is infinitely long for all practical purpose (that is the length of n-region is greater than hole diffusion-length $D_p^{1/2}t_p^{1/2}$). We put the origin of coordinate system at the point at which the holes are injected into the n-region. If no voltage is applied to the junction, the concentration at x=0 is equal to the equilibrium concentration p_n. If a voltage V is applied to the diode, the hole concentration at x=0 becomes

$$p = p_n \mathrm{EXP}(eV/kT) \qquad \text{(B-11)}$$

In particular a d-c voltage V_o and a small a-c voltage, $V_1 EXP(jwt)$, are applied, Eq. (B-11) may be written as

$$p = p_n + p_o' + p_1' EXP(jwt) \qquad (B\text{-}12)$$

where

$$p_o' = p_n\left\{EXP(eV_o/kT) - 1\right\} \qquad (B\text{-}13)$$

$$p_1' = p_n(eV_1/kT)EXP(eV_o/kT) \qquad (B\text{-}14)$$

From the transmission line analogy, we know that an infinite transmission line of the characteristic-impedance Z_o with applied voltage E gives input current of $I=E/Z_o$. Applying this fact directly to p-n junction, we have for the d-c hole current at x=0,

$$I_p = p_o'/Z_{oo} = I_{po}\left\{EXP(eV_o/kT)-1\right\} \qquad (B\text{-}15)$$

where

$$I_{po} = ep_n(D_p/t_p)^{1/2} \qquad (B\text{-}16)$$

$$Z_{oo} = Z_o(jw=0) = \left(\frac{e^2 D_p}{t_p}\right)^{-1/2} \qquad (B\text{-}17)$$

In the same way, we have the a-c hole current at x=0,

$$i_p = I_1 EXP(jwt) = p_1' EXP(jwt)/Z_o \qquad (B\text{-}18)$$

$$= G_o(1+jwt_p)^{1/2} V_1 EXP(jwt) \qquad (B\text{-}19)$$

Consequently, a-c conductance of junction becomes

$$Y = G + jB = \frac{I_1}{V_1} = G_o(1+jwt_p)^{1/2} \qquad (B\text{-}20)$$

where G_o is the d-c conductance of the junction given by

$$G_o = (e/kT)e(D_p/t_p)^{1/2}p_n EXP(eV_o/kT) \qquad (B-21)$$

$$= (e/kT)(I_p+I_{po}) \qquad (B-22)$$

Eq. (B-20) may be rewritten as

$$G = G_o(1/2(1+w^2t_p^2)^{1/2}+1/2)^{1/2} \qquad (B-23)$$

$$B = G_o(1/2(1+w^2t_p^2)^{1/2}-1/2)^{1/2} \qquad (B-24)$$

Eqs. (B-22) and (B-23) are refered in Eq. (2-6).

Finally the d-c hole concentration in the n-region is given by

$$p'(x) = p'EXP(-r_o x) = p_o'EXP(-x/(D_p t_p)^{1/2}) \qquad (B-25)$$

The shot-noise in the p-n junction is caused by two mechanisms. One mechanism is random hole-electron pair recombination and generation, another mechanism is random diffusion. Both mechanisms are statistically independent. Their effect should, therefore, be discussed separately and the results will be added quadratically.

(1) The random hole-electron recombination and generation:

We split the semiconductor n-region into section of dx. For stationary current flow $\partial p'/\partial t=0$ in Eq. (B-5),

$$\frac{\partial i_p}{\partial x} = -\left(\frac{e}{t_p}\right)p' \qquad (B-26)$$

or the current fluctuation between x+dx and x is

$$\frac{e(p'+p_n)}{t_p}\,dx - \frac{ep_n}{t_p}dx \qquad \text{(B-27)}$$

The first term is considered to be hole-electron pair recombination and the second term is considered to be hole-electron pair generation. Since pair recombination and pair generation are independent random processes, the two current fluctuate independently. Because the indivisual events are independent and random, one should expect full shot-noise effect for these currents. Current spectral density of these fluctuating current are

$$S_{i,dx} = 2e\left\{e(p'+p_n)/t_p + ep_n/t_p\right\}dx \qquad \text{(B-28)}$$

$$= \left\{\frac{2e^2(p'+2p_n)}{t_p}\right\}dx \qquad \text{(B-29)}$$

In the transmission line analogy, a current generator dI_i (corresponds to $S^{1/2}_{i,dx}$) connected across the line at distance x from the input gives rise to a current dI in the lead short circuiting the input as shown in Fig. B-2,

$$dI = dI_i \mathrm{EXP}(-rx) \qquad \text{(B-30)}$$

$$S_{i,o} = S_{i,dx}\mathrm{EXP}(-2rx) \qquad \text{(B-31)}$$

$$= \frac{2e^2(p'+2p_n)}{t_p}\mathrm{EXP}(-2ax) \qquad \text{(B-32)}$$

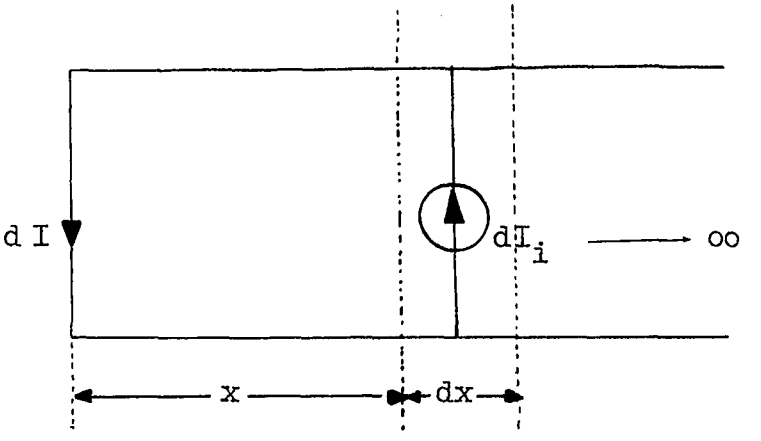

Fig. B-2-a Transmission line analogy of recombination fluctuation.

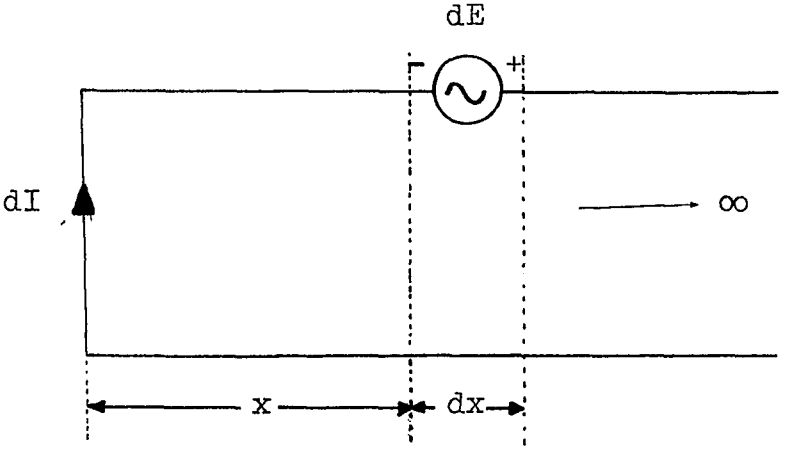

Fig. B-2-b Transmission line analogy of diffusion fluctuation.

where a is the real part of r:

$$a = \frac{\left\{(1+w^2t_p^2)^{1/2}+1\right\}^{1/2}}{(2D_pt_p)^{1/2}} = r_o\left(\frac{G}{G_o}\right) \qquad \text{(B-33)}$$

(2) Effect of random diffusion process:

We split the n-region into section of length dx and calculate the density dluctuation. The result is

$$S_{v,dx} = \left\{\frac{4(p'+p_n)}{D_p}\right\}dx \qquad \text{(B-34)}$$

In the transmission analogy, a fluctuating emf dE in series with line between x and x+dx in lead short circuit input as shown in Fig. B-2-b,

$$dI = \frac{dE}{Z_o}\,EXP(-rx) \qquad \text{(B-35)}$$

Therefore, current-spectral density in the lead short-circuiting the input of the junction, due to diffusion fluctuation is

$$S_{v,o} = \left\{\frac{S_{v,dx}}{Z_o^2}\right\}EXP(-2ax)$$

$$= \frac{4e^2(p'+p_n)}{t_p}\,(1+w^2t_p^2)^{1/2}EXP(-2ax) \qquad \text{(B-36)}$$

We now add Eqs. (B-32) and (B-36) and integrate with respect to x. This yields for spectral density of hole current fluctuation at x=0 which is equal to the current fluctuation in the external circuit. Thus,

$$S_{total} = S_{i,o}+S_{v,o}$$

$$= \frac{2e^2}{t_p}\left\{\int_0^\infty (p'+2p_n)\mathrm{EXP}(-2ax)dx \right.$$

$$\left. +2(1+w^2t_p^2)^{1/2}\int_0^\infty (p'+p_n)\mathrm{EXP}(-2ax)dx\right\}$$

$$= 4kTG + 2eI_p \qquad \text{(B-37)}$$

Eq. (B-37) is refered as Eq. (2-6) in chapter 2.

APPENDIX C

Probability Distribution of Carrier Entry Times

Suppose that the time interval (t,t+a) is partitioned into K adjacent subintervals a_1, a_2,....., a_K, and each carrier entry times, t_k, falls into a_k.

$$\sum_{k=1}^{K} a_k = a \qquad \text{(C-1)}$$

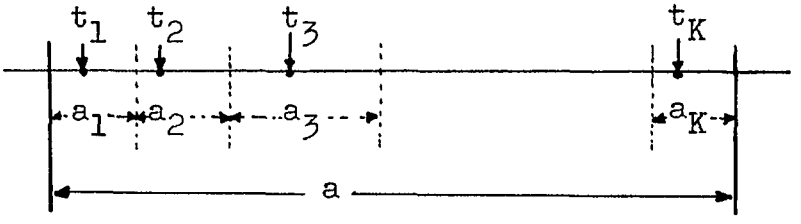

From the definition of conditional probability,

$$p(1,a_1;1,a_2;.....,1,a_K/K,a) = \frac{p(K,a;1,a_1;....,1,a_K)}{p(K,a)} \qquad \text{(C-2)}$$

Since a_k is statistically independent from K,

$$p(K,a;1,a_1;.....,1,a_K) = \prod_{k=1}^{K} p(1,a_k) \qquad \text{(C-3)}$$

Substituting Eq. (C-3) into Eq. (C-2), we have

$$p(1,a_1;1,a_2;.....,1,a_K/K,a) = \frac{\prod_{k=1}^{K} p(1,a_k)}{p(K,a)} \qquad \text{(C-4)}$$

$$= \frac{\prod_{k=1}^{K} \frac{(\bar{n}\cdot a_k)^1 EXP(-\bar{n}\cdot a_k)}{1\ !}}{\frac{(\bar{n}\cdot a)^K EXP(-\bar{n}\cdot a)}{K\ !}}$$

$$= \frac{K!}{a^K} \prod_{k=1}^{K} a_k \qquad \text{(C-5)}$$

since we have assumed that $p(K,2T)$ is Poisson type with $E\left[p(K,2T)\right] = \bar{n}$.

The same result may be obtained if we assume that the carrier entry times, t_k, are statistically independent random variable with an uniform distribution

$$p(t_k) = \begin{cases} \frac{1}{a} & \text{for } t \le t_k \le t+a \\ 0 & \text{otherwise} \end{cases} \qquad \text{(C-6)}$$

since $p(1,a_1;1,a_2;\ldots;1,a_K/K,a) = p(1,a_1,1,a_2;\ldots\ldots;1,a_K)$ and

$$p(1,a_1;1,a_2;\ldots;1,a_K) = K\frac{a_1}{a}(K-1)\frac{a_2}{a}\cdot\ldots\ldots(K-k)\frac{a_k}{a}\ldots\ldots$$

$$= \prod_{k=1}^{K}\left\{K-(k-1)\right\}\frac{a_k}{a}$$

$$= \frac{K!}{a^K}\prod_{k=1}^{K} a_k \qquad \text{(C-7)}$$

APPENDIX D

Current Pulse Induced at External Circuit due to the Motion of a Carrier

We will assume an one-dimensional p-n junction whose depletion layer width is d, and the applied potential across the depletion layer is V_j. The potential distribution, V(x), in the depletion layer may be obtained from the Poisson equation. However, if electric-field is high enough that we can neglect the effect of space-charge, the Poisson equation may be reduced to the Laplace equation

$$\frac{d^2V(x)}{dx^2} = 0 \qquad \text{(D-1)}$$

The electric field intensity E is given by

$$E = \frac{V_j}{d} \qquad \text{(D-2)}$$

From the Lorentz equation, we obtain

$$\frac{d^2x}{dt^2} = \frac{qV_j}{md} \qquad \text{(D-3)}$$

where m is the effective mass of the carrier, and q is the electronic charge. Eq. (D-3) is the differential equation governing the motion of a carrier in the

depletion layer.

The velocity v and the position x of a carrier at time t may be obtained by direct integration of Eq. (D-3). Thus

$$v = (\frac{qV_j}{md})t \qquad (D-4)$$

and

$$x = (\frac{qV_j}{md})\tfrac{1}{2}t^2 \qquad (D-5)$$

under the assumption that initial drift velocity is negligible. The carrier transit time t_a is given by

$$t_a = (\frac{2m}{qV_j})^{\frac{1}{2}}d \qquad (D-6)$$

The carrier velocity v expressed in Eq. (D-4) can now be expressed in terms of the carrier transit time t_a as

$$v = (\frac{qV_j}{md})t = (\frac{2d}{t_a^2})t \qquad (D-7)$$

The energy U gained by a carrier moving through a potential difference V(x) is

$$U = qV(x) = \frac{qV_j}{d}x \qquad (D-8)$$

This energy is equal to the amount of work U' that must be done to induce the charge q' at the external circuit

when depletion layer potential is V_j. Thus,

$$U = U' = q'V_j \tag{D-9}$$

or

$$q' = \frac{qx}{d} \tag{D-10}$$

The current pulse induced at the external circuit, $i_o(t)$, due to the motion of a carriers is

$$i_o(t) = \frac{dq'}{dt} = \frac{q}{d} v = \frac{2q}{t_a^2} t \tag{D-11}$$

for $0 \leq t \leq t_a$. Eq. (D-11) is refered as Eq. (4-5) in chapter 4.

APPENDIX E

Current Pulse Train due to M_k Random Ionizations

One of the major difficulties in evaluating the current pulse train due to M_k random ionizations expressed as Eq. (4-6), in chapter 4, is that

$$i_{M_k}(t) = \sum_{s=1}^{M_k} \frac{2q}{t_{as}^2}(t-t_{ds})G(t_{ds},t_{ds}+t_{as}) \qquad \text{(E-1)}$$

is a (M_k^2+1)-fold random process. At present, (M_k^2+1)-fold joint probability

$$p(t_{d1},t_{a1};t_{d2},t_{a2};\ldots;t_{dM_k},t_{aM_k}/M_k) \qquad \text{(B-2)}$$

is not determined.

In the early stage of this research, the author attempted to approximate the current pulse train by a random square wave of equal height as shown below:

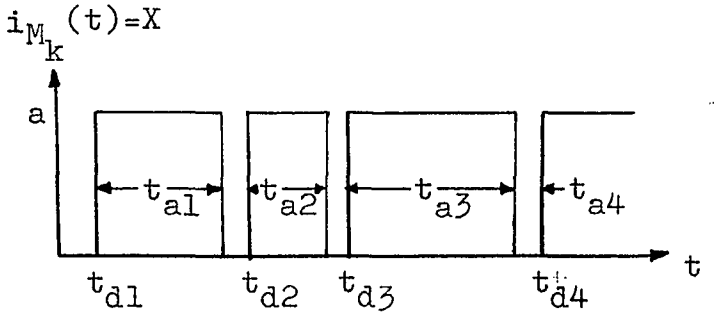

If a transition from a state X=0 to the other state X=a is a random process

$$E(X) = 0 \cdot p(X=0) + a \cdot p(X=a) = a \cdot p(X=a) = \tfrac{1}{2}a \tag{E-3}$$

Furthermore, if we assume that the probability that n transitions occur in a time interval of T is given by the Poisson distribution,

$$p(k,T) = \frac{(\bar{n}T)^k}{k!} \, EXP(-\bar{n}T) \tag{E-4}$$

The autocorrelation function of $i_{M_k}(t)$, R(s), is given by definition,

$$R(s) = E(X_1, X_2) \tag{E-5}$$

where $X_1 = X(t=t_1)$ and $X_2 = X(t=t_1+s=t_2)$. X_1 and X_2 are both discrete random variable having the two possible values, zero, and a. Therefore,

$$\begin{aligned} R(s) &= (0 \cdot 0)p(X_1=0, X_2=0) + (0 \cdot a)p(X_1=0, X_2=a) \\ &\quad + (a \cdot 0)p(X_1=a, X_2=0) + (a \cdot a)p(X_1=a, X_2=a) \\ &= a^2 p(X_1=a, X_2=a) \end{aligned} \tag{E-6}$$

$p(X_1=a, X_2=a)$ is the probability that $X_1=X_2=a$ which is the same as the probability that $X_1=a$ and that an even number of transition occur between $s=t_2-t_1$. Hence,

$$p(X_1=a, X_2=a) = p(X_1=a, k=\text{even})$$

$$= p(X_1=a)p(k=\text{even}) = \tfrac{1}{2}p(k=\text{even}) \qquad \text{(E-7)}$$

since events $X_1=a$ and k=even are statistically independent. Using the Poisson distribution, we have

$$R(s) = \tfrac{1}{2}a^2 \text{EXP}(-\bar{n}|s|) \sum_{k=0}^{\infty} \frac{(\bar{n}|s|)^k}{k!}$$

$$= \tfrac{1}{2}a^2 \left\{ \text{EXP}(\bar{n}|s|) + \text{EXP}(-\bar{n}|s|) \right\}$$

$$= \tfrac{1}{4}a^2 \left\{ 1 + \text{EXP}(-2\bar{n}|s|) \right\} \qquad \text{(E-8)}$$

From the Wiener-Khintchine theorem, the current-spectral density is found to be

$$S_i(w) = \frac{1}{4}a^2 \int_{-\infty}^{+\infty} \left\{ 1 + \text{EXP}(-2\bar{n}|s|) \right\} \text{EXP}(-jws)\,ds$$

$$= \frac{1}{4}\, a^2 \left\{ \delta(w) + \frac{\bar{n}}{\bar{n}^2 + \frac{1}{4}w^2} \right\} \qquad \text{(E-9)}$$

Examination of Eq. (E-9) indicates 1/f type noise spectral density. The idea of using the random square wave of equal height to approximate $i_{M_k}(t)$ was abandoned since an experimental fact presented in Fig. 4-1 contradicts the result shown in Eq. (E-9).

APPENDIX F

Derivation of $S_i(w)$ from R(s) by the Wiener-Khintchine Theorem

The autocorrelation function of the noise current pulse train I(t) was found to be:

$$R(s) = E(M_k^2)\frac{E(K)}{2T}\frac{4q^2}{\bar{t}_{as}^4}\left\{\frac{\bar{t}_{as}^3}{3} - \frac{\bar{t}_{as}^2}{2}s + \frac{1}{6}s^3\right\}$$

$$+ E(M_k \cdot M_j)_{k\neq j}\frac{E(K^2-K)}{4T^2}q^2 \qquad \text{(F-1)}$$

for $0 \leq t \leq \bar{t}_{as}$.

The noise-current spectral density, $S_i(w)$, may be obtained by taking Fourier transform of the autocorrelation function R(s):

$$S_i(w) = 2\int_0^\infty R(s)\cos(ws)ds \qquad \text{(F-2)}$$

since R(s) is an even function with respect to s.

If we rearrange the first term as

$$E(M_k^2)\frac{E(K)}{2T}\frac{2q^2}{3\bar{t}_{as}^4}(2\bar{t}_{as}^3 - 3\bar{t}_{as}^2 s + s^3) \qquad \text{(F-3)}$$

and using the trigonometry identities

$$\int X\cos X dX = X\sin X + \cos X$$

$$\int X^3\cos X dX = X^3\sin X + 3X^3\cos X - 6X\sin X - 6\cos X$$

We have

$$\int_0^{\infty}(2\bar{t}_{as}^3-3\bar{t}_{as}^2 s+s^3)\cos(ws)ds$$

$$=\left\{\frac{6\bar{t}_{as}^4}{(w\bar{t}_{as})^4}+\frac{3\bar{t}_{as}^4}{(w\bar{t}_{as})^4}-\frac{6\bar{t}_{as}^4}{(w\bar{t}_{as})^4}\cos(w\bar{t}_{as})\right.$$

$$\left.-\frac{6\bar{t}_{as}^4}{(w\bar{t}_{as})^3}\sin(w\bar{t}_{as})\right\} \qquad (F-4)$$

For the second term:

$$E(M_k\cdot M_j)_{k\neq j}\frac{E(K^2-K)}{4T^4}\,q^2\int_{-\infty}^{+\infty}e^{-jws}ds$$

$$=E(M_k\cdot M_j)_{k\neq j}\frac{E(K^2-K)}{4T^2}\,q^2\delta(w) \qquad (F-5)$$

$\delta(w)$, the impulse at $w=0$, is due to the average component of the multiplication current.

APPENDIX G

Mean-Square of the Number of Carriers Emerging from the Multiplication Zone Assuming Poisson-Distribution

If we assume the probability that a primary carrier will produce M_k ionization events is given by the Poisson distribution,

$$p(M_k) = \frac{(\overline{M}_k)^{M_k} EXP(-\overline{M}_k)}{M_k!} \qquad (G\text{-}1)$$

the mean-square of the number of carriers emerging from the multiplication zone, $E(M_k^2)$, may be found by the following manner:

$$E(M_k^2) = \sum_{M_k=0}^{\infty} M_k^2 \frac{(\overline{M}_k)^{M_k} EXP(-\overline{M}_k)}{M_k!}$$

$$= \sum_{M_k=0}^{\infty} (M_k^2 - M_k) \frac{(\overline{M}_k)^{M_k}}{(M_k-2)!} + \sum_{M_k=0}^{\infty} M_k \frac{(\overline{M}_k)^{M_k} EXP(-M_k)}{M_k!}$$

$$= (\overline{M}_k)^2 EXP(-M_k) \sum_{M_k=2}^{\infty} \frac{(\overline{M}_k)^{(M_k-2)}}{(M_k-2)!} + \sum_{M_k=0}^{\infty} M_k \frac{(\overline{M}_k)^{M_k} EXP(-\overline{M}_k)}{M_k!}$$

$$= (\overline{M}_k)^2 + \overline{M}_k \qquad (G\text{-}2)$$

APPENDIX H

A DIGITAL COMPUTER PROGRAM FOR MULTI-CORRELATION ANALYSIS

This digital computer program is written by the author to analyze the data obtained during life-test experiment. The average of parameters ($\bar{X}_i$), Standard-deviation (s_{X_i}), Multi-correlation coefficients between the parameters X_i and X_j (R_{ij}), and Standard-error of correlation coefficient (e_{ij}) will be computed as well as some cross products.

Although this program can handle up to 16 parameters, it may be easily re-assembled to increase the size of parameters if larger memory is available. The input-format and output-format of the program are as follows:

Input-Format (card)*

1-st card	N (number of parameters)
2-nd card	X_1, X_2, X_3, X_4, X_5
3-rd card	X_6, X_7, X_8, X_9, X_{10}
4-th card	X_{11}, X_{12}, X_{13}, X_{14}, X_{15}
5-th card	X_{16} (leave for blank)

---

*N: I2

X_1 through X_{16}: F12.8

Output-Format (Card)

Parameter	$\bar{X}_i$	s_{X_i}	$\sum X_i$	$\sum X_i^2$
1	X_1	s_{X_1}	$\sum X_1$	$\sum X_1^2$
.	.	.	.	.
.	.	.	.	.
16	$\bar{X}_{16}$	$s_{X_{16}}$	$\sum X_{16}$	$\sum X_{16}^2$

J (Sample-size)

Parameters between	$R_{i,j}$	$\sum X_i X_j$	$e_{i,j}$
1 2	$R_{1,2}$	$\sum X_1 X_2$	$e_{1,2}$
1 3	.	.	.
. .			
1 N	.	.	.
2 1	.	.	.
(N-1) N	$R_{N-1,N}$	.	$e_{N-1,N}$

The multi-correlation coefficients, $R_{i,j}$, and Standard-deviation, s_{X_i}, were computed from the following formulas:

$$R_{i,j} = \frac{J\sum X_i X_j - (\sum X_i)(\sum X_j)}{\sqrt{J\sum X_i^2 - (\sum X_i)^2}\sqrt{J\sum X_j^2 - (\sum X_j)^2}}$$

$$s_{X_i} = \frac{1}{J}\sqrt{J\sum X_i^2 - (\sum X_i)^2} \qquad \text{if } J > 30$$

$$s_{X_i} = \sqrt{\frac{1}{J(J-1)}\ J\sum X_i^2 - (\sum X_i)^2} \qquad \text{if } J \leqslant 30$$

where J is the sample-size.

```
C       APPENDIX H.
C       CORRELATION ANALYSIS PROGRAM BY Y.D. KIM


C       J= NO.OF VARIABLES OBSERVED
C       CORRELATION ROUTINE
        DIMENSION SUM(16),X(16),SUMXY(16,16)
  777 FORMAT(I3)
  888 FORMAT(I3,4F16.2)
  999 FORMAT(2I3,3F16.2)
        IF(SENSE SWITCH 9)18,18
   18 N=0
        READ,J
C  CLEAR ALL ARRAYS TO 0.0
        DO 1 I=1,J
        SUM(I)=0.0
        DO 1 K=1,J
    1 SUMXY(I,K)=0.0
C  READ A CARD AND FORM SUMS,AND COUNT NO.OF OBSERVATIONS
    3 DO 2 I=1,J
        READ, X(I)
    2 SUM(I)= SUM(I) + X(I)
        DO 4 I=1,J
        DO 4 K=I,J
    4 SUMXY(I,K)= SUMXY(I,K)+ X(I)* X(K)
        N= N+1
        IF (SENSE SWITCH 9) 5,3
C  ALL CARDS READ AND ALL PRODUCTS FORMED
C  NOW COMPUTE CORRELATION COEFFICIENTS
    5 FN =N
        IF(N-30) 25,25,26
   25 FN1=(FN*(FN-1.0))**0.5
        GO TO 27
   26  FN1= FN
   27  JM1 = J-1
        DO 9 I= 1,JM1
        AMEAN = SUM(I)/FN
        DENOM =      ( FN * SUMXY(I,I) -SUM(I)**2)**0.5
        STDEV = DENOM/ FN1
        IF (SENSE SWITCH 1) 12,13
   12 PRINT888,I,AMEAN,STDEV,SUM(I),SUMXY(I,I)
   13 PUNCH888,I,AMEAN,STDEV,SUM(I),SUMXY(I,I)
        KK= I+1
        DO 9 K=KK,J
        DENM2 =     (FN* SUMXY(K,K)-SUM(K)**2)**0.5
    9 SUMXY(K,I)= (FN*SUMXY(I,K)- SUM(I)*SUM(K))/(DENOM * DENM2)
```

```
C       ALL BUT THE LAST VARIABLE.DO THAT NEXT.
        AMEAN= SUM(J)/FN
        STDEV= DENM2/FN1
        IF(SENSE SWITCH 1) 10,11
   10   PRINT888,I,AMEAN,STDEV,SUM(J),SUMXY(J,J)
        PRINT777,N
   11   PUNCH888,I,AMEAN,STDEV,SUM(J),SUMXY(J,J)
        PUNCH777,N
C   OUTPUT THE CORRELATION COEFFICIENT AND SUM OF CROSS PRODUCTS
        DO15I=1,JM1
        KK= I+1
        DO 15 K= KK,J
        SIGMA   = (1.0-SUMXY(K,I)**2)/(FN**0.5)
        IF(SENSE SWITCH 1) 16,17
   16   PRINT999,I,K,SUMXY(K,I),SUMXY(I,K),SIGMA
   17   PUNCH999,I,K,SUMXY(K,I),SUMXY(I,K),SIGMA
   15   CONTINUE
        PAUSE
        IF(SENSE SWITCH 2) 3,18
        END
```

APPENDIX I

G315 Life-Test Data

(1) Input Data Format

x_1 x_2 x_3 x_4 x_5

x_6 x_7 x_8 x_9 x_{10}

x_{11} x_{12} x_{13} x_{14} x_{15}

x_{16}

(2) Description of Input-data

x_1: Sample number

x_2: Noise-voltage spectral density at 1-kHz and I_r=100-ua in $uV/Hz^{1/2}$.

x_3: " " " at I_r=200 ua.

x_4: " " " at I_r=300-ua.

x_5: Noise-voltage spectral density at 10-Hz and at I_r=100-ua.

x_6: " " " at I_r=200-ua.

x_7: " " " at I_r=300-ua.

x_8: a-c impedance at 1-kHz, and I_r=200-ua in ohms.

x_9: " " " at I_r=300-ua.

x_{10}: Noise-voltage spectral density at the first peak in $uV/Hz^{1/2}$.

x_{11}: I_r to observe x_{10}, in ua.

x_{12}: Noise-voltage spectral density at the second peak in $uv/Hz^{1/2}$.

x_{13}: I_r to observe x_{12}, in ua.

x_{14}: Percent-degradation at I_r=100-ua.

x_{15}: " " " at I_r=200-ua.

x_{16}: " " " at I_r=300-ua.

(3) $R_{x_i x_j}$ are computed by the correlation analysis digital computer program presented in Appendix H.

LIFE-TEST NO.1 (G315) INPUT-DATA
(TYPE-1)

1.000	230.0	10.00	.8000	300.0
150.0	50.00	90.00	60.00	340.0
40.00	0.000	0.000	0.000	0.000
-.2141				
3.000	4.000	1.200	.7000	4.100
1.900	1.300	120.0	60.00	8.400
15.00	0.000	0.000	1.063	1.063
1.063				
5.000	140.0	4.000	.4000	265.0
180.0	165.0	150.0	100.0	315.0
50.00	0.000	0.000	-.6355	-.4237
-.4237				
8.000	13.00	35.00	1.300	34.00
39.00	15.00	10.00	3.000	22.00
35.00	0.000	0.000	-.4228	-.4228
-.4228				
10.00	28.00	8.000	1.300	32.00
32.00	35.00	70.00	35.00	60.00
30.00	0.000	0.000	.4219	.2109
.4219				
12.00	3.000	190.0	10.00	100.0
180.0	120.0	200.0	120.0	195.0
190.0	0.000	0.000	.6315	.2096
.4201				
14.00	82.00	20.00	6.200	65.00
50.00	45.00	75.00	35.00	88.00
115.0	0.000	0.000	.4201	.2100
.2100				
15.00	24.00	9.000	2.000	140.0
105.0	130.0	90.00	45.00	205.0
35.00	0.000	0.000	.6302	.6302
.6302				
16.00	27.00	4.000	1.500	45.00
22.00	23.00	10.00	4.000	35.00
50.00	0.000	0.000	.4201	.4201
.4201				
19.00	18.00	5.000	1.000	68.00
35.00	16.00	80.00	45.00	72.00
30.00	0.000	0.000	-.8385	-.4201
-.6289				
20.00	43.00	5.000	1.500	67.00
40.00	40.00	45.00	45.00	95.00
30.00	0.000	0.000	-.4192	-.2096
-.2096				

21.00	45.00	6.000	1.000	77.00
35.00	40.00	70.00	35.00	50.00
40.00	0.000	0.000	-1.449	-.4192
-.4184				
22.00	90.00	1.000	.8000	230.0
120.0	300.0	120.0	60.00	430.0
43.00	0.000	0.000	-.6276	-.6276
-.8350				
27.00	40.00	4.000	.9000	30.00
13.00	8.000	40.00	55.00	97.00
37.00	0.000	0.000	.2087	.2092
.4184				
31.00	24.00	5.000	1.000	47.00
22.00	46.00	100.0	48.00	100.0
28.00	0.000	0.000	1.250	1.041
1.250				
32.00	45.00	3.000	15.00	120.0
90.00	30.00	300.0	50.00	14.00
40.00	0.000	0.000	0.000	-.2074
-.2070				
34.00	25.00	63.00	1.600	45.00
68.00	33.00	130.0	70.00	96.00
162.0	0.000	0.000	1.039	1.043
1.043				
35.00	140.0	3.000	.4000	150.0
105.0	75.00	120.0	140.0	300.0
43.00	0.000	0.000	0.000	0.000
0.000				
36.00	45.00	5.000	1.600	76.00
40.00	27.00	90.00	45.00	130.0
30.00	0.000	0.000	-.6224	-.6224
-.6224				
38.00	15.00	5.000	.8000	21.00
27.00	40.00	75.00	50.00	81.00
25.00	0.000	0.000	.6211	.8298
.8298				
42.00	25.00	2.000	1.000	13.00
80.00	85.00	95.00	50.00	225.0
35.00	0.000	0.000	-.4140	-.2070
-.2070				
43.00	55.00	12.00	2.500	52.00
28.00	10.00	45.00	30.00	80.00
50.00	0.000	0.000	0.000	0.000
0.000				
44.00	52.00	13.00	1.900	65.00
39.00	40.00	90.00	45.00	62.00
127.0	0.000	0.000	.4132	.4140
.6211				

```
 47.00      300.0      10.00      .7000      380.0
 360.0      450.0      100.0      50.00      470.0
 43.00      0.000      0.000      -.6185     -.6185
-.6185
 48.00      38.00      3.000      1.000      36.00
 18.00      11.00      75.00      25.00      38.00
 100.0      0.000      0.000      -.2061     -.2061
-.2061
 49.00      65.00      100.0      3.000      55.00
 90.00      44.00      90.00      50.00      95.00
 90.00      0.000      0.000      -.6172     -.6185
-.4123
 53.00      18.00      5.000      2.600      20.00
 10.00      9.000      180.0      65.00      32.00
 43.00      0.000      0.000      -.8213     -.6160
-.6147
 56.00      11.00      32.00      7.000      50.00
 38.00      55.00      120.0      60.00      55.00
 235.0      0.000      0.000      .6147      .6160
 .6160
 61.00      30.00      5.000      10.00      94.00
 31.00      18.00      70.00      30.00      103.0
 30.00      0.000      0.000      1.431      1.635
 1.428
 63.00      .6000      12.00      3.000      10.00
 10.00      26.00      45.00      35.00      27.00
 238.0      0.000      0.000      -.2044     -.4081
-.4081
 64.00      38.00      5.000      4.500      59.00
 25.00      16.00      70.00      35.00      92.00
 40.00      0.000      0.000      -.2040     0.000
 0.000
 67.00      200.0      10.00      .8000      350.0
 250.0      140.0      90.00      65.00      370.0
 50.00      0.000      0.000      0.000      .2040
 0.000
 69.00      160.0      10.00      .7000      320.0
 150.0      90.00      150.0      90.00      600.0
 38.00      0.000      0.000      .8163      .6109
 .4065
 74.00      8.000      28.00      4.000      11.00
 10.00      14.00      45.00      40.00      32.00
 212.0      0.000      0.000      -1.829     -1.832
-1.832
 77.00      3.500      1.500      .8000      4.500
 4.000      3.500      14.00      12.00      4.000
 40.00      0.000      0.000      0.000      .2032
 0.000
```

79.00 32.00 6.000 1.800 68.00
60.00 23.00 80.00 40.00 105.0
25.00 0.000 0.000 -.6085 -.6085
-.6085
85.00 120.0 3.000 1.300 140.0
120.0 140.0 190.0 90.00 170.0
37.00 0.000 0.000 1.010 1.008
1.006
86.00 12.00 3.000 2.000 47.00
50.00 58.00 85.00 45.00 83.00
20.00 0.000 0.000 -.4032 -.4040
-.4040
87.00 190.0 15.00 1.000 210.0
80.00 35.00 85.00 50.00 195.0
90.00 0.000 0.000 .4032 .4032
.4032
90.00 67.00 17.00 .7000 97.00
49.00 150.0 60.00 35.00 22.00
25.00 0.000 0.000 0.000 .2016
0.000
91.00 105.0 3.000 .6000 150.0
140.0 135.0 70.00 50.00 250.0
40.00 0.000 0.000 -.6036 -.4024
-.4024
93.00 50.00 9.000 1.000 56.00
32.00 18.00 85.00 45.00 62.00
50.00 0.000 0.000 -.8032 -.8048
-.8048
96.00 25.00 2.000 1.400 45.00
50.00 80.00 80.00 40.00 125.0
30.00 0.000 0.000 .2004 .2004
.2004
102.0 270.0 10.00 .5000 480.0
460.0 400.0 150.0 95.00 340.0
75.00 0.000 0.000 -.3992 -.3984
-.3984
105.0 100.0 10.00 5.600 120.0
60.00 40.00 100.0 55.00 410.0
45.00 0.000 0.000 -14.25 -.1980
0.000
107.0 25.00 2.000 .4000 15.00
13.00 7.000 110.0 140.0 35.00
28.00 0.000 0.000 -.3937 -.3937
-.5893

LIFE-TEST NO.1 (G315) INPUT-DATA
(TYPE-2)

6.000	75.00	30.00	.4000	135.0
105.0	35.00	300.0	200.0	145.0
30.00	170.0	140.0	-.3270	-.3090
-.3120				
7.000	13.00	7.000	3.000	40.00
40.00	45.00	40.00	30.00	45.00
25.00	20.00	150.0	-.1120	-.1120
-.1100				
11.00	390.0	380.0	1.000	280.0
320.0	410.0	150.0	85.00	400.0
50.00	390.0	165.0	-.8390	-.8260
-.8210				
13.00	27.00	24.00	4.000	38.00
37.00	50.00	55.00	30.00	30.00
55.00	255.0	212.0	-.2110	-.2110
-.3290				
17.00	36.00	22.00	1.300	36.00
32.00	25.00	70.00	50.00	55.00
30.00	45.00	135.0	-.1350	-.1350
-.1410				
18.00	65.00	40.00	3.000	90.00
80.00	80.00	75.00	40.00	80.00
40.00	109.0	140.0	-.2250	-.2350
-.2380				
23.00	63.00	159.0	15.00	120.0
126.0	90.00	90.00	50.00	117.0
37.00	165.0	206.0	-.3150	-.3390
-.3250				
24.00	265.0	75.00	.3000	150.0
160.0	70.00	200.0	150.0	290.0
40.00	340.0	135.0	-.8130	-.8050
-.8050				
25.00	76.00	9.000	3.000	67.00
50.00	20.00	75.00	30.00	95.00
137.0	96.00	118.0	-.2450	-.2390
-.2390				
26.00	58.00	21.00	.5000	90.00
68.00	35.00	100.0	50.00	77.00
35.00	65.00	135.0	-.2170	-.2140
-.2140				
37.00	30.00	46.00	1.500	30.00
53.00	60.00	30.00	25.00	35.00
130.0	46.00	205.0	-.1350	-.1310
-.1310				

40.00	210.0	140.0	100.0	65.00
39.00	.6211	.6224	.4140	315.0
40.00	247.4	118.0	-.2160	-.1080
-.1080				
46.00	117.0	35.00	1.500	157.0
142.0	123.0	80.00	50.00	145.0
45.00	123.0	120.0	-.3140	-.3140
-.3080				
50.00	49.00	15.00	1.000	135.0
110.0	45.00	80.00	45.00	98.00
40.00	68.00	40.00	.1170	.1090
.1090				
51.00	100.0	20.00	.6000	130.0
45.00	20.00	110.0	100.0	280.0
38.00	225.0	65.00	.1280	9.800
9.800				
52.00	75.00	5.000	4.300	105.0
45.00	65.00	70.00	45.00	150.0
35.00	100.0	87.00	-.6250	-.6250
-.6990				
55.00	42.00	7.000	.3000	52.00
30.00	24.00	150.0	80.00	30.00
25.00	48.00	125.0	.1820	.1220
.1220				
59.00	24.00	19.00	6.000	26.00
27.00	25.00	90.00	45.00	32.00
35.00	43.00	155.0	-.3650	-.3520
-.3520				
60.00	24.00	15.00	8.000	70.00
19.00	19.00	65.00	25.00	107.0
30.00	35.00	155.0	.2130	.2130
.2130				
62.00	22.00	2.000	1.000	18.00
10.00	4.000	150.0	80.00	29.00
30.00	22.00	100.0	-.6250	-.6880
-.7440				
65.00	24.00	28.00	7.000	39.00
35.00	20.00	60.00	30.00	82.00
30.00	33.00	180.0	.1450	.1520
.1590				
68.00	300.0	15.00	.7000	300.0
190.0	75.00	150.0	70.00	330.0
50.00	300.0	95.00	-.1680	-.1120
-.1080				
70.00	70.00	175.0	15.00	200.0
280.0	180.0	130.0	75.00	126.0
75.00	190.0	215.0	.1350	.1550
.1690				

71.00	12.00	11.00	5.000	13.00
8.000	4.000	70.00	30.00	28.00
20.00	21.00	155.0	.2650	.2680
.2680				
73.00	190.0	120.0	3.000	190.0
160.0	65.00	70.00	35.00	160.0
40.00	240.0	160.0	-.6210	-.7050
-.7050				
80.00	145.0	10.00	1.500	12.00
65.00	30.00	110.0	60.00	230.0
37.00	150.0	105.0	-.8520	-.7690
-.7990				
83.00	25.00	70.00	1.300	120.0
185.0	155.0	110.0	60.00	45.00
18.00	100.0	70.00	.2840	.2550
.1280				
92.00	230.0	25.00	1.200	180.0
115.0	85.00	180.0	75.00	330.0
40.00	240.0	110.0	.1250	.1250
.1210				
94.00	30.00	15.00	5.000	35.00
28.00	18.00	80.00	40.00	58.00
60.00	33.00	160.0	.1950	.1820
.1820				
95.00	30.00	11.00	7.000	62.00
65.00	30.00	100.0	50.00	140.0
35.00	49.00	75.00	-.2080	-.2050
-.2050				
99.00	57.00	2.000	8.200	78.00
25.00	15.00	85.00	40.00	110.0
37.00	72.00	80.00	-.2120	-.2090
-.2090				
101.0	20.00	125.0	.8000	110.0
145.0	90.00	130.0	80.00	42.00
35.00	150.0	82.00	-.5600	-.5520
-.5580				
104.0	15.00	63.00	10.00	125.0
180.0	100.0	60.00	35.00	96.00
40.00	180.0	56.00	.2350	.2110
.2110				
106.0	55.00	65.00	.8000	180.0
180.0	150.0	150.0	90.00	145.0
28.00	165.0	65.00	-.3670	-.3610
-.3610				
108.0	175.0	25.00	2.000	110.0
110.0	105.0	90.00	55.00	75.00
20.00	265.0	130.0	-.8630	-.8520
-.8500				

LIFE-TEST NO.1 (G315) INPUT-DATA
(TYPE-3)

98.00	15.00	19.00	10.00	38.00
23.00	20.00	13.00	13.00	20.00
106.0	35.00	225.0	-.6880	-.6440
-.6210				

LIFE-TEST NO.1 (G315) INPUT-DATA
(TYPE-4)

2.000	105.0	3.000	.6000	195.0
100.0	90.00	110.0	70.00	300.0
45.00	0.000	0.000	-.2132	-.2132
0.000				
29.00	20.00	70.00	.3000	80.00
140.0	60.00	140.0	120.0	200.0
150.0	0.000	0.000	-2.500	-2.500
-2.291				
39.00	19.00	13.00	2.000	70.00
85.00	127.0	100.0	60.00	123.0
28.00	0.000	0.000	1.560	1.560
1.560				
45.00	8.000	14.00	40.00	32.00
40.00	18.00	10.00	5.000	43.00
225.0	0.000	0.000	-.4198	-.5198
-.5198				
58.00	190.0	10.00	.5000	280.0
240.0	100.0	200.0	85.00	430.0
45.00	0.000	0.000	-.9179	-.9134
-.9156				
81.00	12.00	65.00	.2000	150.0
230.0	330.0	500.0	500.0	470.0
145.0	0.000	0.000	.2210	.3580
.5210				
82.00	150.0	20.00	21.00	150.0
135.0	45.00	90.00	45.00	165.0
115.0	0.000	0.000	.4040	.6072
.6072				
84.00	32.00	20.00	3.000	35.00
31.00	45.00	80.00	35.00	48.00
130.0	0.000	0.000	.6060	.4040
.4040				
97.00	13.00	9.000	4.000	24.00
17.00	9.000	18.00	12.00	15.00
145.0	0.000	0.000	-.6000	-.6000
-.6000				

LIFE-TEST NO.1 (G315) INPUT-DATA
(TYPE-5)

33.00	85.00	20.00	1.400	76.00
51.00	25.00	80.00	40.00	103.0
125.0	0.000	0.000	-.6237	-.4175
-.4175				
57.00	100.0	3.000	.6000	225.0
85.00	45.00	85.00	70.00	280.0
40.00	0.000	0.000	-.6147	-.6147
-.6134				
66.00	12.00	32.00	1.200	23.00
43.00	20.00	40.00	30.00	53.00
195.0	0.000	0.000	-1.020	-1.020
-1.020				
72.00	105.0	40.00	.4000	85.00
105.0	35.00	150.0	90.00	185.0
140.0	0.000	0.000	.4065	.5670
.5670				
75.00	23.00	4.000	2.600	39.00
57.00	68.00	90.00	50.00	68.00
32.00	0.000	0.000	.4065	.6109
.4065				
88.00	45.00	80.00	.3000	105.0
160.0	60.00	220.0	150.0	190.0
155.0	0.000	0.000	-.4032	-.6048
-.6048				
89.00	100.0	60.00	1.000	370.0
425.0	230.0	85.00	45.00	160.0
150.0	0.000	0.000	0.000	0.000
-.2020				
103.0	10.00	4.500	3.200	23.00
23.00	10.00	12.00	7.000	140.0
130.0	0.000	0.000	-.7936	-.5964
-.3976				

LIFE-TEST NO.1 (G315) INPUT-DATA
(TYPE-6)

4.000	8.000	1.000	.7000	35.00
22.00	17.00	90.00	50.00	105.0
23.00	0.000	0.000	1.273	1.273
1.486				
9.000	20.00	6.000	8.200	64.00
45.00	65.00	25.00	23.00	18.00
40.00	0.000	0.000	.9860	.9880
.9880				
41.00	12.00	3.000	1.100	25.00
25.00	21.00	25.00	17.00	14.00
30.00	0.000	0.000	-1.035	-1.035
-1.035				
54.00	43.00	2.000	.6000	48.00
12.00	15.00	95.00	60.00	67.00
30.00	0.000	0.000	-.2053	-.2053
-.2049				

LIFE-TEST NO.1 (G315) INPUT-DATA
(TYPE-7)

28.00	11.00	4.000	.8000	18.00
12.00	7.000	150.0	80.00	12.00
85.00	0.000	0.000	1.250	1.252
1.041				
30.00	14.00	5.000	1.400	22.00
20.00	16.00	100.0	50.00	15.00
31.00	0.000	0.000	-.8333	-.6250
-.6250				
76.00	140.0	50.00	4.600	12.00
135.0	90.00	110.0	60.00	190.0
120.0	0.000	0.000	0.000	0.000
0.000				
78.00	80.00	5.000	3.200	180.0
160.0	140.0	150.0	70.00	150.0
40.00	0.000	0.000	.8130	.8130
.6085				
100.0	40.00	14.00	5.000	60.00
55.00	58.00	50.00	25.00	40.00
125.0	0.000	0.000	-.7984	-.7984
-.7984				

CORRELATION ANALYSIS LIFE-TEST NO.1 (G315)
(TYPE-1)

1	49.50	31.00	2277.00	156945.00
2	66.98	71.99	3081.10	444801.61
3	15.53	31.13	714.70	55689.69
4	2.38	2.93	109.60	656.62
5	105.73	109.25	4863.60	1063270.00
6	78.51	89.47	3611.90	651907.61
7	72.53	94.19	3336.80	650177.94
8	94.76	51.73	4359.00	536171.00
9	53.73	28.93	2472.00	171348.00
10	148.16	140.52	6815.40	1918135.50
11	63.13	56.30	2904.00	329182.00
12	.00	.00	.00	.00
13	.00	.00	.00	.00
14	-.04	1.18	-5.79	24.35
15	.02	.62	.29	17.70
16	.02	.63	-.10	18.33

SAMPLE SIZE (46)

1	2	.15	168256.30	.14
1	3	-.17	27551.10	.14
1	4	-.06	5144.20	.14
1	5	.09	256161.80	.14
1	6	.10	192818.70	.14
1	7	.10	179566.40	.14
1	8	.00	215288.00	.14
1	9	.11	127065.00	.14
1	10	.08	353910.20	.14
1	11	.01	144739.00	.14
1	12	.00	.00	.14
1	13	.00	.00	.14
1	14	-.29	-1703.64	.13
1	15	-.15	-125.15	.14
1	16	-.18	-172.31	.14
2	3	-.13	34213.25	.14
2	4	-.24	4972.70	.13
2	5	.92	659896.15	.02
2	6	.82	487450.60	.04
2	7	.70	441963.05	.07
2	8	.20	326886.00	.14
2	9	.32	196822.00	.13
2	10	.76	812022.80	.06
2	11	-.14	166763.80	.14
2	12	.00	.00	.14
2	13	.00	.00	.14
2	14	-.08	-1671.77	.14
2	15	-.07	-143.80	.14

2	16	-.11	-250.56	.14
3	4	.37	3264.64	.12
3	5	-.05	66447.67	.14
3	6	.14	74693.28	.14
3	7	.01	54414.81	.14
3	8	.22	84245.00	.14
3	9	.24	48716.00	.13
3	10	-.02	101380.08	.14
3	11	.51	86449.00	.10
3	12	.00	.00	.14
3	13	.00	.00	.14
3	14	.05	-59.50	.14
3	15	.00	9.93	.14
3	16	.07	66.16	.14
4	5	-.14	9484.97	.14
4	6	-.08	7577.03	.14
4	7	-.17	5696.01	.14
4	8	.46	13615.20	.11
4	9	-.03	5768.00	.14
4	10	-.18	12709.38	.14
4	11	.32	9416.20	.13
4	12	.00	.00	.14
4	13	.00	.00	.14
4	14	-.09	-64.66	.14
4	15	.11	10.45	.14
4	16	.14	12.05	.14
5	6	.90	789659.79	.02
5	7	.77	721387.08	.05
5	8	.31	543465.00	.13
5	9	.36	314633.00	.12
5	10	.82	1302269.40	.04
5	11	-.12	271534.50	.14
5	12	.00	.00	.14
5	13	.00	.00	.14
5	14	-.02	-1978.21	.14
5	15	-.04	-114.50	.14
5	16	-.10	-327.98	.14
6	7	.87	600615.47	.03
6	8	.36	419609.00	.12
6	9	.40	242448.00	.12
6	10	.71	946412.96	.07
6	11	-.02	223303.50	.14
6	12	.00	.00	.14
6	13	.00	.00	.14
6	14	.00	-1174.23	.14
6	15	-.10	-257.44	.14
6	16	-.12	-332.75	.14

7 8	.25	373785.00	.13
7 9	.28	214950.00	.13
7 10	.65	891167.92	.08
7 11	-.05	196548.50	.14
7 12	.00	.00	.14
7 13	.00	.00	.14
7 14	.01	-1012.87	.14
7 15	-.13	-345.15	.14
7 16	-.15	-435.44	.14
8 9	.60	275788.00	.09
8 10	.25	732394.00	.13
8 11	.04	281325.00	.14
8 12	.00	.00	.14
8 13	.00	.00	.14
8 14	.03	-1299.12	.14
8 15	.09	163.09	.14
8 16	.10	145.43	.14
9 10	.42	446383.00	.12
9 11	.06	160919.00	.14
9 12	.00	.00	.14
9 13	.00	.00	.14
9 14	.02	-786.58	.14
9 15	.03	40.59	.14
9 16	.02	15.82	.14
10 11	-.15	373472.00	.14
10 12	.00	.00	.14
10 13	.00	.00	.14
10 14	-.25	-5976.86	.13
10 15	-.02	-72.30	.14
10 16	-.06	-272.59	.14
11 12	.00	.00	.14
11 13	.00	.00	.14
11 14	.04	-737.75	.14
11 15	-.10	-148.68	.14
11 16	-.05	-101.53	.14
12 13	.00	.00	.14
12 14	.00	.00	.14
12 15	.00	.00	.14
12 16	.00	.00	.14
13 14	.00	.00	.14
13 15	.00	.00	.14
13 16	.00	.00	.14
14 15	.34	21.23	.13
14 16	.29	18.81	.13
15 16	.98	17.68	.00

CORRELATION ANALYSIS LIFE-TEST NO.1 (G315)
(TYPE-2)

1	56.88	31.36	1991.00	147685.00
2	89.68	91.28	3139.00	573187.00
3	52.31	72.59	1831.00	280241.00
4	6.40	16.49	224.20	10957.02
5	102.51	70.38	3588.00	541194.00
6	94.54	75.39	3309.00	511775.00
7	67.64	73.71	2367.62	350347.38
8	101.58	54.06	3555.62	463525.38
9	58.15	36.49	2035.41	164975.17
10	130.05	100.66	4552.00	946714.00
11	42.62	25.00	1492.00	85478.00
12	137.15	99.15	4800.40	1002513.70
13	126.97	45.34	4444.00	636232.00
14	-.21	.34	-7.54	5.71
15	-.21	.33	-7.51	5.59
16	-.22	.34	-7.89	5.82

SAMPLE SIZE (35)

1	2	-.11	167093.00	.16
1	3	-.17	90476.00	.16
1	4	-.05	11777.20	.16
1	5	.04	207933.00	.16
1	6	.08	195627.00	.16
1	7	-.04	131316.84	.16
1	8	-.01	201349.89	.16
1	9	-.13	110546.56	.16
1	10	-.06	251770.00	.16
1	11	-.21	78859.00	.16
1	12	-.06	265610.00	.16
1	13	-.45	230244.00	.13
1	14	.12	-384.08	.16
1	15	.11	-384.57	.16
1	16	.11	-404.92	.16
2	3	.52	287107.00	.12
2	4	.15	28084.30	.16
2	5	.69	478845.00	.08
2	6	.54	428272.00	.11
2	7	.51	333856.43	.12
2	8	.30	371975.70	.15
2	9	.26	214006.94	.15
2	10	.88	691297.00	.03
2	11	.03	136957.00	.16
2	12	.83	694798.00	.05
2	13	.00	399700.00	.16
2	14	-.47	-1200.44	.13
2	15	-.45	-1161.94	.13

2	16	-.42	-1174.85	.13
3	4	.24	21893.60	.15
3	5	.54	285919.00	.11
3	6	.73	314098.00	.07
3	7	.81	276936.95	.05
3	8	.10	199927.13	.16
3	9	.11	117137.96	.16
3	10	.45	353438.00	.13
3	11	.08	83485.00	.16
3	12	.58	398496.00	.11
3	13	.28	265547.00	.15
3	14	-.29	-646.60	.15
3	15	-.28	-637.05	.15
3	16	-.26	-643.64	.15
4	5	-.10	18667.00	.16
4	6	-.10	16543.60	.16
4	7	-.15	8747.31	.16
4	8	-.38	10900.24	.14
4	9	-.34	5867.40	.14
4	10	.26	44503.10	.15
4	11	.00	9530.50	.16
4	12	.15	39461.30	.16
4	13	.05	29820.20	.16
4	14	.06	-35.34	.16
4	15	.11	-24.90	.16
4	16	.12	-25.49	.16
5	6	.85	497798.00	.04
5	7	.68	367618.37	.08
5	8	.43	422425.45	.13
5	9	.38	243171.91	.14
5	10	.66	630586.00	.09
5	11	.00	153099.00	.16
5	12	.72	669133.00	.08
5	13	-.14	439372.00	.16
5	14	-.16	-911.06	.16
5	15	-.16	-905.85	.16
5	16	-.14	-928.39	.16
6	7	.86	391497.22	.04
6	8	.37	389179.27	.14
6	9	.34	225651.14	.14
6	10	.46	553463.00	.13
6	11	.05	144567.00	.16
6	12	.66	627280.60	.09
6	13	-.01	418267.00	.16
6	14	-.20	-898.45	.16
6	15	-.20	-892.19	.16
6	16	-.19	-918.53	.16

7	8	.23	272770.38	.15
7	9	.20	156955.25	.16
7	10	.39	410765.64	.14
7	11	.04	103794.84	.16
7	12	.55	467935.66	.11
7	13	.09	312163.28	.16
7	14	-.26	-747.11	.15
7	15	-.27	-744.58	.15
7	16	-.26	-770.17	.15
8	9	.94	271875.25	.01
8	10	.31	522146.05	.15
8	11	-.19	142329.89	.16
8	12	.33	550618.98	.15
8	13	-.14	438958.44	.16
8	14	-.22	-910.94	.16
8	15	-.23	-912.49	.15
8	16	-.22	-947.28	.16
9	10	.30	303815.41	.15
9	11	-.19	80651.56	.16
9	12	.36	325907.42	.14
9	13	-.13	250358.85	.16
9	14	-.27	-557.74	.15
9	15	-.28	-558.86	.15
9	16	-.27	-578.29	.15
10	11	.00	194259.00	.16
10	12	.75	888572.00	.07
10	13	-.16	551317.00	.16
10	14	-.28	-1319.15	.15
10	15	-.24	-1264.33	.15
10	16	-.21	-1287.38	.16
11	12	.02	206502.00	.16
11	13	.30	201543.00	.15
11	14	.02	-313.82	.16
11	15	.03	-309.32	.16
11	16	.04	-321.65	.16
12	13	.03	614621.20	.16
12	14	-.43	-1555.54	.13
12	15	-.41	-1522.06	.13
12	16	-.41	-1571.29	.14
13	14	-.01	-968.96	.16
13	15	-.01	-964.83	.16
13	16	.00	-1006.87	.16
14	15	.99	5.63	.00
14	16	.98	5.72	.00
15	16	.99	5.69	.00

CORRELATION ANALYSIS LIFE-TEST NO.1 (G315)
(TYPE-4)

1	57.44	31.23	517.00	37505.00
2	61.00	69.18	549.00	71787.00
3	24.88	24.76	224.00	10480.00
4	7.95	13.69	71.60	2070.74
5	112.88	87.21	1016.00	175550.00
6	113.11	81.58	1018.00	168400.00
7	91.55	97.30	824.00	151184.00
8	138.66	147.29	1248.00	346624.00
9	103.55	152.90	932.00	283544.00
10	199.33	167.67	1794.00	582532.00
11	114.22	63.94	1028.00	150134.00
12	.00	.00	.00	.00
13	.00	.00	.00	.00
14	-.20	1.13	-1.85	10.68
15	-.20	1.14	-1.81	10.85
16	-.13	1.10	-1.23	9.95

SAMPLE SIZE (9)

1	2	-.08	30132.00	.33
1	3	.05	13211.00	.33
1	4	.05	4295.10	.33
1	5	-.25	52838.00	.31
1	6	-.06	57248.00	.33
1	7	.05	48556.00	.33
1	8	.13	76576.00	.32
1	9	.15	59409.00	.32
1	10	-.18	95159.00	.32
1	11	.33	64427.00	.29
1	12	.00	.00	.33
1	13	.00	.00	.33
1	14	.23	-40.48	.31
1	15	.24	-33.93	.31
1	16	.20	-14.36	.31
2	3	-.37	8511.00	.28
2	4	-.07	3822.40	.33
2	5	.84	102593.00	.09
2	6	.50	85058.00	.24
2	7	-.10	44474.00	.32
2	8	.00	76624.00	.33
2	9	-.18	41106.00	.32
2	10	.45	152002.00	.26
2	11	-.53	43642.00	.23
2	12	.00	.00	.33
2	13	.00	.00	.33
2	14	-.05	-145.66	.33
2	15	-.01	-119.94	.33

7	8	.95	223992.00	.02
7	9	.95	198418.00	.03
7	10	.75	263215.00	.14
7	11	-.17	85336.00	.32
7	12	.00	.00	.33
7	13	.00	.00	.33
7	14	.24	42.56	.31
7	15	.28	86.47	.30
7	16	.33	171.77	.29
8	9	.97	304616.00	.01
8	10	.83	413690.00	.10
8	11	-.08	135860.00	.33
8	12	.00	.00	.33
8	13	.00	.00	.33
8	14	.02	-220.69	.33
8	15	.07	-150.16	.33
8	16	.11	-16.39	.32
9	10	.71	333430.00	.16
9	11	.06	111745.00	.33
9	12	.00	.00	.33
9	13	.00	.00	.33
9	14	.02	-158.75	.33
9	15	.07	-88.29	.33
9	16	.11	33.01	.32
10	11	-.38	171509.00	.28
10	12	.00	.00	.33
10	13	.00	.00	.33
10	14	-.14	-594.21	.32
10	15	-.09	-508.35	.33
10	16	-.05	-326.92	.33
11	12	.00	.00	.33
11	13	.00	.00	.33
11	14	-.33	-406.38	.29
11	15	-.34	-411.71	.29
11	16	-.36	-347.23	.28
12	13	.00	.00	.33
12	14	.00	.00	.33
12	15	.00	.00	.33
12	16	.00	.00	.33
13	14	.00	.00	.33
13	15	.00	.00	.33
13	16	.00	.00	.33
14	15	.99	10.71	.00
14	16	.98	10.18	.00
15	16	.99	10.34	.00

CORRELATION ANALYSIS LIFE-TEST NO.1 (G315)
(TYPE-5)

1	72.87	21.68	583.00	45777.00
2	60.00	41.82	480.00	41048.00
3	30.43	28.42	243.50	13069.25
4	1.33	1.04	10.70	22.01
5	118.25	120.86	946.00	214130.00
6	118.62	131.00	949.00	232703.00
7	61.62	70.82	493.00	65499.00
8	95.25	64.38	762.00	101594.00
9	60.25	43.96	482.00	42574.00
10	147.37	73.88	1179.00	211967.00
11	120.87	56.58	967.00	139299.00
12	.00	.00	.00	.00
13	.00	.00	.00	.00
14	-.33	.54	-2.64	2.93
15	-.25	.59	-2.07	3.00
16	-.28	.53	-2.28	2.64

SAMPLE SIZE (8)

1	2	-.39	32472.00	.29
1	3	.28	18966.50	.32
1	4	.30	828.40	.32
1	5	.08	70435.00	.35
1	6	.31	75475.00	.31
1	7	.29	39110.00	.32
1	8	.03	55836.00	.35
1	9	.04	35446.00	.35
1	10	.06	86657.00	.35
1	11	.19	72135.00	.34
1	12	.00	.00	.35
1	13	.00	.00	.35
1	14	.14	-180.40	.34
1	15	.07	-144.14	.35
1	16	.11	-156.90	.34
2	3	.20	16321.00	.33
2	4	-.65	440.70	.20
2	5	.68	81013.00	.18
2	6	.48	75617.00	.26
2	7	.40	37904.00	.29
2	8	.33	52120.00	.31
2	9	.29	32680.00	.32
2	10	.62	84330.00	.21
2	11	-.14	55676.00	.34
2	12	.00	.00	.35
2	13	.00	.00	.35
2	14	.36	-100.77	.30
2	15	.32	-68.79	.31

2 16	.29	-91.57	.32
3 4	-.63	193.00	.21
3 5	.34	37190.50	.31
3 6	.63	45482.50	.21
3 7	.46	21592.00	.27
3 8	.70	32249.00	.17
3 9	.66	20501.50	.19
3 10	.12	37698.00	.34
3 11	.63	36573.00	.21
3 12	.00	.00	.35
3 13	.00	.00	.35
3 14	.14	-64.89	.34
3 15	-.04	-68.77	.35
3 16	-.10	-80.81	.34
4 5	-.43	879.50	.28
4 6	-.37	910.80	.30
4 7	-.19	556.80	.33
4 8	-.68	694.40	.18
4 9	-.71	412.40	.17
4 10	-.52	1291.60	.25
4 11	-.26	1184.70	.32
4 12	.00	.00	.35
4 13	.00	.00	.35
4 14	-.09	-3.90	.35
4 15	.07	-2.45	.35
4 16	.12	-2.54	.34
5 6	.87	209717.00	.07
5 7	.85	109742.00	.09
5 8	.13	97211.00	.34
5 9	.12	61641.00	.34
5 10	.53	172794.00	.25
5 11	-.07	110898.00	.35
5 12	.00	.00	.35
5 13	.00	.00	.35
5 14	.20	-219.35	.33
5 15	.09	-198.69	.35
5 16	-.01	-276.54	.35
6 7	.96	121091.00	.02
6 8	.25	105506.00	.33
6 9	.19	64866.00	.34
6 10	.24	156253.00	.33
6 11	.22	126224.00	.33
6 12	.00	.00	.35
6 13	.00	.00	.35
6 14	.33	-144.83	.31
6 15	.20	-133.53	.33
6 16	.09	-226.34	.35

7	8	.12	50865.00	.34
7	9	.04	30720.00	.35
7	10	.11	76934.00	.34
7	11	.05	61001.00	.35
7	12	.00	.00	.35
7	13	.00	.00	.35
7	14	.40	-53.91	.29
7	15	.30	-39.36	.32
7	16	.16	-97.67	.34
8	9	.97	65259.00	.01
8	10	.38	125110.00	.30
8	11	.05	93490.00	.35
8	12	.00	.00	.35
8	13	.00	.00	.35
8	14	.44	-143.61	.28
8	15	.26	-126.63	.32
8	16	.23	-159.70	.33
9	10	.48	82040.00	.27
9	11	.02	58760.00	.35
9	12	.00	.00	.35
9	13	.00	.00	.35
9	14	.30	-107.70	.31
9	15	.11	-103.64	.34
9	16	.09	-121.47	.35
10	11	-.28	134136.00	.32
10	12	.00	.00	.35
10	13	.00	.00	.35
10	14	.05	-375.28	.35
10	15	-.04	-321.15	.35
10	16	-.01	-339.17	.35
11	12	.00	.00	.35
11	13	.00	.00	.35
11	14	-.36	-397.19	.30
11	15	-.41	-348.02	.29
11	16	-.39	-358.96	.29
12	13	.00	.00	.35
12	14	.00	.00	.35
12	15	.00	.00	.35
12	16	.00	.00	.35
13	14	.00	.00	.35
13	15	.00	.00	.35
13	16	.00	.00	.35
14	15	.97	2.87	.02
14	16	.92	2.63	.04
15	16	.97	2.76	.01

CORRELATION ANALYSIS LIFE-TEST NO.1 (G315)
(TYPE-6)

1	27.00	24.34	108.00	4694.00
2	20.75	15.64	83.00	2457.00
3	3.00	2.16	12.00	50.00
4	2.65	3.70	10.60	69.30
5	43.00	16.87	172.00	8250.00
6	26.00	13.83	104.00	3278.00
7	29.50	23.79	118.00	5180.00
8	58.75	39.02	235.00	18375.00
9	37.50	20.76	150.00	6918.00
10	51.00	43.32	204.00	16034.00
11	30.75	6.99	123.00	3929.00
12	.00	.00	.00	.00
13	.00	.00	.00	.00
14	.25	1.07	1.01	3.70
15	.25	1.07	1.02	3.71
16	.30	1.14	1.23	4.29

SAMPLE SIZE (4)

1	2	.68	3026.00	.26
1	3	-.22	289.00	.47
1	4	-.48	154.10	.38
1	5	-.25	4333.00	.46
1	6	-.63	2166.00	.29
1	7	-.49	2324.00	.37
1	8	.13	6740.00	.49
1	9	.19	4344.00	.48
1	10	-.23	4774.00	.47
1	11	-.03	3302.00	.49
1	12	.00	.00	.50
1	13	.00	.00	.50
1	14	-.85	-39.55	.13
1	15	-.85	-39.53	.13
1	16	-.86	-38.66	.12
2	3	.00	250.00	.49
2	4	-.06	208.60	.49
2	5	.44	3924.00	.39
2	6	-.40	1892.00	.41
2	7	-.10	2333.00	.49
2	8	.39	5605.00	.42
2	9	.54	3644.00	.35
2	10	.00	4249.00	.49
2	11	.24	2634.00	.46
2	12	.00	.00	.50
2	13	.00	.00	.50
2	14	-.24	8.65	.46
2	15	-.24	8.69	.46

2	16	-.28	10.41	.45
3	4	.94	54.40	.05
3	5	.67	590.00	.27
3	6	.88	391.00	.11
3	7	.94	500.00	.05
3	8	-.79	505.00	.18
3	9	-.67	359.00	.27
3	10	-.79	389.00	.18
3	11	.97	413.00	.02
3	12	.00	.00	.50
3	13	.00	.00	.50
3	14	.08	3.67	.49
3	15	.08	3.68	.49
3	16	.02	3.89	.49
4	5	.79	605.60	.18
4	6	.93	419.10	.06
4	7	.99	577.00	.00
4	8	-.62	352.50	.30
4	9	-.51	278.30	.36
4	10	-.54	276.70	.34
4	11	.88	395.10	.10
4	12	.00	.00	.50
4	13	.00	.00	.50
4	14	.42	7.71	.41
4	15	.42	7.73	.41
4	16	.36	7.88	.43
5	6	.54	4851.00	.35
5	7	.76	6000.00	.20
5	8	-.08	9935.00	.49
5	9	.07	6527.00	.49
5	10	-.17	8393.00	.48
5	11	.75	5555.00	.21
5	12	.00	.00	.50
5	13	.00	.00	.50
5	14	.51	71.92	.36
5	15	.51	72.05	.36
5	16	.45	79.53	.39
6	7	.94	4004.00	.05
6	8	-.76	4870.00	.20
6	9	-.71	3280.00	.24
6	10	-.57	4274.00	.33
6	11	.75	3416.00	.21
6	12	.00	.00	.50
6	13	.00	.00	.50
6	14	.39	44.03	.42
6	15	.39	44.12	.42
6	16	.35	48.81	.43

7	8	-.65	5105.00	.28
7	9	-.55	3602.00	.34
7	10	-.57	4254.00	.33
7	11	.88	4071.00	.10
7	12	.00	.00	.50
7	13	.00	.00	.50
7	14	.40	60.91	.41
7	15	.40	61.04	.41
7	16	.34	64.67	.43
8	9	.98	11200.00	.01
8	10	.91	16615.00	.08
8	11	-.67	6670.00	.26
8	12	.00	.00	.50
8	13	.00	.00	.50
8	14	.27	93.84	.46
8	15	.27	93.89	.46
8	16	.30	113.09	.45
9	10	.84	9922.00	.14
9	11	-.53	4380.00	.35
9	12	.00	.00	.50
9	13	.00	.00	.50
9	14	.27	56.41	.46
9	15	.27	56.46	.46
9	16	.29	67.13	.45
10	11	-.77	5565.00	.19
10	12	.00	.00	.50
10	13	.00	.00	.50
10	14	.51	123.16	.36
10	15	.51	123.20	.36
10	16	.55	145.59	.34
11	12	.00	.00	.50
11	13	.00	.00	.50
11	14	.00	31.51	.49
11	15	.00	31.59	.49
11	16	-.06	36.50	.49
12	13	.00	.00	.50
12	14	.00	.00	.50
12	15	.00	.00	.50
12	16	.00	.00	.50
13	14	.00	.00	.50
13	15	.00	.00	.50
13	16	.00	.00	.50
14	15	.99	3.70	.00
14	16	.99	3.97	.00
15	16	.99	3.98	.00

CORRELATION ANALYSIS LIFE-TEST NO.1 (G315)
(TYPE-7)

1	62.40	31.91	312.00	23544.00
2	57.00	54.01	285.00	27917.00
3	15.60	19.65	78.00	2762.00
4	3.00	1.87	15.00	59.00
5	58.40	70.53	292.00	36952.00
6	76.40	67.47	382.00	47394.00
7	62.20	54.82	311.00	31369.00
8	112.00	41.47	560.00	69600.00
9	57.00	21.09	285.00	18025.00
10	81.40	82.82	407.00	60569.00
11	80.20	43.73	401.00	39811.00
12	.00	.00	.00	.00
13	.00	.00	.00	.00
14	.08	.93	.43	3.55
15	.12	.89	.64	3.25
16	.04	.78	.22	2.48

SAMPLE SIZE (5)

1	2	.55	21608.00	.30
1	3	.39	5852.00	.37
1	4	.95	1163.60	.04
1	5	.43	22116.00	.36
1	6	.61	29176.00	.27
1	7	.68	24236.00	.23
1	8	-.50	32260.00	.33
1	9	-.56	16260.00	.30
1	10	.52	30926.00	.32
1	11	.54	28050.00	.31
1	12	.00	.00	.44
1	13	.00	.00	.44
1	14	-.27	-6.42	.41
1	15	-.35	-.12	.39
1	16	-.35	-21.97	.38
2	3	.85	8074.00	.12
2	4	.67	1128.40	.24
2	5	.15	18986.00	.43
2	6	.86	34312.00	.11
2	7	.73	26421.00	.20
2	8	.05	32450.00	.44
2	9	.07	16580.00	.44
2	10	.96	40542.00	.02
2	11	.37	26369.00	.38
2	12	.00	.00	.44
2	13	.00	.00	.44
2	14	.05	35.18	.44
2	15	.00	38.12	.44

2	16	.03	19.44	.44
3	4	.62	326.20	.27
3	5	-.36	2522.00	.38
3	6	.47	8468.00	.34
3	7	.29	6120.00	.40
3	8	-.21	8050.00	.42
3	9	-.10	4270.00	.44
3	10	.70	10933.00	.22
3	11	.63	8445.00	.26
3	12	.00	.00	.44
3	13	.00	.00	.44
3	14	-.17	-6.27	.43
3	15	-.21	-5.22	.42
3	16	-.17	-7.09	.43
4	5	.19	976.40	.43
4	6	.59	1445.60	.28
4	7	.60	1180.00	.28
4	8	-.59	1496.00	.29
4	9	-.60	759.00	.28
4	10	.58	1584.60	.29
4	11	.65	1416.40	.25
4	12	.00	.00	.44
4	13	.00	.00	.44
4	14	-.40	-1.55	.37
4	15	-.47	-1.26	.34
4	16	-.47	-2.08	.34
5	6	.63	34376.00	.26
5	7	.78	30238.00	.17
5	8	.30	36220.00	.40
5	9	.12	17360.00	.44
5	10	.36	32226.00	.38
5	11	-.41	18352.00	.37
5	12	.00	.00	.44
5	13	.00	.00	.44
5	14	.29	102.60	.40
5	15	.27	107.22	.41
5	16	.24	66.61	.42
6	7	.97	38144.00	.02
6	8	.23	45400.00	.42
6	9	.15	22635.00	.43
6	10	.94	52294.00	.04
6	11	.04	31115.00	.44
6	12	.00	.00	.44
6	13	.00	.00	.44
6	14	.20	84.50	.42
6	15	.16	88.69	.43
6	16	.17	53.44	.43

7	8	.17	36450.00	.43
7	9	.06	18010.00	.44
7	10	.84	40744.00	.12
7	11	-.02	24741.00	.44
7	12	.00	.00	.44
7	13	.00	.00	.44
7	14	.17	62.93	.43
7	15	.13	66.27	.43
7	16	.12	36.16	.43
8	9	.98	35350.00	.01
8	10	.22	48700.00	.42
8	11	-.49	41300.00	.33
8	12	.00	.00	.44
8	13	.00	.00	.44
8	14	.88	186.20	.09
8	15	.91	207.33	.07
8	16	.91	145.00	.07
9	10	.20	24610.00	.42
9	11	-.37	21475.00	.38
9	12	.00	.00	.44
9	13	.00	.00	.44
9	14	.89	95.28	.09
9	15	.92	105.86	.06
9	16	.93	74.66	.05
10	11	.18	35285.00	.43
10	12	.00	.00	.44
10	13	.00	.00	.44
10	14	.18	92.51	.43
10	15	.14	95.66	.43
10	16	.16	62.45	.43
11	12	.00	.00	.44
11	13	.00	.00	.44
11	14	-.13	13.13	.43
11	15	-.20	19.76	.42
11	16	-.17	-6.35	.43
12	13	.00	.00	.44
12	14	.00	.00	.44
12	15	.00	.00	.44
12	16	.00	.00	.44
13	14	.00	.00	.44
13	15	.00	.00	.44
13	16	.00	.00	.44
14	15	.99	3.38	.00
14	16	.99	2.95	.00
15	16	.99	2.82	.00

APPENDIX J

G321 Life-Test Data

(1) Input-data format:

x_1 x_2 x_3 x_4 x_5

(2) Description of input-data format:

x_1: Sample number.

x_2: Initial leakage in 10^{-9} amperes.

x_3: Leakage current after 1000-hours life-test, in nano-amperes.

x_4: Percent-degradation.

x_5: Noise-voltage spectral density measured at f=1-kHz, and I_r=10-ua after 1000-hours life-test.

(3) $R_{i,j}$ are computed by the correlation analysis program presented in Appendix H.

LIFE-TEST NO.2 (S2A-436 UNITS)

SAMPLE	IR(0)	IR(1000)	DEG	SV(10UA)
451.	11.5	12.5	8.69	18.5
452.	13.3	16.1	21.0	10.5
453.	12.3	16.0	30.0	6.00
454.	12.9	16.8	30.2	8.00
456.	16.9	20.0	18.3	10.0
457.	16.3	17.9	9.81	8.00
458.	27.7	25.6	-7.58	20.0
459.	23.3	26.4	13.3	13.0
460.	15.2	17.7	16.4	20.0
461.	10.7	13.2	23.3	10.0
462.	14.6	17.4	19.1	8.00
463.	10.1	12.7	25.7	22.0
464.	24.1	27.4	13.6	9.00
465.	14.7	18.4	25.1	23.0
466.	19.1	23.7	24.0	50.0
467.	15.5	20.6	32.9	19.0
468.	24.6	23.7	-3.65	9.50
469.	13.9	17.5	25.8	12.0
470.	8.60	13.0	51.1	10.0
471.	11.5	13.0	13.0	19.0
472.	17.9	19.8	10.6	12.0
473.	13.1	15.2	16.0	8.00
474.	25.9	29.7	14.6	18.0
475.	15.9	19.8	24.5	12.0
476.	10.8	11.4	5.55	14.0
477.	25.4	26.7	5.11	14.0
478.	23.1	22.9	-.865	15.0
479.	14.3	14.5	1.39	40.0
480.	31.9	32.4	1.56	20.0
481.	11.9	12.5	5.04	11.0
482.	15.9	15.0	-5.66	11.5
483.	36.9	33.4	-9.48	19.0
484.	32.8	30.1	-8.23	30.0
485.	14.7	14.1	-4.08	43.0
486.	18.6	17.2	-7.52	17.0
487.	16.3	14.5	-11.0	10.5
488.	17.2	15.9	-7.55	22.0
489.	13.3	12.8	-3.75	18.0
490.	22.3	23.5	5.38	15.0
491.	8.00	10.2	27.5	7.00
492.	9.50	12.6	32.6	10.0
493.	11.3	15.3	35.3	18.0
494.	32.9	34.9	6.07	12.0
495.	20.6	25.2	22.3	8.00

496.	17.8	21.2	19.1	18.0
497.	13.1	15.0	14.5	8.00
499.	9.20	11.2	21.7	10.0
500.	15.0	17.1	14.0	14.0
501.	18.1	20.8	14.9	13.5
502.	12.5	15.1	20.8	15.0
503.	11.6	14.6	25.8	30.0
504.	17.5	20.5	17.1	12.0
505.	20.6	22.8	10.6	16.0
506.	23.5	26.5	12.7	14.0
507.	13.2	15.1	14.3	21.0
508.	10.8	11.8	9.25	12.0
509.	21.0	23.6	12.3	11.0
510.	21.2	25.0	17.9	41.0
511.	17.3	17.8	2.89	7.00
512.	12.4	12.8	3.22	19.0
513.	19.3	21.2	9.84	9.00
514.	13.9	14.8	6.47	10.0
515.	9.70	10.2	5.15	59.0
516.	18.6	20.3	9.13	10.0
517.	11.6	11.6	0.00	20.0
518.	12.9	14.0	8.52	12.0
519.	17.3	17.4	.578	7.00
520.	13.3	14.0	5.26	20.0
521.	14.0	12.4	-11.4	5.00
522.	31.2	28.7	-8.01	11.0
523.	15.7	13.2	-15.9	16.0
524.	31.7	28.1	-11.3	16.0
526.	26.2	23.6	-9.92	10.0
527.	11.5	10.4	-9.56	10.0
528.	25.8	24.9	-3.48	22.0
529.	9.40	8.50	-9.57	10.0
530.	28.0	28.2	.714	12.0
531.	14.8	16.2	9.45	7.00
532.	15.3	16.7	9.15	50.0
533.	12.7	14.1	11.0	10.0
534.	8.30	8.40	1.20	20.0
535.	19.4	19.5	.515	4.00
536.	9.10	9.10	0.00	17.0
537.	8.20	7.80	-4.87	6.00
538.	20.2	20.2	0.00	11.0
539.	14.7	16.2	10.2	10.0
540.	24.8	23.9	-3.62	17.0
541.	27.4	26.4	-3.64	6.00
542.	23.6	24.6	4.23	7.50
543.	18.5	19.6	5.94	18.0
544.	12.7	13.8	8.66	7.00
545.	17.1	18.1	5.84	13.0
546.	23.7	21.0	-11.3	11.0

547.	23.9	24.8	3.76	15.0
548.	11.2	12.6	12.5	10.0
549.	18.5	18.6	.540	9.00
550.	14.5	15.3	5.51	14.5
551.	28.1	26.1	-7.11	19.0
552.	16.0	16.2	1.25	9.00
553.	11.7	12.4	5.98	20.0
554.	16.9	20.8	23.0	12.0
555.	10.8	12.2	12.9	18.0
556.	21.3	23.4	9.85	10.0
557.	25.0	22.9	-8.40	14.0
558.	18.4	18.6	1.08	16.0
559.	17.3	17.0	-1.73	4.00
560.	9.20	8.40	-8.69	21.0
561.	21.4	19.0	-11.2	12.0
562.	11.3	11.5	1.76	12.0
563.	26.0	22.5	-13.4	6.00
564.	24.7	22.1	-10.5	100.
565.	21.1	19.2	-9.00	17.0
566.	27.8	24.8	-10.7	11.0
567.	19.0	16.9	-11.0	15.0
568.	13.2	12.5	-5.30	8.00
569.	16.5	17.0	3.03	18.0
571.	23.4	26.5	13.2	9.00
572.	23.4	25.8	10.2	15.0
573.	12.3	12.8	4.06	8.00
574.	31.7	28.1	-11.3	10.0
575.	11.7	12.3	5.12	8.00
576.	19.5	21.3	9.23	17.0
577.	13.1	13.9	6.10	16.0
578.	11.4	11.6	1.75	17.0
579.	11.6	12.8	10.3	22.0
580.	20.7	21.9	5.79	15.0
581.	29.2	31.5	7.87	11.0
582.	16.2	16.4	1.23	9.00
583.	13.3	14.3	7.51	9.00
584.	11.8	12.1	2.54	15.0
586.	15.4	15.5	.649	4.00
587.	26.7	28.0	4.86	14.0
588.	12.9	14.2	10.0	9.00
589.	12.0	14.1	17.5	9.00
590.	14.9	16.3	9.39	14.0
591.	14.1	14.6	3.54	9.00
592.	28.5	29.8	4.56	11.0
593.	14.7	16.1	9.52	6.20
594.	13.5	14.3	5.92	9.00
595.	14.0	15.3	9.28	10.0
596.	19.9	21.9	10.0	10.0
597.	14.5	14.9	2.75	22.0

598.	13.5	12.6	-6.66	18.0
599.	21.8	21.4	-1.83	20.0
600.	23.1	24.6	6.49	7.00
601.	10.6	10.2	-3.77	39.0
602.	10.1	9.80	-2.97	15.0
603.	28.7	24.5	-14.6	60.0
604.	33.8	32.2	-4.73	200.
605.	25.0	21.6	-13.6	10.0
606.	16.3	15.8	-3.06	9.00
607.	12.3	11.4	-7.31	11.0
608.	30.0	27.5	-8.33	14.5
609.	23.4	20.4	-12.8	13.0
610.	19.7	19.9	1.01	10.0
611.	11.2	12.5	11.6	9.00
612.	20.7	23.7	14.4	23.0
613.	19.3	22.2	15.0	9.00
614.	21.9	20.8	-5.02	11.0
615.	14.4	16.8	16.6	9.00
616.	32.4	37.7	16.3	16.0
617.	15.0	15.9	6.00	6.00
618.	23.9	24.4	2.09	10.0
619.	19.9	22.0	10.5	14.0
620.	11.4	12.6	10.5	9.20
621.	14.7	15.9	8.16	8.00
622.	17.5	19.1	9.14	11.0
623.	31.0	30.7	-.967	14.5
624.	12.6	13.6	7.93	16.0
625.	14.9	15.0	.671	7.80
626.	30.7	33.6	9.44	9.00
627.	15.1	15.7	3.97	10.0
628.	15.2	16.2	6.57	12.0
629.	22.3	26.1	17.0	6.00
630.	17.3	20.6	19.0	13.0
631.	11.6	11.7	.862	7.00
632.	11.5	11.8	2.60	9.00
633.	18.3	21.3	16.3	8.00
634.	24.0	27.2	13.3	20.0
635.	12.1	13.7	13.2	23.0
636.	12.2	13.8	13.1	8.00
637.	14.2	16.3	14.7	8.00
638.	18.1	19.7	8.83	11.0
639.	13.9	14.8	6.47	9.00
640.	32.1	27.8	-13.3	7.50
641.	28.6	24.7	-13.6	4.00
642.	19.4	17.4	-10.3	9.00
643.	23.5	18.9	-19.5	9.50
644.	17.4	15.2	-12.6	300.
645.	15.5	13.5	-12.9	8.00
646.	18.7	17.6	-5.88	22.0

647.	23.8	22.7	-4.62	120.
648.	12.1	10.6	-12.3	10.0
649.	16.8	16.2	-3.57	8.00
650.	12.1	11.5	-4.95	8.00
651.	19.8	22.1	11.6	18.0
652.	11.1	11.6	4.50	7.80
653.	26.5	26.5	0.00	10.0
654.	21.0	25.0	19.0	76.0
655.	18.4	18.7	1.63	13.0
656.	22.9	20.1	-12.2	22.0
657.	22.4	24.3	8.48	22.0
658.	19.1	19.0	-.523	8.00
660.	20.9	21.6	3.34	8.00
661.	27.9	29.6	6.09	21.0
662.	18.1	18.3	1.10	9.00
663.	26.3	27.1	3.04	7.50
664.	18.4	19.1	3.80	10.0
665.	18.2	18.7	2.74	14.0
666.	32.3	35.0	8.35	12.0
667.	10.8	13.5	25.0	21.0
668.	26.5	28.8	8.67	14.0
669.	16.5	23.3	41.2	18.5
670.	16.0	21.3	33.1	13.0
671.	16.0	15.7	-1.87	7.00
672.	19.3	19.5	1.03	13.0
673.	13.3	16.4	23.3	14.0
674.	19.5	23.5	20.5	8.50
675.	13.1	16.1	22.9	4.00
676.	12.1	13.0	7.43	13.0
677.	32.6	34.9	7.05	14.0
678.	19.7	19.7	0.00	8.00
679.	17.2	17.8	3.48	9.60
680.	39.0	36.8	-5.64	20.0
681.	18.6	16.9	-9.13	10.0
682.	26.8	24.7	-7.83	7.00
683.	11.2	9.00	-19.6	20.0
684.	22.6	18.7	-17.2	12.0
686.	18.9	22.9	21.1	12.0
687.	24.1	24.4	1.24	56.0
688.	13.7	14.7	7.29	28.0
689.	14.6	14.3	-2.05	10.0
690.	10.0	10.0	0.00	7.00
691.	19.8	21.7	9.59	18.0
693.	12.5	12.3	-1.60	7.00
694.	17.8	15.3	-14.0	17.0
695.	32.3	30.8	-4.64	12.0
696.	17.9	16.5	-7.82	10.0
697.	15.6	14.1	-9.61	12.0
698.	8.60	8.00	-6.97	9.00

699.	11.4	10.9	-4.38	12.0
700.	16.1	12.3	-23.6	19.0
701.	17.9	15.9	-11.1	62.0
702.	23.2	21.1	-9.05	29.0
703.	17.0	15.6	-8.23	14.0
704.	16.1	14.3	-11.1	10.0
705.	30.3	26.6	-12.2	13.0
706.	34.9	32.3	-7.44	10.5
707.	18.1	17.6	-2.76	12.0
708.	13.9	14.0	.719	7.00
709.	21.6	22.6	4.62	39.0
710.	17.7	17.9	1.12	8.20
711.	19.7	18.4	-6.59	10.5
712.	19.0	18.4	-3.15	22.0
713.	12.9	13.7	6.20	9.80
714.	23.6	25.4	7.62	14.0
715.	24.6	24.4	-.813	10.0
716.	22.6	24.1	6.63	200.
717.	15.1	15.8	4.63	8.50
718.	18.9	19.5	3.17	17.0
719.	27.1	24.7	-8.85	6.00
720.	15.8	15.4	-2.53	9.50
721.	36.8	70.5	91.5	12.0
722.	27.3	24.5	-10.2	12.0
723.	14.4	11.9	-17.3	9.00
724.	21.2	17.2	-18.8	9.20
725.	33.2	28.0	-15.6	8.00
727.	26.7	23.2	-13.1	11.0
728.	17.6	16.6	-5.68	12.5
729.	22.5	20.0	-11.1	16.5
730.	10.8	10.8	0.00	21.5
731.	7.00	8.20	17.1	20.0
732.	11.5	13.3	15.6	16.0
733.	9.00	9.30	3.33	12.0
735.	9.40	9.30	-1.06	7.00
736.	12.9	13.0	.775	10.0
737.	26.5	25.7	-3.01	19.0
738.	10.6	10.8	1.88	21.5
739.	14.2	14.9	4.92	11.0
740.	16.5	17.1	3.63	9.00
741.	14.0	17.4	24.2	12.0
742.	12.8	15.9	24.2	8.00
743.	10.4	11.3	8.65	9.00
744.	21.3	22.0	3.28	6.00
745.	26.1	23.4	-10.3	8.20
746.	26.1	27.3	4.59	12.0
747.	21.3	23.7	11.2	7.00
748.	12.1	15.0	23.9	50.0
749.	13.7	15.5	13.1	13.8

750.	17.7	18.8	6.21	8.00
751.	10.5	10.4	-.952	10.0
752.	15.5	16.4	5.80	22.0
753.	23.1	25.7	11.2	13.0
754.	31.0	35.0	12.9	12.0
755.	16.8	19.0	13.0	6.80
756.	20.7	23.4	13.0	9.70
757.	14.3	17.1	19.5	7.50
758.	32.3	31.7	-1.85	9.00
759.	14.9	15.3	-2.68	8.50
760.	28.1	26.9	-4.27	20.0
761.	19.8	16.9	-14.6	9.30
762.	30.5	29.0	-4.91	17.0
763.	21.6	19.1	-11.5	11.0
764.	23.4	19.6	-16.2	7.00
765.	30.4	28.0	-7.89	9.00
766.	34.1	30.7	-9.97	180.
767.	16.8	16.1	-4.16	10.0
768.	18.7	19.2	2.67	8.00
769.	12.9	12.9	0.00	6.00
770.	12.5	12.5	0.00	14.0
771.	16.5	18.8	13.9	16.0
772.	10.8	12.5	15.7	11.0
773.	19.3	20.6	6.73	8.00
774.	25.0	24.5	-2.00	6.00
775.	21.8	23.2	6.42	10.0
776.	13.0	13.8	6.15	10.0
777.	17.8	18.6	4.49	11.0
778.	24.9	24.4	-2.00	10.0
779.	27.1	31.8	17.3	40.0
780.	15.1	18.5	22.5	22.0
781.	11.6	13.5	16.3	7.00
782.	26.3	31.0	17.8	15.0
783.	31.8	36.8	15.7	24.0
784.	15.9	21.9	37.7	40.0
785.	14.5	17.2	18.6	7.00
786.	14.2	14.7	3.52	10.0
787.	16.5	17.0	3.03	13.0
788.	15.7	18.5	17.8	23.0
789.	17.2	18.7	8.72	18.0
790.	25.3	27.8	9.88	13.0
791.	20.1	20.6	2.48	7.00
792.	16.8	17.8	5.95	16.0
793.	10.4	11.7	12.5	13.0
794.	16.0	18.0	12.5	20.0
795.	14.6	15.1	3.42	8.00
796.	12.0	15.3	27.5	18.0
797.	20.7	22.2	7.24	8.00
798.	13.9	14.4	3.59	10.0

799.	30.8	30.0	-2.59	11.0
800.	33.4	34.1	2.09	12.0
801.	23.5	24.1	2.55	10.0
802.	26.2	24.3	-7.25	20.0
803.	22.2	20.0	-9.90	12.0
804.	22.2	19.0	-14.4	15.0
805.	18.2	16.1	-11.5	16.0
806.	8.30	7.30	-12.0	22.0
807.	19.3	19.8	2.59	20.0
808.	12.6	11.5	-8.73	22.0
809.	23.0	21.7	-5.65	8.00
810.	15.8	14.9	-5.69	6.00
811.	6.70	7.20	7.46	17.0
812.	28.2	35.2	24.8	18.0
813.	12.8	13.3	3.90	8.00
814.	14.8	16.1	8.78	11.0
815.	26.0	25.3	-2.69	23.0
816.	17.4	17.1	-1.72	6.80
817.	22.7	23.0	1.32	28.0
818.	21.4	23.1	7.94	11.0
819.	11.8	12.6	6.77	13.0
820.	8.20	8.80	7.31	15.0
822.	18.8	23.3	23.9	50.0
823.	21.5	25.4	18.1	11.0
824.	12.1	13.0	7.43	8.00
825.	18.2	18.6	2.19	18.0
826.	12.9	13.4	3.87	11.0
827.	16.9	19.0	12.4	14.2
828.	13.4	14.7	9.70	13.0
829.	13.9	16.5	18.7	12.0
830.	14.8	18.2	22.9	15.0
831.	19.9	20.1	1.00	12.0
832.	24.3	23.2	-4.52	7.00
833.	21.5	29.5	37.2	17.0
834.	27.4	36.4	32.8	5.00
835.	21.7	23.0	5.99	7.00
836.	14.3	15.5	8.39	10.0
838.	11.0	10.7	-2.72	12.0
839.	10.8	10.8	0.00	8.00
841.	18.7	18.0	-3.74	9.00
842.	17.5	15.7	-10.2	12.0
843.	20.2	18.9	-6.43	16.0
844.	24.6	21.5	-12.6	13.0
845.	17.1	15.2	-11.1	6.00
846.	9.30	8.30	-10.7	8.00
847.	32.3	28.0	-13.3	9.50
848.	17.9	15.7	-12.2	35.0
849.	11.1	9.30	-16.2	15.0
851.	19.0	19.9	4.73	5.00

852.	11.7	13.3	13.6	8.00
853.	22.6	23.7	4.86	16.0
854.	12.4	12.9	4.03	7.50
855.	18.9	19.8	4.76	12.0
856.	16.5	16.8	1.81	10.0
857.	12.8	12.8	0.00	18.0
858.	10.8	12.6	16.6	10.0
859.	17.0	16.9	-.588	8.80
860.	12.5	12.7	1.60	13.7
861.	30.2	31.8	5.29	8.00
862.	23.4	23.7	1.28	12.0
863.	11.9	13.7	15.1	12.5
865.	23.1	24.1	4.32	7.00
866.	11.5	12.4	7.82	14.0
867.	11.3	13.2	16.8	22.0
868.	26.5	27.7	4.52	18.0
869.	11.0	12.6	14.5	15.0
870.	13.1	13.3	1.52	6.00
871.	13.7	14.3	4.37	8.00
872.	22.2	21.1	-4.95	8.00
873.	33.0	33.3	.909	43.0
874.	13.3	16.1	21.0	8.00
875.	15.2	17.1	12.5	6.00
876.	21.0	21.2	.952	19.0
877.	34.0	32.3	-5.00	12.0
878.	13.4	15.9	18.6	65.0
879.	20.1	20.4	1.49	13.0
880.	12.2	11.5	-5.73	20.0
881.	15.9	16.2	1.88	9.00
882.	24.2	23.0	-4.95	11.0
883.	21.5	19.6	-8.83	32.0
884.	27.4	26.2	-4.37	11.0
885.	11.4	9.90	-13.1	18.0
886.	20.1	19.7	-1.99	14.5
887.	22.9	20.9	-8.73	11.0
888.	23.3	23.0	-1.28	20.0
889.	11.2	10.5	-6.25	20.0
890.	22.4	21.5	-4.01	5.00
891.	31.8	31.6	-.628	18.0
892.	8.00	8.10	1.25	9.00
893.	15.0	17.0	13.3	12.0
894.	9.70	10.9	12.3	8.00
895.	8.90	10.4	16.8	17.0
896.	9.00	10.3	14.4	22.0
897.	18.4	20.7	12.5	9.00
898.	15.2	16.5	8.55	7.00
899.	15.7	18.6	18.4	10.0
900.	24.2	29.8	23.1	37.0

CORRELATION ANALYSIS LIFE-TEST NO.2 (G321)

1	675.53	130.05	294534.00	206342930.00
2	18.41	6.53	8028.50	166444.31
3	19.05	6.80	8310.00	178559.70
4	4.44	12.24	1939.62	73954.52
5	16.61	23.10	7245.60	353080.60

SAMPLE SIZE (436)

1	2	.04	5439797.60	.04
1	3	.02	5623885.40	.04
1	4	-.09	1242498.80	.04
1	5	-.01	4874239.90	.04
2	3	.92	170890.31	.00
2	4	-.22	28026.05	.04
2	5	.12	141559.44	.04
3	4	.14	42116.16	.04
3	5	.09	144885.55	.04
4	5	-.05	25686.23	.04

APPENDIX E

S2A Life-Test Data

(1) Input-data Format:

* Sample Number

x_1	x_2	x_3	x_4	x_5
x_6	x_7	x_8	x_9	x_{10}
x_{11}	x_{12}	x_{13}	x_{14}	
y_1	y_2	y_3	y_4	y_5
y_6	y_7	y_8	y_9	y_{10}
y_{11}	y_{12}	y_{13}	y_{14}	
z_1	z_2	z_3	z_4	z_5
z_6	z_7	z_8	z_9	z_{10}
z_{11}	z_{12}	z_{13}	z_{14}	

(2) Description of Input-data:

x_1: Reverse-bias at I_r=1-ua, at zero-hour in volts.

x_2: Noise-voltage spectral density at f=10-Hz and I_r=1-ua, at zero-hour in uv/$Hz^{\frac{1}{2}}$

x_3: " " " at 1-kHz.

x_4: Ratio of x_2/x_3.

x_5: Excess noise figure at I_r=1-ua (see page 104).

x_6: Reverse-bias at I_r=10-ua, at zero-hour in volts.

x_7: Noise-voltage spectral density at f=10-Hz and I_r=10-ua, at zero-hour in uv/$Hz^{\frac{1}{2}}$

x_8: " " " at f=1-kHz.

x_9: Ratio of x_7/x_8.

x_{10}: Excess noise figure at I_r=10-ua (see page 104).

x_{11}: Differential impedance in ohms.

x_{12}: I_r at V_b=200 volts.

x_{13}: Stress-factor = $200/x_6$.

x_{14}: Percent-degradation=I_{final}/x_{12}.

y_1 through y_{14} are identical with x_1 through x_{14} respectively except measured at 500-hours later.

z_1 through z_{14} are identical with x_1 through x_{14} respectively except measured at 1000-hours later.

(3) $R_{i,j}$ are computed by the correlation analysis program presented in Appendix H.

LIFE-TEST NO.3 (S2A) INPUT-DATA

*SAMPLE NUMBER 1

98	20	3	6.667	9.371
135	120	180	.667	17777.776
4.111	420.000	1.481	1.548	
80	15	2	7.500	6.250
120	100	100	1.000	6944.444
4.444	600.000	1.667	1.083	
75	15	2	7.500	7.111
115	100	100	1.000	7561.437
4.444	650.000			

*SAMPLE NUMBER 2

115	30	10	3.000	75.614
130	50	38	1.316	854.438
1.667	262.000	1.538	1.527	
105	35	6	5.833	32.653
125	45	40	1.125	1024.000
2.222	380.000	1.600	1.053	
100	40	6	6.667	36.000
120	40	38	1.053	1002.778
2.222	400.000			

*SAMPLE NUMBER 3

158	40	5	8.000	10.014
175	70	65	1.077	1379.592
1.889	32.000	1.143	5.000	
155	40	8	5.000	26.639
165	75	62	1.210	1411.938
1.111	120.000	1.212	1.333	
120	20	8	2.500	44.444
148	90	77	1.169	2706.812
3.111	160.000			

*SAMPLE NUMBER 4

155	20	5	4.000	10.406
165	25	16	1.563	94.031
1.111	150.000	1.212	1.067	
150	10	3	3.333	4.000
160	20	16	1.250	100.000
1.111	160.000	1.250	1.000	
150	10	3	3.333	4.000
160	20	16	1.250	100.000
1.111	160.000			

*SAMPLE NUMBER 5

155	25	3	8.333	3.746
178	60	40	1.500	504.987
2.556	200.000	1.124	1.150	
150	25	3	8.333	4.000
175	60	50	1.200	816.327

```
     2.778    225.000      1.143        1.022
       140         15          2        7.500         2.041
       170         60         50        1.200       865.052
     3.333    230.000
*SAMPLE NUMBER  6
       125         18          2        9.000         2.560
       155         45         38        1.184       601.041
     3.333    130.000      1.290        1.077
       120         10          2        5.000         2.778
       150         40         35        1.143       544.444
     3.333    140.000      1.333        1.000
       115         10          2        5.000         3.025
       150         40         35        1.143       544.444
     3.889    140.000
*SAMPLE NUMBER  7
       145         25          8        3.125        30.440
       165         50         44        1.136       711.111
     2.222    100.000      1.212        1.200
       140         30          6        5.000        18.367
       165         55         45        1.222       743.802
     2.778    100.000      1.212        1.200
       138         25          5        5.000        13.127
       160         50         44        1.136       756.250
     2.444    120.000
*SAMPLE NUMBER  8
       165         60          8        7.500        23.508
       170         70         58        1.207      1164.014
      .556    460.000      1.176        1.043
       165         60          8        7.500        23.508
       170         70         50        1.400       865.052
      .556    480.000      1.176        1.000
       160         60          9        6.667        31.641
       170         70         52        1.346       935.640
     1.111    480.000
*SAMPLE NUMBER  9
       150         20         10        2.000        44.444
       165         50         20        2.500       146.924
     1.667    170.000      1.212        1.059
       150         20         10        2.000        44.444
       165         50         20        2.500       146.924
     1.667    170.000      1.212        1.059
       150         20         10        2.000        44.444
       160         50         20        2.500       156.250
     1.111    180.000
*SAMPLE NUMBER 10
       125         35         15        2.333       144.000
       135         70         25        2.800       342.936
     1.111    200.000      1.481        1.000
       110         25         10        2.500        82.645
```

128	70	26	2.692	412.598
2.000	200.000	1.563	1.000	
105	20	9	2.222	73.469
125	50	26	1.923	432.640
2.222	200.000			
*SAMPLE NUMBER 11				
150	20	8	2.500	28.444
160	5	8	.625	25.000
1.111	150.000	1.250	3.333	
130	20	5	4.000	14.793
150	7	10	.700	44.444
2.222	200.000	1.333	2.500	
80	10	1	10.000	1.563
145	50	40	1.250	760.999
7.222	500.000			
*SAMPLE NUMBER 12				
178	50	10	5.000	31.562
190	55	28	1.964	217.175
1.333	110.000	1.053	1.091	
175	40	6	6.667	11.755
185	50	30	1.667	262.966
1.111	120.000	1.081	1.000	
170	30	4	7.500	5.536
182	50	40	1.250	483.033
1.333	120.000			
*SAMPLE NUMBER 13				
75	50	5	10.000	44.444
110	350	30	11.667	743.802
3.889	56.000	1.818	.964	
65	60	10	6.000	236.686
110	400	40	10.000	1322.314
5.000	56.000	1.818	.964	
60	70	12	5.833	400.000
105	400	50	8.000	2267.574
5.000	54.000			
*SAMPLE NUMBER 14				
148	18	4	4.500	7.305
165	25	28	.893	287.971
1.889	65.000	1.212	1.015	
145	20	4	5.000	7.610
160	30	28	1.071	306.250
1.667	68.000	1.250	.971	
143	20	4	5.000	7.824
160	30	28	1.071	306.250
1.889	66.000			
*SAMPLE NUMBER 15				
55	10	2	5.000	13.223
155	85	28	3.036	326.327
11.111	45.000	1.290	1.222	

```
        40          20           2          10.000        25.000
       135          90          40           2.250       877.915
    10.556      52.000       1.481           1.058
        34          20           2          10.000        34.602
       125          90          40           2.250      1024.000
    10.111      55.000
*SAMPLE NUMBER 16
       158          25           5           5.000        10.014
       185          45          20           2.250       116.874
     3.000      38.000       1.081           1.158
       155          20           3           6.667         3.746
       180          40          28           1.429       241.975
     2.778      42.000       1.111           1.048
       152          20           3           6.667         3.895
       175          40          28           1.429       256.000
     2.556      44.000
*SAMPLE NUMBER 17
       178          30           5           6.000         7.890
       192          55          48           1.146       625.000
     1.556      40.000       1.042           1.000
       170          30           5           6.000         8.651
       185          50          42           1.190       515.413
     1.667      44.000       1.081            .909
       152          20           3           6.667         3.895
       175          40          38           1.053       471.510
     2.556      40.000
*SAMPLE NUMBER 18
       185          25           8           3.125        18.700
       198          25          15           1.667        57.392
     1.444      25.000       1.010           1.120
       180          30           6           5.000        11.111
       195          40          21           1.905       115.976
     1.667      26.000       1.026           1.077
       180          30           5           6.000         7.716
       195          40          20           2.000       105.194
     1.667      28.000
*SAMPLE NUMBER 19
       120          25           5           5.000        17.361
       160         140           8          17.500        25.000
     4.444     138.000       1.250           1.014
       120          25           2          12.500         2.778
       160         140           9          15.556        31.641
     4.444     140.000       1.250           1.000
       125          30           3          10.000         5.760
       165         180          12          15.000        52.893
     4.444     140.000
*SAMPLE NUMBER 20
       170          15           5           3.000         8.651
       205          80          45           1.778       481.856
```

3.889	12.000	.976	1.333	
160	10	2	5.000	1.563
200	70	42	1.667	441.000
4.444	12.000	1.000	1.333	
140	10	1	10.000	.510
192	70	60	1.167	976.563
5.778	16.000			
*SAMPLE NUMBER 21				
135	28	8	3.500	35.117
158	50	25	2.000	250.361
2.556	130.000	1.266	1.077	
130	25	5	5.000	14.793
150	50	15	3.333	100.000
2.222	140.000	1.333	1.000	
130	20	5	4.000	14.793
150	50	15	3.333	100.000
2.222	140.000			
*SAMPLE NUMBER 22				
120	25	5	5.000	17.361
185	45	10	4.500	29.218
7.222	110.000	1.081	1.136	
100	20	2	10.000	4.000
180	40	29	1.379	259.568
8.889	120.000	1.111	1.042	
80	18	2	9.000	6.250
175	40	25	1.600	204.082
10.556	125.000			
*SAMPLE NUMBER 23				
115	30	10	3.000	75.614
140	70	40	1.750	816.327
2.778	255.000	1.429	1.020	
110	35	8	4.375	52.893
138	80	55	1.455	1588.427
3.111	260.000	1.449	1.000	
108	30	6	5.000	30.864
135	80	47	1.702	1212.071
3.000	260.000			
*SAMPLE NUMBER 24				
170	25	4	6.250	5.536
182	45	38	1.184	435.938
1.333	38.000	1.099	1.316	
165	30	5	6.000	9.183
150	50	40	1.250	711.111
-1.667	40.000	1.333	1.250	
155	30	6	5.000	14.984
170	70	43	1.628	639.792
1.667	50.000			
*SAMPLE NUMBER 25				
230	10	2	5.000	.756

310	100	10	10.000	10.406
8.889	.700	.645	1.000	
230	10	2	5.000	.756
310	100	10	10.000	10.406
8.889	.700	.645	1.000	
230	10	2	5.000	.756
310	100	10	10.000	10.406
8.889	.700			
*SAMPLE NUMBER 26				
150	20	5	4.000	11.111
178	70	68	1.029	1459.412
3.111	180.000	1.124	1.444	
150	20	3	6.667	4.000
180	70	67	1.045	1385.494
3.333	200.000	1.111	1.300	
155	20	4	5.000	6.660
180	70	65	1.077	1304.013
2.778	260.000			
*SAMPLE NUMBER 27				
232	400	80	5.000	1189.061
320	800	160	5.000	2500.000
9.778	.040	.625	1.000	
232	400	80	5.000	1189.061
320	800	160	5.000	2500.000
9.778	.040	.625	1.000	
230	400	80	5.000	1209.830
320	800	160	5.000	2500.000
10.000	.040			
*SAMPLE NUMBER 28				
115	2000	40	50.000	1209.830
220	4000	700	5.714	101239.650
11.667	2.000	.909	4.000	
110	2000	40	50.000	1322.314
220	5000	900	5.556	167355.330
12.222	8.000	.909	1.000	
100	3000	60	50.000	3600.000
210	4000	900	4.444	183673.450
12.222	8.000			
*SAMPLE NUMBER 29				
130	75	25	3.000	369.823
225	750	80	9.375	1264.198
10.556	6.000	.889	1.500	
125	100	20	5.000	256.000
215	800	80	10.000	1384.532
10.000	8.000	.930	1.125	
120	200	15	13.333	156.250
210	800	70	11.429	1111.111
10.000	9.000			
*SAMPLE NUMBER 30				

175	30	3	10.000	2.939
198	150	15	10.000	57.392
2.556	12.000	1.010	2.667	
165	20	4	5.000	5.877
190	100	10	10.000	27.701
2.778	28.000	1.053	1.143	
160	20	4	5.000	6.250
185	60	10	6.000	29.218
2.778	32.000			
*SAMPLE NUMBER 31				
160	40	3	13.333	3.516
198	75	15	5.000	57.392
4.222	12.000	1.010	1.333	
150	30	5	6.000	11.111
195	70	12	5.833	37.870
5.000	16.000	1.026	1.000	
148	20	4	5.000	7.305
190	60	12	5.000	39.889
4.667	16.000			
*SAMPLE NUMBER 32				
180	50	9	5.556	25.000
190	150	18	8.333	89.751
1.111	30.000	1.053	1.200	
178	50	8	6.250	20.199
190	130	16	8.125	70.914
1.333	34.000	1.053	1.059	
170	60	8	7.500	22.145
185	100	15	6.667	65.741
1.667	36.000			
*SAMPLE NUMBER 33				
80	20	1	20.000	1.563
198	60	58	1.034	858.076
13.111	11.000	1.010	1.455	
75	30	3	10.000	16.000
195	100	70	1.429	1288.626
13.333	12.000	1.026	1.333	
65	60	3	20.000	21.302
185	1000	200	5.000	11687.361
13.333	16.000			
*SAMPLE NUMBER 34				
260	15	8	1.875	9.467
270	45	38	1.184	198.080
1.111	.020	.741	1.000	
260	20	5	4.000	3.698
275	50	40	1.250	211.570
280.000	50.000	40.000	1.250	
1	0	0	1.000	.000
265	20	5	4.000	3.560
1.667	.020			

*SAMPLE NUMBER 35				
125	25	5	5.000	16.000
200	120	15	8.000	56.250
8.333	10.000	1.000	1.300	
115	20	2	10.000	3.025
195	100	10	10.000	26.298
8.889	12.000	1.026	1.083	
110	20	2	10.000	3.306
188	100	10	10.000	28.293
8.667	13.000			
*SAMPLE NUMBER 36				
185	35	6	5.833	10.519
202	45	40	1.125	392.118
1.889	10.000	.990	1.600	
180	30	5	6.000	7.716
200	40	39	1.026	380.250
2.222	10.000	1.000	1.600	
178	30	5	6.000	7.890
195	40	38	1.053	379.750
1.889	16.000			
*SAMPLE NUMBER 37				
100	20	3	6.667	9.000
202	100	15	6.667	55.142
11.333	10.000	.990	1.000	
100	20	2	10.000	4.000
200	90	9	10.000	20.250
11.111	10.000	1.000	1.000	
100	10	2	5.000	4.000
200	80	8	10.000	16.000
11.111	10.000			
*SAMPLE NUMBER 38				
110	30	5	6.000	20.661
230	90	75	1.200	1063.327
13.333	7.000	.870	1.429	
90	30	3	10.000	11.111
210	100	70	1.429	1111.111
13.333	8.000	.952	1.250	
70	30	2	15.000	8.163
200	150	50	3.000	625.000
14.444	10.000			
*SAMPLE NUMBER 39				
150	30	5	6.000	11.111
200	150	50	3.000	625.000
5.556	10.000	1.000	1.600	
138	40	3	13.333	4.726
195	150	30	5.000	236.686
6.333	14.000	1.026	1.143	
138	40	3	13.333	4.726
190	150	30	5.000	249.307

5.778	16.000			
*SAMPLE NUMBER 40				
195	30	8	3.750	16.831
210	150	80	1.875	1451.247
1.667	8.000	.952	2.500	
185	40	10	4.000	29.218
200	120	68	1.765	1156.000
1.667	10.000	1.000	2.000	
180	40	10	4.000	30.864
195	70	68	1.029	1216.042
1.667	20.000			
*SAMPLE NUMBER 41				
165	20	9	2.222	29.752
215	50	30	1.667	194.700
5.556	8.000	.930	1.250	
160	20	9	2.222	31.641
210	50	30	1.667	204.082
5.556	9.000	.952	1.111	
160	20	9	2.222	31.641
200	50	30	1.667	225.000
4.444	10.000			
*SAMPLE NUMBER 42				
68	100	10	10.000	216.263
380	1000	100	10.000	692.521
34.667	2.000	.526	2.500	
60	100	10	10.000	277.778
380	1000	100	10.000	692.521
35.556	3.000	.526	1.667	
60	100	9	11.111	225.000
380	1000	100	10.000	692.521
35.556	5.000			
*SAMPLE NUMBER 43				
50	125	8	15.625	256.000
250	120	5	24.000	4.000
22.222	5.000	.800	1.200	
35	100	10	10.000	816.327
240	100	6	16.667	6.250
22.778	5.000	.833	1.200	
25	15	10	1.500	1600.000
218	100	6	16.667	7.575
21.444	6.000			
*SAMPLE NUMBER 44				
160	160	4	40.000	6.250
202	70	40	1.750	392.118
4.667	9.000	.990	1.000	
160	160	4	40.000	6.250
202	70	40	1.750	392.118
4.667	9.000	.990	1.000	
160	40	4	10.000	6.250

202	70	15	4.667	55.142
4.667	9.000			
*SAMPLE NUMBER 45				
180	5	1	5.000	.309
230	70	8	8.750	12.098
5.556	3.000	.870	1.333	
150	10	1	10.000	.444
220	80	8	10.000	13.223
7.778	3.000	.909	1.333	
132	10	1	10.000	.574
218	100	9	11.111	17.044
9.556	4.000			
*SAMPLE NUMBER 46				
125	5	2	2.500	2.560
220	80	15	5.333	46.488
10.556	7.000	.909	1.143	
110	30	2	15.000	3.306
210	100	10	10.000	22.676
11.111	8.000	.952	1.000	
85	30	2	15.000	5.536
202	150	10	15.000	24.507
13.000	8.000			
*SAMPLE NUMBER 47				
75	200	20	10.000	711.111
205	60	64	.938	974.658
14.444	8.000	.976	1.500	
55	200	20	10.000	1322.314
205	60	62	.968	914.694
16.667	8.000	.976	1.500	
50	200	20	10.000	1600.000
198	70	60	1.167	918.274
16.444	12.000			
*SAMPLE NUMBER 48				
175	60	20	3.000	130.612
250	150	30	5.000	144.000
8.333	5.000	.800	2.000	
170	40	9	4.444	28.028
220	100	20	5.000	82.645
5.556	7.000	.909	1.429	
178	30	5	6.000	7.890
200	50	15	3.333	56.250
2.444	10.000			
*SAMPLE NUMBER 49				
195	45	10	4.500	26.298
230	75	40	1.875	302.457
3.889	6.000	.870	1.667	
180	30	6	5.000	11.111
200	60	45	1.333	506.250
2.222	10.000	1.000	1.000	

172	20	4	5.000	5.408
200	60	45	1.333	506.250
3.111	10.000			
*SAMPLE NUMBER 50				
170	25	2	12.500	1.384
195	45	35	1.286	322.156
2.778	8.000	1.026	1.250	
175	20	5	4.000	8.163
200	40	33	1.212	272.250
2.778	10.000	1.000	1.000	
185	20	5	4.000	7.305
200	40	33	1.212	272.250
1.667	10.000			
*SAMPLE NUMBER 51				
118	28	3	9.333	6.464
255	200	20	10.000	61.515
15.222	3.000	.784	1.333	
115	30	2	15.000	3.025
250	200	14	14.286	31.360
15.000	4.000	.800	1.000	
90	30	2	15.000	4.938
235	200	14	14.286	35.491
16.111	4.000			
*SAMPLE NUMBER 52				
188	20	4	5.000	4.527
208	45	10	4.500	23.114
2.222	9.000	.962	1.111	
185	20	3	6.667	2.630
200	40	8	5.000	16.000
1.667	10.000	1.000	1.000	
185	15	3	5.000	2.630
200	40	8	5.000	16.000
1.667	10.000			
*SAMPLE NUMBER 53				
72	6	1	6.000	1.929
320	100	100	1.000	976.563
27.556	3.000	.625	1.000	
68	5	1	5.000	2.163
320	100	100	1.000	976.563
28.000	3.000	.625	1.000	
65	5	1	5.000	2.367
320	100	100	1.000	976.563
28.333	3.000			
*SAMPLE NUMBER 54				
168	35	4	8.750	5.669
202	110	11	10.000	29.654
3.778	10.000	.990	1.000	
165	30	3	10.000	3.306
200	100	10	10.000	25.000

3.889	10.000	1.000	1.000	
150	20	2	10.000	1.778
200	70	11	6.364	30.250
5.556	10.000			
*SAMPLE NUMBER 55				
230	48	9	5.333	15.312
245	110	80	1.375	1066.223
1.667	.100	.816	2.000	
220	40	8	5.000	13.223
240	100	25	4.000	108.507
2.222	.200	.833	1.000	
215	30	8	3.750	13.845
235	80	23	3.478	95.790
2.222	.200			
*SAMPLE NUMBER 56				
150	300	18	16.667	144.000
325	1200	900	1.333	76686.378
19.444	4.000	.615	1.000	
120	320	20	16.000	277.778
320	1500	800	1.875	62499.995
22.222	4.000	.625	1.000	
100	330	20	16.500	400.000
320	1500	800	1.875	62499.995
24.444	4.000			
*SAMPLE NUMBER 57				
178	28	8	3.500	20.199
262	50	40	1.250	233.087
9.333	3.000	.763	1.000	
175	20	8	2.500	20.898
260	50	30	1.667	133.136
9.444	3.000	.769	1.000	
175	15	8	1.875	20.898
260	60	27	2.222	107.840
9.444	3.000			
*SAMPLE NUMBER 58				
192	55	15	3.667	61.035
218	120	80	1.500	1346.688
2.889	3.000	.917	2.667	
185	50	10	5.000	29.218
210	120	85	1.412	1638.322
2.778	6.000	.952	1.333	
180	40	10	4.000	30.864
205	100	83	1.205	1639.262
2.778	8.000			
*SAMPLE NUMBER 59				
75	220	19	11.579	641.778
250	620	100	6.200	1600.000
19.444	2.000	.800	1.500	
60	200	17	11.765	802.778

245	500	35	14.286	204.082
20.556	3.000	.816	1.000	
50	180	15	12.000	900.000
242	300	36	8.333	221.296
21.333	3.000			
*SAMPLE NUMBER 60				
145	20	2	10.000	1.902
245	600	230	2.609	8812.995
11.111	2.000	.816	2.500	
135	18	2	9.000	2.195
240	500	150	3.333	3906.250
11.667	5.000	.833	1.000	
128	20	2	10.000	2.441
240	500	146	3.425	3700.694
12.444	5.000			
*SAMPLE NUMBER 61				
188	20	5	4.000	7.073
230	200	15	13.333	42.533
4.667	4.000	.870	1.250	
175	15	4	3.750	5.224
220	100	10	10.000	20.661
5.000	5.000	.909	1.000	
175	15	4	3.750	5.224
218	40	11	3.636	25.461
4.778	5.000			
*SAMPLE NUMBER 62				
182	55	15	3.667	67.927
222	130	85	1.529	1465.993
4.444	5.000	.901	1.400	
180	50	10	5.000	30.864
220	130	80	1.625	1322.314
4.444	5.000	.909	1.400	
180	50	10	5.000	30.864
215	130	80	1.625	1384.532
3.889	7.000			
*SAMPLE NUMBER 63				
168	65	8	8.125	22.676
338	185	125	1.480	1367.687
18.889	3.000	.592	2.000	
160	60	5	12.000	9.766
230	200	120	1.667	2722.117
7.778	4.000	.870	1.500	
155	60	4	15.000	6.660
228	250	118	2.119	2678.516
8.111	6.000			
*SAMPLE NUMBER 64				
128	32	4	8.000	9.766
382	300	30	10.000	61.676
28.222	3.000	.524	1.000	

125	30	3	10.000	5.760
380	300	30	10.000	62.327
28.333	3.000	.526	1.000	
122	30	3	10.000	6.047
380	300	30	10.000	62.327
28.667	3.000			
*SAMPLE NUMBER 65				
218	12	4	3.000	3.367
275	65	40	1.625	211.570
6.333	.300	.727	1.000	
215	10	4	2.500	3.461
270	50	25	2.000	85.734
6.111	.300	.741	1.000	
212	10	5	2.000	5.562
268	40	22	1.818	67.387
6.222	.300			
*SAMPLE NUMBER 66				
180	22	8	2.750	19.753
235	250	23	10.870	95.790
6.111	2.000	.851	2.500	
180	20	7	2.857	15.123
232	100	25	4.000	116.119
5.778	4.000	.862	1.250	
178	20	7	2.857	15.465
230	50	25	2.000	118.147
5.778	5.000			
*SAMPLE NUMBER 67				
190	22	8	2.750	17.729
205	45	20	2.250	95.181
1.667	9.000	.976	1.111	
190	20	6	3.333	9.972
202	40	10	4.000	24.507
1.333	10.000	.990	1.000	
190	20	6	3.333	9.972
200	40	10	4.000	25.000
1.111	10.000			
*SAMPLE NUMBER 68				
180	45	8	5.625	19.753
210	180	80	2.250	1451.247
3.333	7.000	.952	1.429	
180	50	5	10.000	7.716
205	100	45	2.222	481.856
2.778	9.000	.976	1.111	
178	60	4	15.000	5.050
200	70	48	1.458	576.000
2.444	10.000			
*SAMPLE NUMBER 69				
155	10	1	10.000	.416
240	120	45	2.667	351.563

9.444	2.000	.833	1.500	
155	10	1	10.000	.416
235	100	40	2.500	289.724
8.889	2.000	.851	1.500	
100	10	1	10.000	1.000
215	40	26	1.538	146.241
12.778	3.000			
*SAMPLE NUMBER 70				
178	12	4	3.000	5.050
248	45	30	1.500	146.332
7.778	2.000	.806	1.000	
180	10	3	3.333	2.778
240	40	20	2.000	69.444
6.667	2.000	.833	1.000	
186	10	3	3.333	2.601
240	40	20	2.000	69.444
6.000	2.000			
*SAMPLE NUMBER 71				
195	35	8	4.375	16.831
215	60	40	1.500	346.133
2.222	8.000	.930	1.125	
190	30	6	5.000	9.972
210	50	45	1.111	459.184
2.222	8.000	.952	1.125	
188	30	6	5.000	10.186
202	50	45	1.111	496.275
1.556	9.000			
*SAMPLE NUMBER 72				
198	25	6	4.167	9.183
240	60	20	3.000	69.444
4.667	3.000	.833	1.333	
190	20	5	4.000	6.925
225	50	25	2.000	123.457
3.889	4.000	.889	1.000	
180	20	5	4.000	7.716
220	40	25	1.600	129.132
4.444	4.000			
*SAMPLE NUMBER 73				
28	25	2	12.500	51.020
445	205	12	17.083	7.272
46.333	2.000	.449	1.000	
12	30	2	15.000	277.778
440	200	12	16.667	7.438
47.556	2.000	.455	1.000	
12	30	2	15.000	277.778
440	200	11	18.182	6.250
47.556	2.000			
*SAMPLE NUMBER 74				
25	45	3	15.000	144.000

278	320	18	17.778	41.923
28.111	2.000	.719	1.000	
18	40	2	20.000	123.457
375	305	15	20.333	16.000
39.667	2.000	.533	1.000	
15	40	2	20.000	177.778
370	300	15	20.000	16.435
39.444	2.000			
*SAMPLE NUMBER 75				
195	25	5	5.000	6.575
222	50	10	5.000	20.291
3.000	5.000	.901	1.600	
190	25	5	5.000	6.925
210	50	12	4.167	32.653
2.222	6.000	.952	1.333	
180	70	12	5.833	44.444
202	70	13	5.385	41.418
2.444	8.000			
*SAMPLE NUMBER 76				
198	18	5	3.600	6.377
215	50	35	1.429	265.008
1.889	4.000	.930	2.250	
190	20	4	5.000	4.432
210	40	29	1.379	190.703
2.222	5.000	.952	1.800	
190	20	4	5.000	4.432
208	30	29	1.034	194.388
2.000	9.000			
*SAMPLE NUMBER 77				
188	15	8	1.875	18.108
305	45	20	2.250	42.999
13.000	2.000	.656	1.000	
182	12	5	2.400	7.547
302	42	15	2.800	24.670
13.333	2.000	.662	1.000	
182	10	5	2.000	7.547
300	40	13	3.077	18.778
13.111	2.000			
*SAMPLE NUMBER 78				
185	38	10	3.800	29.218
216	50	28	1.786	168.038
3.444	5.000	.926	1.800	
180	30	9	3.333	25.000
210	50	25	2.000	141.723
3.333	6.000	.952	1.500	
178	30	9	3.333	25.565
202	60	25	2.400	153.171
2.667	9.000			
*SAMPLE NUMBER 79				

170	10	1	10.000	.346
245	40	30	1.333	149.938
8.333	3.000	.816	1.000	
170	10	1	10.000	.346
245	40	25	1.600	104.123
8.333	3.000	.816	1.000	
155	10	1	10.000	.416
240	40	29	1.379	146.007
9.444	3.000			
*SAMPLE NUMBER 80				
200	10	1	10.000	.250
250	100	28	3.571	125.440
5.556	1.000	.800	2.000	
190	10	1	10.000	.277
245	100	40	2.500	266.556
6.111	2.000	.816	1.000	
170	10	1	10.000	.346
240	60	42	1.429	306.250
7.778	2.000			
*SAMPLE NUMBER 81				
198	158	125	1.264	3985.563
238	600	460	1.304	37356.117
4.444	2.000	.840	4.000	
195	150	120	1.250	3786.982
235	600	400	1.500	28972.380
4.444	4.000	.851	2.000	
192	150	120	1.250	3906.250
232	500	400	1.250	29726.514
4.444	8.000			
*SAMPLE NUMBER 82				
218	25	8	3.125	13.467
245	55	46	1.196	352.520
3.000	.300	.816	1.333	
215	20	5	4.000	5.408
240	50	43	1.163	321.007
2.778	.400	.833	1.000	
210	20	5	4.000	5.669
238	50	40	1.250	282.466
3.111	.400			
*SAMPLE NUMBER 83				
197	30	3	10.000	2.319
265	42	20	2.100	56.960
7.556	2.000	.755	1.000	
190	20	2	10.000	1.108
260	40	28	1.429	115.976
7.778	2.000	.769	1.000	
188	10	2	5.000	1.132
255	30	27	1.111	112.111
7.444	2.000			

*SAMPLE NUMBER 84				
198	35	5	7.000	6.377
225	120	40	3.000	316.049
3.000	2.000	.889	1.000	
190	30	3	10.000	2.493
220	100	45	2.222	418.388
3.333	2.000	.909	1.000	
183	30	3	10.000	2.687
218	70	47	1.489	464.818
3.889	2.000			
*SAMPLE NUMBER 85				
287	22	3	7.333	1.093
320	80	48	1.667	225.000
3.667	.100	.625	1.000	
285	20	2	10.000	.492
320	80	45	1.778	197.754
3.889	.100	.625	1.000	
285	20	2	10.000	.492
320	80	45	1.778	197.754
3.889	.100			
*SAMPLE NUMBER 86				
192	22	4	5.500	4.340
285	115	25	4.600	76.947
10.333	2.000	.702	1.000	
180	20	2	10.000	1.235
270	100	28	3.571	107.545
10.000	2.000	.741	1.000	
160	20	2	10.000	1.563
262	90	28	3.214	114.212
11.333	2.000			
*SAMPLE NUMBER 87				
198	22	5	4.400	6.377
215	95	38	2.500	312.385
1.889	2.000	.930	2.500	
190	15	3	5.000	2.493
210	100	40	2.500	362.812
2.222	4.000	.952	1.250	
180	10	2	5.000	1.235
208	70	45	1.556	468.057
3.111	5.000			
*SAMPLE NUMBER 88				
148	25	3	8.333	4.109
225	190	20	9.500	79.012
8.556	3.000	.889	1.667	
140	20	2	10.000	2.041
220	200	20	10.000	82.645
8.889	3.000	.909	1.667	
120	20	2	10.000	2.778
212	200	20	10.000	89.000

10.222	5.000			
*SAMPLE NUMBER 89				
165	54	4	13.500	5.877
240	88	55	1.600	525.174
8.333	2.000	.833	2.000	
160	50	3	16.667	3.516
240	80	40	2.000	277.778
8.889	2.000	.833	2.000	
132	50	3	16.667	5.165
235	80	40	2.000	289.724
11.444	4.000			
*SAMPLE NUMBER 90				
182	35	5	7.000	7.547
248	158	32	4.938	166.493
7.333	2.000	.806	1.000	
180	30	3	10.000	2.778
240	150	30	5.000	156.250
6.667	2.000	.833	1.000	
185	30	3	10.000	2.630
235	150	28	5.357	141.965
5.556	2.000			
*SAMPLE NUMBER 91				
98	12	1	12.000	1.041
312	55	42	1.310	181.213
23.778	.300	.641	1.000	
92	10	1	10.000	1.181
305	55	42	1.310	189.626
23.667	.300	.656	1.000	
90	10	1	10.000	1.235
300	50	45	1.111	225.000
23.333	.300			
*SAMPLE NUMBER 92				
248	39	5	7.800	4.065
268	125	30	4.167	125.306
2.222	.100	.746	1.000	
240	30	4	7.500	2.778
265	100	20	5.000	56.960
2.778	.100	.755	1.000	
240	30	4	7.500	2.778
260	120	19	6.316	53.402
2.222	.100			
*SAMPLE NUMBER 93				
192	10	1	10.000	.271
245	62	8	7.750	10.662
5.889	2.000	.816	1.000	
190	10	1	10.000	.277
250	60	9	6.667	12.960
6.667	2.000	.800	1.000	
190	10	1	10.000	.277

245	60	9	6.667	13.494
6.111	2.000			
*SAMPLE NUMBER 94				
205	22	2	11.000	.952
262	110	100	1.100	1456.792
6.333	.100	.763	12.000	
200	20	2	10.000	1.000
260	110	90	1.222	1198.225
6.667	.100	.769	12.000	
195	20	2	10.000	1.052
255	120	100	1.200	1537.870
6.667	1.200			
*SAMPLE NUMBER 95				
238	52	6	8.667	6.355
270	96	65	1.477	579.561
3.556	.100	.741	7.000	
230	50	5	10.000	4.726
250	80	63	1.270	635.040
2.222	.100	.800	7.000	
229	30	6	5.000	6.865
245	70	63	1.111	661.224
1.778	.700			
*SAMPLE NUMBER 96				
175	28	3	9.333	2.939
320	125	12	10.417	14.063
16.111	2.000	.625	1.000	
172	25	2	12.500	1.352
320	120	10	12.000	9.766
16.444	2.000	.625	1.000	
170	25	2	12.500	1.384
330	120	10	12.000	9.183
17.778	2.000			
*SAMPLE NUMBER 97				
198	38	7	5.429	12.499
235	195	20	9.750	72.431
4.111	2.000	.851	1.500	
190	40	7	5.714	13.573
235	200	20	10.000	72.431
5.000	2.000	.851	1.500	
190	60	5	12.000	6.925
230	250	20	12.500	75.614
4.444	3.000			
*SAMPLE NUMBER 98				
198	18	8	2.250	16.325
212	55	22	2.500	107.690
1.556	4.000	.943	1.500	
195	20	7	2.857	12.886
210	50	20	2.500	90.703
1.667	4.000	.952	1.500	

190	30	7	4.286	13.573
208	50	20	2.500	92.456
2.000	6.000			
*SAMPLE NUMBER 99				
222	32	7	4.571	9.942
242	72	40	1.800	273.205
2.222	.100	.826	2.000	
220	30	6	5.000	7.438
240	70	45	1.556	351.563
2.222	.100	.833	2.000	
220	30	6	5.000	7.438
240	70	46	1.522	367.361
2.222	.200			
*SAMPLE NUMBER100				
215	10	1	10.000	.216
270	40	35	1.143	168.038
6.111	.700	.741	1.143	
215	10	1	10.000	.216
270	40	36	1.111	177.778
6.111	.700	.741	1.143	
210	10	1	10.000	.227
272	40	38	1.053	195.177
6.889	.800			
*SAMPLE NUMBER101				
210	40	6	6.667	8.163
260	180	180	1.000	4792.899
5.556	.200	.769	4.000	
210	40	6	6.667	8.163
280	200	200	1.000	5102.041
7.778	.800	.714	1.000	
212	60	6	10.000	8.010
280	250	190	1.316	4604.592
7.556	.800			
*SAMPLE NUMBER102				
232	7	1	7.000	.186
305	55	42	1.310	189.626
8.111	.600	.656	1.000	
228	9	1	9.000	.192
300	52	40	1.300	177.778
8.000	.600	.667	1.000	
228	10	1	10.000	.192
300	50	38	1.316	160.444
8.000	.600			
*SAMPLE NUMBER103				
200	20	4	5.000	4.000
228	160	45	3.556	389.543
3.111	1.000	.877	1.000	
200	20	4	5.000	4.000
225	100	40	2.500	316.049

2.778	1.000	.889	1.000	
200	20	3	6.667	2.250
225	60	42	1.429	348.444
2.778	1.000			
*SAMPLE NUMBER104				
205	35	7	5.000	11.660
222	62	15	4.133	45.654
1.889	.800	.901	2.500	
200	30	5	6.000	6.250
218	60	10	6.000	21.042
2.000	2.000	.917	1.000	
200	30	5	6.000	6.250
215	60	10	6.000	21.633
1.667	2.000			
*SAMPLE NUMBER105				
230	28	6	4.667	6.805
248	90	18	5.000	52.680
2.000	.100	.806	2.000	
220	30	7	4.286	10.124
245	100	20	5.000	66.639
2.778	.100	.816	2.000	
218	30	7	4.286	10.311
240	100	21	4.762	76.563
2.444	.200			
*SAMPLE NUMBER106				
195	20	4	5.000	4.208
218	45	8	5.625	13.467
2.556	2.000	.917	1.500	
195	20	4	5.000	4.208
218	40	10	4.000	21.042
2.556	2.000	.917	1.500	
195	20	4	5.000	4.208
215	40	10	4.000	21.633
2.222	3.000			
*SAMPLE NUMBER107				
275	25	5	5.000	3.306
300	120	20	6.000	44.444
2.778	.100	.667	1.000	
270	20	4	5.000	2.195
300	120	20	6.000	44.444
3.333	.100	.667	1.000	
260	25	5	5.000	3.698
300	120	20	6.000	44.444
4.444	.100			
*SAMPLE NUMBER108				
252	20	5	4.000	3.937
298	150	20	7.500	45.043
5.111	.400	.671	1.250	
245	22	.3	7.333	1.499

290	150	25	6.000	74.316
5.000	.400	.690	1.250	
232	22	3	7.333	1.672
290	120	27	4.444	86.683
6.444	.500			
*SAMPLE NUMBER109				
212	22	4	5.500	3.560
235	32	8	4.000	11.589
2.556	.500	.851	1.000	
210	20	3	6.667	2.041
230	30	6	5.000	6.805
2.222	.500	.870	1.000	
210	20	3	6.667	2.041
230	30	6	5.000	6.805
2.222	.500			
*SAMPLE NUMBER110				
285	40	6	6.667	4.432
303	70	45	1.556	220.567
2.000	.050	.660	1.000	
285	45	7	6.429	6.033
300	70	43	1.628	205.444
1.667	.050	.667	1.000	
285	40	6	6.667	4.432
300	78	45	1.733	225.000
1.667	.050			
*SAMPLE NUMBER111				
232	25	3	8.333	1.672
325	135	120	1.125	1363.314
10.333	.500	.615	1.000	
222	20	2	10.000	.812
320	125	110	1.136	1181.641
10.889	.500	.625	1.000	
220	20	2	10.000	.826
320	120	97	1.237	918.848
11.111	.500			
*SAMPLE NUMBER112				
205	52	9	5.778	19.274
227	125	125	1.000	3032.273
2.444	.800	.881	1.250	
202	50	8	6.250	15.685
225	120	125	.960	3086.420
2.556	.800	.889	1.250	
200	60	8	7.500	16.000
220	120	120	1.000	2975.207
2.222	1.000			
*SAMPLE NUMBER113				
210	20	6	3.333	8.163
292	50	15	3.333	26.389
9.111	.600	.685	1.333	

210	30	6	5.000	8.163
290	60	18	3.333	38.526
8.889	.600	.690	1.333	
210	20	5	4.000	5.669
290	100	17	5.882	34.364
8.889	.800			
*SAMPLE NUMBER114				
252	75	4	18.750	2.520
275	35	32	1.094	135.405
2.556	.050	.727	1.000	
250	20	3	6.667	1.440
272	40	40	1.000	216.263
2.444	.050	.735	1.000	
250	20	3	6.667	1.440
260	40	40	1.000	236.686
1.111	.050			
*SAMPLE NUMBER115				
288	55	9	6.111	9.766
288	80	20	4.000	48.225
.000	.200	.694	1.000	
275	50	7	7.143	6.479
285	100	20	5.000	49.246
1.111	.200	.702	1.000	
270	50	9	5.556	11.111
282	150	28	5.357	98.587
1.333	.200			
*SAMPLE NUMBER116				
232	38	8	4.750	11.891
262	85	42	2.024	256.978
3.333	.020	.763	1.500	
228	36	6	6.000	6.925
248	80	45	1.778	329.247
2.222	.030	.806	1.000	
220	30	6	5.000	7.438
240	80	45	1.778	351.563
2.222	.030			
*SAMPLE NUMBER117				
242	35	3	11.667	1.537
282	128	15	8.533	28.293
4.444	.400	.709	1.250	
230	32	4	8.000	3.025
280	130	17	7.647	36.862
5.556	.400	.714	1.250	
225	30	3	10.000	1.778
280	150	17	8.824	36.862
6.111	.500			
*SAMPLE NUMBER118				
248	18	5	3.600	4.065
282	30	12	2.500	18.108

3.778	.030	.709	1.667	
245	15	3	5.000	1.499
265	35	10	3.500	14.240
2.222	.040	.755	1.250	
240	20	4	5.000	2.778
250	30	10	3.000	16.000
1.111	.050			
*SAMPLE NUMBER119				
200	40	9	4.444	20.250
225	100	25	4.000	123.457
2.778	1.000	.889	1.000	
200	40	9	4.444	20.250
220	100	25	4.000	129.132
2.222	1.000	.909	1.000	
200	50	10	5.000	25.000
218	100	27	3.704	153.396
2.000	1.000			
*SAMPLE NUMBER120				
218	22	8	2.750	13.467
220	45	11	4.091	25.000
.222	.200	.909	1.500	
215	20	4	5.000	3.461
230	50	10	5.000	18.904
1.667	.200	.870	1.500	
215	20	4	5.000	3.461
230	60	10	6.000	18.904
1.667	.300			
*SAMPLE NUMBER121				
218	55	8	6.875	13.467
225	130	18	7.222	64.000
.778	.700	.889	1.286	
210	50	8	6.250	14.512
220	100	20	5.000	82.645
1.111	.800	.909	1.125	
205	40	8	5.000	15.229
220	90	21	4.286	91.116
1.667	.900			
*SAMPLE NUMBER122				
200	20	10	2.000	25.000
232	55	30	1.833	167.212
3.556	1.000	.862	1.000	
200	20	8	2.500	16.000
230	50	25	2.000	118.147
3.333	1.000	.870	1.000	
200	20	7	2.857	12.250
230	50	25	2.000	118.147
3.333	1.000			
*SAMPLE NUMBER123				
212	18	3	6.000	2.002

212	42	9	4.667	18.022
.000	1.000	.943	1.200	
200	20	3	6.667	2.250
210	40	8	5.000	14.512
1.111	1.000	.952	1.200	
195	40	4	10.000	4.208
210	40	7	5.714	11.111
1.667	1.200			
*SAMPLE NUMBER124				
205	40	10	4.000	23.795
228	120	80	1.500	1231.148
2.556	.700	.877	1.000	
205	40	10	4.000	23.795
225	100	85	1.176	1427.160
2.222	.700	.889	1.000	
205	40	10	4.000	23.795
225	80	85	.941	1427.160
2.222	.700			
*SAMPLE NUMBER125				
212	42	10	4.200	22.250
228	55	18	3.056	62.327
1.778	.700	.877	1.429	
205	40	8	5.000	15.229
225	50	15	3.333	44.444
2.222	.900	.889	1.111	
202	40	8	5.000	15.685
222	60	15	4.000	45.654
2.222	1.000			
*SAMPLE NUMBER126				
208	55	15	3.667	52.006
228	105	82	1.280	1293.475
2.222	.900	.877	1.111	
205	50	10	5.000	23.795
225	100	80	1.250	1264.198
2.222	.900	.889	1.111	
202	50	10	5.000	24.507
220	100	82	1.220	1389.256
2.000	1.000			
*SAMPLE NUMBER127				
225	48	3	16.000	1.778
232	36	6	6.000	6.688
.778	.030	.862	1.333	
220	50	6	8.333	7.438
230	40	8	5.000	12.098
1.111	.030	.870	1.333	
220	30	8	3.750	13.223
325	40	10	4.000	9.467
11.667	.040			
*SAMPLE NUMBER128				

284	22	8	2.750	7.935
292	42	9	4.667	9.500
.889	.100	.685	2.000	
270	20	5	4.000	3.429
288	40	8	5.000	7.716
2.000	.100	.694	2.000	
260	20	5	4.000	3.698
288	40	8	5.000	7.716
3.111	.200			
*SAMPLE NUMBER129				
222	22	9	2.444	16.435
252	120	48	2.500	362.812
3.333	.200	.794	1.000	
220	20	5	4.000	5.165
240	100	40	2.500	277.778
2.222	.200	.833	1.000	
220	20	4	5.000	3.306
238	50	42	1.190	311.419
2.000	.200			
*SAMPLE NUMBER130				
245	72	15	4.800	37.484
258	85	62	1.371	577.489
1.444	.030	.775	1.333	
230	60	13	4.615	31.947
240	80	68	1.176	802.778
1.111	.040	.833	1.000	
220	60	13	4.615	34.917
230	80	68	1.176	874.102
1.111	.040			
*SAMPLE NUMBER131				
286	27	11	2.455	14.793
308	52	18	2.889	34.154
2.444	.030	.649	1.000	
282	28	9	3.111	10.186
302	50	17	2.941	31.687
2.222	.030	.662	1.000	
282	35	8	4.375	8.048
300	50	17	2.941	32.111
2.000	.030			
*SAMPLE NUMBER132				
272	20	4	5.000	2.163
288	30	10	3.000	12.056
1.778	.040	.694	1.000	
265	20	4	5.000	2.278
285	40	10	4.000	12.311
2.222	.040	.702	1.000	
262	20	4	5.000	2.331
280	40	10	4.000	12.755
2.000	.040			

*SAMPLE NUMBER133				
320	20	2	10.000	.391
380	100	30	3.333	62.327
6.667	.100	.526	1.000	
320	20	2	10.000	.391
380	100	30	3.333	62.327
6.667	.100	.526	1.000	
320	20	2	10.000	.391
380	100	30	3.333	62.327
6.667	.100			
*SAMPLE NUMBER134				
290	35	10	3.500	11.891
305	52	15	3.467	24.187
1.667	.200	.656	1.000	
290	35	9	3.889	9.631
300	50	14	3.571	21.778
1.111	.200	.667	1.000	
290	35	9	3.889	9.631
300	50	14	3.571	21.778
1.111	.200			
*SAMPLE NUMBER135				
228	55	12	4.583	27.701
248	110	28	3.929	127.471
2.222	.100	.806	10.000	
225	50	10	5.000	19.753
240	100	25	4.000	108.507
1.667	.200	.833	5.000	
200	50	10	5.000	25.000
238	95	23	4.130	93.390
4.222	1.000			
*SAMPLE NUMBER136				
242	55	12	4.583	24.588
268	110	28	3.929	109.156
2.889	.030	.746	1.667	
240	50	10	5.000	17.361
260	120	25	4.800	92.456
2.222	.030	.769	1.667	
240	50	8	6.250	11.111
258	140	23	6.087	79.472
2.000	.050			
*SAMPLE NUMBER137				
315	10	1	10.000	.101
350	80	15	5.333	18.367
3.889	.100	.571	1.000	
315	10	1	10.000	.101
350	80	15	5.333	18.367
3.889	.100	.571	1.000	
315	10	1	10.000	.101
350	80	15	5.333	18.367

3.889	.100			
*SAMPLE NUMBER138				
278	42	8	5.250	8.281
296	110	78	1.410	694.394
2.000	.100	.676	1.000	
270	40	6	6.667	4.938
295	100	70	1.429	563.057
2.778	.100	.678	1.000	
265	40	6	6.667	5.126
292	100	78	1.282	713.548
3.000	.100			
*SAMPLE NUMBER139				
240	32	3	10.667	1.563
322	120	14	8.571	18.904
9.111	.200	.621	1.000	
240	30	3	10.000	1.563
320	100	12	8.333	14.063
8.889	.200	.625	1.000	
240	30	3	10.000	1.563
320	100	12	8.333	14.063
8.889	.200			
*SAMPLE NUMBER140				
242	80	10	8.000	17.075
268	75	8	9.375	8.911
2.889	.100	.746	1.000	
235	50	5	10.000	4.527
260	80	10	8.000	14.793
2.778	.100	.769	1.000	
230	40	4	10.000	3.025
258	90	11	8.182	18.178
3.111	.100			
*SAMPLE NUMBER141				
212	380	120	3.167	3203.987
218	500	180	2.778	6817.608
.667	.100	.917	2.000	
210	400	150	2.667	5102.041
215	500	190	2.632	7809.627
.556	.100	.930	2.000	
208	400	160	2.500	5917.160
210	500	200	2.500	9070.295
.222	.200			
*SAMPLE NUMBER142				
345	100	80	1.250	537.702
432	1000	282	3.546	4261.188
9.667	.080	.463	1.250	
340	100	78	1.282	526.298
430	1000	282	3.546	4300.919
10.000	.100	.465	1.000	
340	100	78	1.282	526.298

430	1000	280	3.571	4240.130
10.000	.100			
*SAMPLE NUMBER143				
280	20	7	2.857	6.250
300	50	40	1.250	177.778
2.222	.030	.667	1.000	
280	20	6	3.333	4.592
300	50	42	1.190	196.000
2.222	.030	.667	1.000	
280	20	6	3.333	4.592
300	50	42	1.190	196.000
2.222	.030			
*SAMPLE NUMBER144				
240	100	12	8.333	25.000
260	100	20	5.000	59.172
2.222	.100	.769	1.000	
233	100	12	8.333	26.525
252	100	20	5.000	62.988
2.111	.100	.794	1.000	
230	50	10	5.000	18.904
250	100	20	5.000	64.000
2.222	.100			
*SAMPLE NUMBER145				
282	38	12	3.167	18.108
298	78	28	2.786	88.284
1.778	.040	.671	1.250	
270	40	10	4.000	13.717
290	80	25	3.200	74.316
2.222	.040	.690	1.250	
265	50	9	5.556	11.534
285	90	22	4.091	59.588
2.222	.050			
*SAMPLE NUMBER146				
212	18	8	2.250	14.240
248	40	14	2.857	31.868
4.000	.300	.806	1.000	
210	20	7	2.857	11.111
245	40	15	2.667	37.484
3.889	.300	.816	1.000	
210	30	7	4.286	11.111
245	40	17	2.353	48.147
3.889	.300			
*SAMPLE NUMBER147				
258	20	5	4.000	3.756
285	120	25	4.800	76.947
3.000	.100	.702	2.000	
250	20	5	4.000	4.000
280	100	25	4.000	79.719
3.333	.200	.714	1.000	

245	50	6	8.333	5.998
278	90	27	3.333	94.327
3.667	.200			
*SAMPLE NUMBER148				
242	38	9	4.222	13.831
268	52	48	1.083	320.784
2.889	.030	.746	1.333	
235	40	8	5.000	11.589
250	60	45	1.333	324.000
1.667	.040	.800	1.000	
228	40	7	5.714	9.426
248	70	43	1.628	300.631
2.222	.040			
*SAMPLE NUMBER149				
278	25	8	3.125	8.281
288	48	15	3.200	27.127
1.111	.020	.694	1.500	
270	20	5	4.000	3.429
280	40	10	4.000	12.755
1.111	.020	.714	1.500	
265	20	4	5.000	2.278
278	30	10	3.000	12.939
1.444	.030			
*SAMPLE NUMBER150				
320	20	3	6.667	.879
378	120	20	6.000	27.995
6.444	.100	.529	1.000	
320	20	2	10.000	.391
375	100	18	5.556	23.040
6.111	.100	.533	1.000	
320	20	2	10.000	.391
375	100	18	5.556	23.040
6.111	.100			
*SAMPLE NUMBER150				
320	20	2	10.000	.391
375	100	18	5.556	23.040
6.111	.100	.533	.200	
340	92	28	3.286	67.820
432	3	76	.039	309.499
10.222	.010	.463	2.000	
340	90	25	3.600	54.066
430	300	75	4.000	304.218
10.000	.020			
*SAMPLE NUMBER151				
340	90	25	3.600	54.066
430	300	70	4.286	265.008
10.000	.020	.465	10.000	
235	50	5	10.000	4.527
250	100	15	6.667	36.000

1.667	.200	.800	1.000	
235	50	5	10.000	4.527
250	100	15	6.667	36.000
1.667	.200			
*SAMPLE NUMBER152				
230	60	5	12.000	4.726
248	100	15	6.667	36.583
2.000	.300	.806	.267	
285	30	4	7.500	1.970
347	250	20	12.500	33.220
6.889	.080	.576	1.000	
280	30	3	10.000	1.148
345	250	20	12.500	33.606
7.222	.080			
*SAMPLE NUMBER154				
285	25	3	8.333	1.108
410	210	11	19.091	7.198
13.889	.200	.488	1.000	
282	22	2	11.000	.503
407	200	10	20.000	6.037
13.889	.200	.491	1.000	
280	20	2	10.000	.510
405	200	10	20.000	6.097
13.889	.200			
*SAMPLE NUMBER155				
292	180	25	7.200	73.302
305	170	30	5.667	96.748
1.444	.080	.656	1.000	
290	180	25	7.200	74.316
300	170	25	6.800	69.444
1.111	.080	.667	1.000	
290	180	23	7.826	62.901
300	170	25	6.800	69.444
1.111	.080			
*SAMPLE NUMBER156				
259	22	5	4.400	3.727
278	100	10	10.000	12.939
2.111	.100	.719	1.000	
250	20	4	5.000	2.560
270	100	10	10.000	13.717
2.222	.100	.741	1.000	
245	20	4	5.000	2.666
265	30	11	2.727	17.230
2.222	.100			
*SAMPLE NUMBER157				
262	32	9	3.556	11.800
297	60	25	2.400	70.854
3.889	.080	.673	1.125	
265	30	8	3.750	9.114

295	60	25	2.400	71.818
3.333	.080	.678	1.125	
250	25	8	3.125	10.240
282	60	25	2.400	78.593
3.556	.090			
*SAMPLE NUMBER158				
298	55	9	6.111	9.121
302	140	25	5.600	68.528
.444	.010	.662	7.000	
295	50	9	5.556	9.308
300	140	25	5.600	69.444
.556	.070	.667	1.000	
295	50	8	6.250	7.354
300	140	23	6.087	58.778
.556	.070			
*SAMPLE NUMBER159				
265	42	12	3.500	20.506
295	105	15	7.000	25.855
3.333	.020	.678	1.000	
262	40	8	5.000	9.323
292	100	13	7.692	19.821
3.333	.020	.685	1.000	
260	40	7	5.714	7.249
292	100	13	7.692	19.821
3.556	.020			
*SAMPLE NUMBER160				
240	35	9	3.889	14.063
275	130	62	2.097	508.298
3.889	.060	.727	1.333	
240	30	6	5.000	6.250
265	100	60	1.667	512.638
2.778	.060	.755	1.333	
180	10	1	10.000	.309
260	80	68	1.176	684.024
8.889	.080			
*SAMPLE NUMBER161				
282	42	12	3.500	18.108
298	80	32	2.500	115.310
1.778	.030	.671	1.333	
270	40	10	4.000	13.717
290	90	30	3.000	107.015
2.222	.030	.690	1.333	
255	40	10	4.000	15.379
270	90	29	3.103	115.364
1.667	.040			
*SAMPLE NUMBER162				
222	22	3	7.333	1.826
242	45	37	1.216	233.761
2.222	.080	.826	1.250	

220	20	3	6.667	1.860
240	40	38	1.053	250.694
2.222	.080	.833	1.250	
215	15	3	5.000	1.947
240	30	38	.789	250.694
2.778	.100			
*SAMPLE NUMBER163				
268	28	5	5.600	3.481
270	32	29	1.103	115.364
.222	.030	.741	1.333	
260	25	4	6.250	2.367
270	30	28	1.071	107.545
1.111	.030	.741	1.333	
250	20	4	5.000	2.560
263	30	28	1.071	113.346
1.444	.040			
*SAMPLE NUMBER164				
455	20	6	3.333	1.739
475	55	20	2.750	17.729
2.222	.050	.421	1.000	
455	18	7	2.571	2.367
475	50	18	2.778	14.360
2.222	.050	.421	1.000	
455	20	6	3.333	1.739
475	50	18	2.778	14.360
2.222	.050			
*SAMPLE NUMBER165				
260	70	10	7.000	14.793
290	300	30	10.000	107.015
3.333	.060	.690	1.000	
260	70	10	7.000	14.793
290	300	30	10.000	107.015
3.333	.060	.690	1.000	
260	70	10	7.000	14.793
290	300	30	10.000	107.015
3.333	.060			
*SAMPLE NUMBER166				
285	32	7	4.571	6.033
305	50	20	2.500	42.999
2.222	.080	.656	1.000	
285	30	6	5.000	4.432
302	50	20	2.500	43.858
1.889	.080	.662	1.000	
285	30	6	5.000	4.432
300	50	19	2.632	40.111
1.667	.080			
*SAMPLE NUMBER167				
320	72	18	4.000	31.641
350	120	30	4.000	73.469

3.333	.020	.571	1.000	
320	70	15	4.667	21.973
350	120	29	4.138	68.653
3.333	.020	.571	1.000	
320	70	15	4.667	21.973
350	120	29	4.138	68.653
3.333	.020			
*SAMPLE NUMBER168				
260	80	9	8.889	11.982
295	120	22	5.455	55.616
3.889	.050	.678	1.200	
260	80	8	10.000	9.467
295	150	20	7.500	45.964
3.889	.050	.678	1.200	
260	70	8	8.750	9.467
290	150	120	1.250	1712.247
3.333	.060			
*SAMPLE NUMBER169				
230	22	8	2.750	12.098
244	32	9	3.556	13.605
1.556	.050	.820	1.000	
228	20	5	4.000	4.809
240	30	9	3.333	14.063
1.333	.050	.833	1.000	
222	20	5	4.000	5.073
232	30	9	3.333	15.049
1.111	.050			
*SAMPLE NUMBER170				
248	32	8	4.000	10.406
265	55	15	3.667	32.040
1.889	.030	.755	1.333	
240	30	6	5.000	6.250
260	50	15	3.333	33.284
2.222	.040	.769	1.000	
235	30	6	5.000	6.519
255	50	15	3.333	34.602
2.222	.040			
*SAMPLE NUMBER171				
238	45	9	5.000	14.300
262	65	20	3.250	58.272
2.667	.050	.763	1.200	
235	30	7	4.286	8.873
258	60	17	3.529	43.417
2.556	.050	.775	1.200	
228	25	6	4.167	6.925
252	60	16	3.750	40.312
2.667	.060			
*SAMPLE NUMBER172				
292	22	7	3.143	5.747

338	60	20	3.000	35.013
5.111	.020	.592	1.000	
290	24	7	3.429	5.826
335	52	20	2.600	35.643
5.000	.020	.597	1.000	
290	20	6	3.333	4.281
335	50	19	2.632	32.168
5.000	.020			
*SAMPLE NUMBER173				
220	20	7	2.857	10.124
252	76	52	1.462	425.800
3.556	.080	.794	1.250	
220	20	6	3.333	7.438
250	70	42	1.667	282.240
3.333	.090	.800	1.111	
205	20	5	4.000	5.949
235	50	40	1.250	289.724
3.333	.100			
*SAMPLE NUMBER174				
305	25	7	3.571	5.267
332	58	17	3.412	26.219
3.000	.040	.602	1.000	
300	20	7	2.857	5.444
330	58	18	3.222	29.752
3.333	.040	.606	1.000	
300	20	6	3.333	4.000
330	60	18	3.333	29.752
3.333	.040			
*SAMPLE NUMBER175				
290	40	10	4.000	11.891
305	50	50	1.000	268.745
1.667	.060	.656	1.000	
290	40	10	4.000	11.891
305	50	45	1.111	217.683
1.667	.060	.656	1.000	
290	40	9	4.444	9.631
305	50	45	1.111	217.683
1.667	.060			
*SAMPLE NUMBER176				
242	65	18	3.611	55.324
242	68	15	4.533	38.420
.000	.030	.826	1.333	
230	50	10	5.000	18.904
240	60	13	4.615	29.340
1.111	.030	.833	1.333	
225	50	8	6.250	12.642
235	60	11	5.455	21.910
1.111	.040			
*SAMPLE NUMBER177				

250	55	9	6.111	12.960
300	100	20	5.000	44.444
5.556	.060	.667	1.000	
248	50	8	6.250	10.406
290	100	22	4.545	57.551
4.667	.060	.690	1.000	
248	50	8	6.250	10.406
290	100	18	5.556	38.526
4.667	.060			
*SAMPLE NUMBER178				
265	25	6	4.167	5.126
275	30	10	3.000	13.223
1.111	.040	.727	1.000	
265	25	6	4.167	5.126
275	30	10	3.000	13.223
1.111	.040	.727	1.000	
260	25	6	4.167	5.325
270	30	10	3.000	13.717
1.111	.040			
*SAMPLE NUMBER179				
250	55	9	6.111	12.960
278	120	85	1.412	934.864
3.111	.030	.719	1.667	
245	40	8	5.000	10.662
275	100	80	1.250	846.261
3.333	.040	.727	1.250	
235	30	6	5.000	6.519
262	90	79	1.139	909.184
3.000	.050			
*SAMPLE NUMBER180				
272	45	9	5.000	10.948
282	72	16	4.500	32.192
1.111	.030	.709	1.000	
265	40	8	5.000	9.114
280	70	15	4.667	28.699
1.667	.030	.714	1.000	
260	40	8	5.000	9.467
278	60	14	4.286	25.361
2.000	.030			
*SAMPLE NUMBER181				
238	38	9	4.222	14.300
258	82	60	1.367	540.833
2.222	.040	.775	1.500	
230	40	8	5.000	12.098
250	80	60	1.333	576.000
2.222	.040	.800	1.500	
225	50	9	5.556	16.000
245	80	68	1.176	770.346
2.222	.060			

*SAMPLE NUMBER182				
275	35	8	4.375	8.463
305	85	20	4.250	42.999
3.333	.060	.656	1.000	
275	30	5	6.000	3.306
300	80	17	4.706	32.111
2.778	.060	.667	1.000	
265	30	4	7.500	2.278
290	80	16	5.000	30.440
2.778	.060			
*SAMPLE NUMBER183				
258	42	10	4.200	15.023
288	52	19	2.737	43.523
3.333	.020	.694	2.500	
250	30	6	5.000	5.760
270	50	17	2.941	39.643
2.222	.030	.741	1.667	
232	20	4	5.000	2.973
260	50	16	3.125	37.870
3.111	.050			
*SAMPLE NUMBER184				
288	250	50	5.000	301.408
500	1500	250	6.000	2500.000
23.556	.020	.400	1.500	
285	250	50	5.000	307.787
500	1500	200	7.500	1600.000
23.889	.030	.400	1.000	
385	250	50	5.000	168.662
500	1500	200	7.500	1600.000
12.778	.030			
*SAMPLE NUMBER185				
282	220	18	12.222	40.742
292	450	35	12.857	143.671
1.111	.030	.685	1.000	
280	200	15	13.333	28.699
290	400	30	13.333	107.015
1.111	.030	.690	1.000	
270	100	14	7.143	26.886
282	200	28	7.143	98.587
1.333	.030			
*SAMPLE NUMBER186				
245	35	6	5.833	5.998
252	42	8	5.250	10.078
.778	.040	.794	1.250	
240	30	5	6.000	4.340
250	40	7	5.714	7.840
1.111	.040	.800	1.250	
238	30	5	6.000	4.414
245	30	7	4.286	8.163

.778	.050			
*SAMPLE NUMBER187				
282	22	8	2.750	8.048
290	52	12	4.333	17.122
.889	.050	.690	1.000	
280	20	7	2.857	6.250
290	50	12	4.167	17.122
1.111	.050	.690	1.000	
280	30	7	4.286	6.250
290	50	12	4.167	17.122
1.111	.050			
*SAMPLE NUMBER188				
218	22	6	3.667	7.575
242	52	10	5.200	17.075
2.667	.200	.826	1.000	
215	20	5	4.000	5.408
240	50	13	3.846	29.340
2.778	.200	.833	1.000	
210	20	5	4.000	5.669
238	50	14	3.571	34.602
3.111	.200			
*SAMPLE NUMBER189				
270	10	5	2.000	3.429
332	70	15	4.667	20.413
6.889	.030	.602	1.000	
255	12	3	4.000	1.384
320	60	12	5.000	14.063
7.222	.030	.625	1.000	
240	15	3	5.000	1.563
315	40	12	3.333	14.512
8.333	.030			
*SAMPLE NUMBER190				
322	35	5	7.000	2.411
338	60	42	1.429	154.406
1.778	.050	.592	1.200	
300	20	4	5.000	1.778
325	50	40	1.250	151.479
2.778	.050	.615	1.200	
285	15	3	5.000	1.108
320	40	40	1.000	156.250
3.889	.060			
*SAMPLE NUMBER191				
342	50	10	5.000	8.550
355	50	45	1.111	160.682
1.444	.030	.563	1.000	
340	50	9	5.556	7.007
350	50	42	1.190	144.000
1.111	.030	.571	1.000	
340	40	8	5.000	5.536

350	50	40	1.250	130.612
1.111	.030			
*SAMPLE NUMBER192				
268	40	8	5.000	8.911
278	52	13	4.000	21.867
1.111	.030	.719	1.667	
268	40	10	4.000	13.923
275	50	15	3.333	29.752
.778	.030	.727	1.667	
250	40	12	3.333	23.040
270	50	16	3.125	35.117
2.222	.050			
*SAMPLE NUMBER193				
232	55	15	3.667	41.803
242	55	18	3.056	55.324
1.111	.030	.826	1.333	
230	50	10	5.000	18.904
240	50	15	3.333	39.063
1.111	.030	.833	1.333	
205	40	14	2.857	46.639
235	50	16	3.125	46.356
3.333	.040			
*SAMPLE NUMBER194				
258	18	8	2.250	9.615
265	38	12	3.167	20.506
.778	.030	.755	1.333	
255	20	7	2.857	7.536
265	40	12	3.333	20.506
1.111	.030	.755	1.333	
248	20	6	3.333	5.853
260	50	12	4.167	21.302
1.333	.040			
*SAMPLE NUMBER195				
272	30	6	5.000	4.866
282	52	45	1.156	254.640
1.111	.010	.709	5.000	
270	30	6	5.000	4.938
282	50	42	1.190	221.820
1.333	.010	.709	5.000	
258	30	6	5.000	5.408
275	50	42	1.190	233.256
1.889	.050			
*SAMPLE NUMBER196				
268	12	5	2.400	3.481
292	50	14	3.571	22.987
2.667	.020	.685	1.500	
265	15	4	3.750	2.278
290	50	12	4.167	17.122
2.778	.020	.690	1.500	

258	20	4	5.000	2.404
278	40	12	3.333	18.633
2.222	.030			
*SAMPLE NUMBER197				
240	16	3	5.333	1.563
272	75	12	6.250	19.464
3.556	.050	.735	1.000	
230	20	5	4.000	4.726
265	60	15	4.000	32.040
3.889	.050	.755	1.000	
228	20	6	3.333	6.925
260	50	17	2.941	42.751
3.556	.050			
*SAMPLE NUMBER198				
228	90	4	22.500	3.078
258	80	40	2.000	240.370
3.333	.030	.775	1.333	
225	70	6	11.667	7.111
250	100	42	2.381	282.240
2.778	.040	.800	1.000	
220	30	6	5.000	7.438
242	200	80	2.500	1092.822
2.444	.040			
*SAMPLE NUMBER199				
320	40	10	4.000	9.766
335	65	20	3.250	35.643
1.667	.030	.597	1.000	
320	35	9	3.889	7.910
330	60	18	3.333	29.752
1.111	.030	.606	1.000	
320	35	9	3.889	7.910
330	60	17	3.529	26.538
1.111	.030			
*SAMPLE NUMBER200				
320	45	8	5.625	6.250
340	100	22	4.545	41.869
2.222	.040	.588	1.000	
315	40	7	5.714	4.938
338	100	22	4.545	42.365
2.556	.040	.592	1.000	
315	40	7	5.714	4.938
338	100	22	4.545	42.365
2.556	.040			

CORRELATION ANALYSIS LIFE-TEST NO.3 (S2A)
(ZERO-HOUR PARAMETERS AND DEGRADATION)

1	210.16	66.60	42032.00	9720722.00
2	54.41	147.93	10883.00	4969399.00
3	9.36	14.68	1873.00	60689.00
4	6.37	5.26	1275.77	13674.96
5	78.26	384.06	15653.32	30726407.00
6	257.97	62.49	51595.00	14091449.00
7	149.86	332.41	29972.00	26590940.00
8	49.00	91.35	9800.00	2149380.00
9	4.10	3.67	821.74	6071.75
10	1590.55	9371.65	318111.66	18071548000.00
11	5.31	6.33	1062.55	13680.69
12	19.32	60.78	3865.50	813646.05
13	.82	.21	164.52	144.27
14	1.56	1.41	313.77	893.88

SAMPLE SIZE (200)

1	2	-.09	2103326.00	.07
1	3	.10	413313.00	.06
1	4	-.25	249902.51	.06
1	5	-.07	2900187.80	.07
1	6	.61	11352015.00	.04
1	7	-.12	5726231.00	.06
1	8	-.12	1909932.00	.06
1	9	-.17	164113.53	.06
1	10	-.14	48796484.00	.06
1	11	-.49	181254.32	.05
1	12	-.34	532530.26	.06
1	13	-.62	32818.01	.04
1	14	.03	66577.95	.07
2	3	.39	272149.00	.05
2	4	.61	165607.26	.04
2	5	.40	5415821.50	.05
2	6	.01	2839467.00	.07
2	7	.90	10506096.00	.01
2	8	.63	2258349.00	.04
2	9	.05	51176.69	.07
2	10	.80	239439230.00	.02
2	11	.12	81793.37	.06
2	12	-.04	126227.12	.07
2	13	-.02	8824.59	.07
2	14	.13	22545.98	.06
3	4	-.06	10882.99	.07
3	5	.89	1156555.80	.01
3	6	.12	505451.00	.06
3	7	.43	705407.00	.05
3	8	.48	222521.00	.05

3 9	-.04	7177.26	.07
3 10	.33	12148556.00	.06
3 11	.01	10237.54	.07
3 12	-.05	26978.22	.07
3 13	-.08	1487.11	.07
3 14	.12	3456.50	.06
4 5	.05	123279.32	.07
4 6	-.01	328447.29	.07
4 7	.53	376802.23	.05
4 8	.37	98508.98	.06
4 9	.17	5922.42	.06
4 10	.50	7038983.60	.05
4 11	.29	8727.19	.06
4 12	-.06	20631.81	.07
4 13	.00	1049.09	.07
4 14	.06	2093.60	.07
5 6	-.01	3949825.10	.07
5 7	.38	12250355.00	.06
5 8	.47	4070775.60	.05
5 9	-.01	60370.61	.07
5 10	.40	313895170.00	.05
5 11	.06	116626.21	.07
5 12	-.03	147268.90	.07
5 13	.01	13076.64	.07
5 14	.12	37788.69	.06
6 7	.15	8383634.00	.06
6 8	.08	2628232.00	.07
6 9	.18	220394.75	.06
6 10	-.01	80227874.00	.07
6 11	.38	304380.88	.06
6 12	-.47	633661.50	.05
6 13	-.92	39999.99	.01
6 14	.02	81309.25	.07
7 8	.75	6040942.00	.03
7 9	.15	161873.42	.06
7 10	.80	549062110.00	.02
7 11	.32	295266.32	.06
7 12	-.06	304451.86	.07
7 13	-.09	23261.98	.07
7 14	.14	60234.55	.06
8 9	-.15	29971.95	.06
8 10	.90	170228290.00	.01
8 11	.23	79811.04	.06
8 12	.01	202737.78	.07
8 13	-.05	7844.57	.07
8 14	.16	19631.44	.06
9 10	-.04	964452.60	.07
9 11	.40	6253.47	.05
9 12	-.13	9938.88	.06

9	13	-.13	655.50	.06
9	14	-.09	1189.45	.07
10	11	.15	3492367.90	.06
10	12	.03	10021323.00	.07
10	13	.01	268740.02	.07
10	14	.12	831266.41	.06
11	12	-.12	11236.73	.06
11	13	-.28	797.98	.06
11	14	-.01	1636.80	.07
12	13	.64	4845.41	.04
12	14	-.05	5128.58	.07
13	14	-.02	256.41	.07

CORRELATION ANALYSIS LIFE-TEST NO.3 (S2A)
(500-HOURS PARAMETERS AND DEGRADATION)

1	204.60	68.27	40920.00	9304540.00
2	52.20	148.21	10440.00	4938504.00
3	8.41	15.73	1682.00	63680.00
4	6.84	4.99	1368.83	14359.21
5	92.28	477.88	18456.81	47378777.00
6	253.20	63.69	50640.00	13633534.00
7	149.94	396.59	29989.00	35953569.00
8	46.64	92.59	9329.00	2149875.00
9	4.17	3.70	835.83	6244.62
10	1730.22	12725.69	346044.57	32987433000.00
11	5.39	6.67	1079.99	14747.00
12	22.62	72.74	4525.05	1160771.90
13	.84	.22	168.42	152.02
14	1.28	.98	256.63	521.71

SAMPLE SIZE (200)

1	2	-.09	1938624.00	.07
1	3	.09	364886.00	.07
1	4	-.33	257319.88	.06
1	5	-.10	3123204.40	.07
1	6	.58	10871781.00	.04
1	7	-.13	5410585.00	.06
1	8	-.12	1744779.00	.06
1	9	-.18	161528.59	.06
1	10	-.13	47309296.00	.06
1	11	-.51	174137.39	.05
1	12	-.34	584115.34	.06
1	13	-.61	32564.74	.04
1	14	.01	52756.93	.07
2	3	.39	273742.00	.05
2	4	.62	163490.18	.04
2	5	.39	6621146.20	.05
2	6	.02	2685296.00	.07
2	7	.93	12515856.00	.00
2	8	.76	2585150.00	.02
2	9	.06	50648.99	.07
2	10	.92	366764970.00	.01
2	11	.13	82963.46	.06
2	12	-.03	151574.33	.07
2	13	-.02	8627.68	.07
2	14	-.01	12957.44	.07
3	4	-.06	10439.99	.07
3	5	.89	1505729.00	.01
3	6	.12	450606.00	.06
3	7	.38	726701.00	.06
3	8	.46	214036.00	.05
3	9	-.03	6576.33	.07

3	10	.26	13639044.00	.06
3	11	.02	9524.43	.07
3	12	-.05	24554.64	.07
3	13	-.08	1355.12	.07
3	14	.03	2276.48	.07
4	5	.04	149993.78	.07
4	6	.00	346612.26	.07
4	7	.58	436966.49	.04
4	8	.44	105091.92	.05
4	9	.28	6790.75	.06
4	10	.59	9955216.50	.04
4	11	.37	9921.37	.06
4	12	-.02	29007.27	.07
4	13	.00	1150.95	.07
4	14	.00	1761.45	.07
5	6	-.01	4576215.30	.07
5	7	.32	15184208.00	.06
5	8	.41	4543622.60	.05
5	9	.02	84284.16	.07
5	10	.30	397055540.00	.06
5	11	.09	161445.11	.07
5	12	-.03	148889.96	.07
5	13	.01	15786.31	.07
5	14	.05	28872.87	.07
6	7	.12	8249230.00	.06
6	8	.06	2443445.00	.07
6	9	.24	223133.25	.06
6	10	-.02	84122322.00	.07
6	11	.39	306860.76	.05
6	12	-.46	712902.12	.05
6	13	-.91	39999.99	.01
6	14	-.02	64695.92	.07
7	8	.84	7569142.00	.02
7	9	.15	170014.17	.06
7	10	.91	971362060.00	.01
7	11	.28	315404.26	.06
7	12	-.05	379367.09	.07
7	13	-.08	23763.39	.07
7	14	-.02	36286.80	.07
8	9	-.13	29988.94	.06
8	10	.87	221389100.00	.01
8	11	.22	77629.47	.06
8	12	.00	216206.97	.07
8	13	-.04	7670.74	.07
8	14	.03	12624.35	.07
9	10	-.01	1304191.10	.07
9	11	.47	6844.96	.05
9	12	-.15	10579.97	.06
9	13	-.18	672.11	.06

9	14	-.12	981.82	.06
10	11	.13	4090326.60	.06
10	12	.00	8456624.20	.07
10	13	.01	299054.49	.07
10	14	-.01	412780.53	.07
11	12	-.10	14309.56	.06
11	13	-.27	826.13	.06
11	14	-.04	1326.54	.07
12	13	.65	5946.29	.04
12	14	-.04	5128.58	.07
13	14	-.01	215.39	.07

CORRELATION ANALYSIS LIFE-TEST NO.3 (S2A)
(AMONG 1000-HOURS PARAMETERS)

1	199.45	71.27	39890.00	8972010.00
2	55.37	215.42	11075.00	9894483.00
3	8.31	16.45	1662.00	67966.00
4	6.83	4.60	1367.72	13603.31
5	114.40	586.77	22881.10	71478314.00
6	250.10	64.88	50020.00	13351886.00
7	146.96	341.73	29393.00	27676709.00
8	48.00	93.28	9600.00	2201404.00
9	4.01	3.63	803.24	5866.97
10	1903.44	13821.44	380688.92	38931108000.00
11	5.62	6.65	1125.55	15181.52
12	25.64	82.76	5128.59	1501501.80

SAMPLE SIZE (200)

1	2	-.09	1929804.00	.07
1	3	.10	356487.00	.06
1	4	-.36	248582.77	.06
1	5	-.12	3486606.00	.06
1	6	.61	10547094.00	.04
1	7	-.11	5285130.00	.06
1	8	-.12	1743135.00	.06
1	9	-.17	151144.80	.06
1	10	-.14	47731852.00	.06
1	11	-.52	175008.90	.05
1	12	-.34	615511.03	.06
2	3	.39	372767.00	.05
2	4	.66	207507.74	.03
2	5	.54	15145282.00	.04
2	6	.00	2761940.00	.07
2	7	.87	14555080.00	.01
2	8	.74	3506299.00	.03
2	9	.02	48908.13	.07
2	10	.94	585267330.00	.00
2	11	.10	92459.47	.06
2	12	-.03	162435.30	.07
3	4	-.01	11074.99	.07
3	5	.87	1873145.60	.01
3	6	.10	438654.00	.06
3	7	.45	753678.00	.05
3	8	.50	234257.00	.05
3	9	-.03	6210.50	.07
3	10	.33	18378915.00	.06
3	11	-.01	9129.65	.07
3	12	-.06	25730.05	.07
4	5	.20	267524.95	.06
4	6	.00	342404.72	.07

4	7	.66	410392.46	.03
4	8	.52	110719.51	.05
4	9	.31	6537.10	.06
4	10	.66	11093005.00	.03
4	11	.44	10424.64	.05
4	12	-.01	33747.48	.07
5	6	-.04	5378289.50	.07
5	7	.48	23004214.00	.05
5	8	.53	6949178.30	.05
5	9	.02	103436.76	.07
5	10	.50	865631760.00	.05
5	11	.10	210186.61	.06
5	12	-.03	210362.45	.07
6	7	.15	8023110.00	.06
6	8	.05	2466956.00	.07
6	9	.27	213627.52	.06
6	10	-.03	88936465.00	.07
6	11	.34	311642.86	.06
6	12	-.45	792227.11	.05
7	8	.85	6848575.00	.01
7	9	.15	156391.53	.06
7	10	.87	879763990.00	.01
7	11	.30	304219.27	.06
7	12	-.05	433237.40	.07
8	9	-.13	29392.93	.06
8	10	.85	239276320.00	.01
8	11	.21	80424.47	.06
8	12	.00	256788.21	.07
9	10	-.02	1252687.70	.07
9	11	.50	6942.53	.05
9	12	-.15	11081.56	.06
10	11	.13	4578281.40	.06
10	12	.00	10441225.00	.07
11	12	-.08	19635.03	.07

REFERENCES

1. Barnes, J.A. and Allan, D.W., "A Statistical Model of Flicker Noise," Proc. IRE, vol. 54, No. 2, pp. 176-178, February 1966.

2. Bardeen, J., "Surface State and Rectification at a Metal Semiconductor Contact," Phys. Rev. vol. 71, pp. 649-744, 1947.

3. Bennett, W.R., Electrical Noise, McGraw-Hill (1960), pp. 91-95.

4. Davenport, W.B. and Root, W.L., Random Signal and Noise,

5. Ekstein, H. and Rostoker, A.B., "Quantum Theory of Fluctuations," Phys. Rev. vol. 100, pp. 1023-1031, 1955.

6. Feller, W., Probability Theory and its Application, Chapter 15, Markov Chains, John Wiley (1950).

7. Fisher, S., "Small Signal Impedance of Avalanching Junction with Unequal Electron and Hole Ionization Rates and Drift Velocities," IEEE Trans. on Electron Devices, vol. ED-14, pp. 313-322, June 1967.

8. Fonger, W.E., "A Determination of 1/f Noise Source in Semiconductor Diodes and Triodes," RCA Lab. Series, Princeton, New Jersey, March 1956.

9. Giacoletto, J.L., "Study of p-n-p Alloy Junction Transistors from d-c through Medium Frequencies," RCA Rev., vol. 15, pp. 506-562, December 1954.

10. Gilden, M. and Hines, M.E., "Electronic Tuning Effects in the Reed Microwave Avalanche Diode," IEEE Trans. on Electron Devices, vol. ED-13, pp. 169-175, January 1966.

11. Göetzberger, A., "Avalanche Effects in Silicon p-n Junction. (I) Localyzed Photomultiplication Studies on Microplasmas," J. Appl. Phys. vol. 34, pp. 1581-1590, June 1963.

12. Göetzberger, A., McDonald, B., Haitz, R.H., and Scarlet, R.M., "Avalanche Effect in Silicon p-n Junction. (II) Structurally Perfect Junctions," J. Appl. Phys. vol. 34, pp. 1591-1600, June 1963.

13. Guggenbuehl, W. and Strutt, M.J.O., "Theory and Experiments on Shot Noise in Semiconductor Diodes and Transistors," Proc. IRE, vol. 45, pp. 839-854, May 1957.

14. Haitz, R.H., "Studies of the Uniformity of Avalanche Breakdown by means of Low-frequency Noise Measurements," Physics of Failure in Electronic Fifth Annual Symposium, Battele Auditorium, Columbs, Ohio, 1966.

15. Haitz, R.H., Research on Solid State Noise Devices, Final Report, Harry Diamond Laboratories, USAMC, Washington, D.C., July 1964.

16. Hyde, F.J., "The Physical Basis of Noise," Noise in Electronic Devices, The Institute of Physical Society, Chapman & Hall Ltd., pp. 35-49, 1959.

17. Johnson, J.B., "Thermal Agitation of Electrons in Conductors," Phys. Rev., vol. 32, pp. 97-110, 1928.

18. Kingston, R.H., Semiconductor Surface Physics, University of Pennsylvania Press, 1957.

19. Kittel, C., Elemental Statistical Physics, John Wiley (1958), pp. 127-158.

20. Laning, J.H. and Battin, R.H., Random Process in Automatic Control, McGraw-Hill (1956), pp. 123-125.

21. Lee, Y.W., Statistical Theory of Communication, John Wiley (1963), Table 1 in page 258.

22. McKay, K.G. and McAfee, K.B., "Electron Multiplication in Silicon and Germanium," Phys. Rev. vol. 91, pp. 1079-1084, September 1953.

23. Miller, S.L., "Avalanche Breakdown in Germanium," Phys. Rev., vol. 99, pp. 1234-1241, August 1955.

24. Misawa, T., "Negative Resistance in p-n Junctions Under Avalanche Breakdown Condition," IEEE Trans. on Electron Devices, vol. ED-13, pp. 137-143, January 1966.

25. Misra, R.P., "Reliability of Semiconductor Devices," Summer Conference on Semiconductors, University of Michigan, June 1962.

26. Montgomery, H.C. and Clark, M.A., "Shot Noise in Junction Transistors," J. Appl. Phys. vol. 24, pp. 1337-1338, October 1953.

27. Newman, R., "Visible Light from a Silicon p-n Junction," Phys. Rev., vol. 100, pp. 700-712, 1955.

28. Newton, G.C., Gould, L.A., and Kaiser, J.F., Analytical Design of Linear Feedback Controls, John Wiley (1957), pp. 87-108.

29. Nyquist, H., "Thermal Agitation on Electron Charge in Conductor", Phys. Rev., vol. 32, 1928.

30. Nussbaum, A., Semiconductor Device Physics, Prentice-Hall (1962), pp. 103-113.

31. Petritz, R.L., "On Noise in p-n Junction Rectifiers and Transistors. (I) Theory", Phys. Rev., vol. 91, pp. 231-244, 1953.

32. Petritz, R.L., "On the Theory in p-n Junctions and Related Devices", Proc. IRE, vol, 40, pp. 1442-1456, 1952.

33. Phillips, A.B., Transistor Engineering, McGraw-Hill (1962), pp. 136-137.

34. Ramos, S., Field and Waves in Modern Radio, John-Wiley (1964), pp. 23-34.

35. Reed, W.T., "A Proposed High-frequency Negative Resistance Diode", Bell System Tech. J., vol. 37, pp. 401-446, March 1958.

36. Ryder, E.J., "Mobility of Holes and Electrons in High Electric Fields", Phys. Rev., vol. 90, pp.766-769, June 1953.

37. Schneider, B. and Strutt, M.J.O., "Theory and Experiments on Shot Noise in Silicon p-n Junction Diode and Transistors", Proc. IRE, vol. 47, pp. 546-554, April 1959

38. Shockley, W., Electrons and Holes in Semiconductors, Van Nostrand (1950), pp. 318-324.

39. Schottky, W., "Shot Effect and Fliker Effect", Phys. Rev., vol. 52, 1926.

40. Shockly, W., "The Theory of p-n Junction in Semiconductors and Transistors", The Bell Tel. Syst. Tech. Pub., Monograph I726, Apendix V, pp. I46-I49, I947.

4I. Van der Ziel, A., "Thermal Noise in Space-charge Limited Diodes", Solid State Electronics, pp. 899-900, I966.

42. Van der Ziel, A., "Theory of Junction Diode and Junction Transistor Noise", Proc. IRE, Vol. 46, pp. 589-594, March I958.

43. Van der Ziel, A. "Theory of Shot Noise in Junction Diodes and Junction Transistors", Proc. IRE, Vol. 45, pp. IOII-IOI8, July I957.

44. Van der Ziel, A., "Theory of Shot Noise in Junction Diodes and Junction Transistors", Proc. IRE, Vol. 43, pp. I639-I647, November I955.

45. Van der Ziel, A., Noise , Prentice-Hall, Chapter 8, I954.

46. Weisskoph, V., "A Theory on Shot Noise", NDRC, MIT Rad. Lab. Series, No. I33, May I943. An outline of th this paper will be found in Torrey, H.C. and Whitmer, op, cit.

47. Zucker, H. and others, "Design and Development of a Standard White Noise Generator and Noise Indicating Instrument", IRE. Trans. on Instruments, Vol. I-7, pp. 279-29I, I958.

VITA

Young-Duck Kim was born in on .

He received B.S.E.E. from the Seoul National University, Seoul, Korea, and M.S.E.E. from the Newark College of Engineering, Newark, New Jersey in 1955 and 1963 respectively. While at Newark College of Engineering, he was the recipient of the graduate fellowship. Since 1967 he has joined U.S. Navy Ammunition Depot, Crane, Indiana.